UNIVERSITA' DEGLI STUDI DI MILANO

Dipartimento di Bioscienze

Doctoral school in Integrative Biomedical Research

Cycle XXX

MODULATORY ROLE OF MONOMERIC AMYLOID BETA ON NEURONAL EXCITABILITY AND ITS IMPLICATIONS ON SYNAPTIC ACTIVITY OF IMMATURE CORTICAL NEURONS

Tutor and Supervisor:

Michele MAZZANTI, PhD

Author:

Erika PIZZI

R11078

Academic Year 2016/2017

You can be anything you want to be
Just turn yourself into anything
you think that you could ever be

Queen*, Innuendo*

Table of contents

Introduction

1. Alzheimer's Disease

Since the turn of the century, a rapidly increase in the life expectancy was driven mainly by improvements in sanitation, education and housing. Nowadays, this trend continues to rise resulting in an increased probability of developing an age-associated disease. Indeed, deaths due to dementias are more than doubled between 2000 and 2015 for people at the age of 85 and older [1]. Alzheimer's Disease (AD) contributes to 60-70% of these cases. Given the social, economical and medical impact of the disease, there is an urgent need to develop an effective therapy. Indeed, despite the constant ongoing studies, no new treatments have been approved for Alzheimer's disease since 2003 [2]. The drugs currently in use to treat AD such as the cholinesterase inhibitors (donepezil, galantamine, rivastigmine) [3] and the N-methyl-D-aspartate receptors antagonist memantine , [4] are palliative rather than curative, merely providing symptomatic relief but not altering the course of the disease, which is still incurable.

Alzheimer: Where are you?
Auguste D.: Here and everywhere. Here and now. You don't mind.

In 1906, at the annual meeting of South-West German psychiatrists, a young doctor presented his results concerning a patient who suffered from an unknown brain disorder. The talk entitled "Über eine eigenartige Erkrankung der Hirnrinde" ("On a peculiar disease of the cerebral cortex"). On that occasion, Dr. Alois Alzheimer described the psychiatric symptoms and the histopathological brain changes of Auguste D., the woman who has been the first person diagnosed with the condition currently called AD [5], [6].
The progressive and irreversible brain degeneration typical of AD leads at first to memory loss, confusion and difficulty speaking followed by mood and personality changes with anxiety and aggressiveness increased over time. More the severity of

AD increase more the patient is unable to communicate and to recognize family, friends or their living environment. At the later stage of the disease, AD sufferers become to be completely dependent on other people (NIH, National Institute of Aging, https://www.nia.nih.gov). It is therefore predictable the huge cost requests for both health-care and long-term care of AD patients that has been estimated to be hundreds of dollars billion worldwide. The lifespan increase and the totally lack of a cure has led to a constant growing of the AD cost that will triple in 2030 [7].

A constant and extensive research is attempting to clarify the pathophysiological changes altering the AD brain structure as well as the key players involved in the development of the disease for over 20 years. However, the fascinating and terrible complexity of AD pathophysiology has not been yet resolved.

The severe cognitive impairment typical of AD goes along with a cerebral atrophy which rate appears to be greater compared to what usually takes place in a healthy aged brain [8], [9], [10]. As reviewed by Fox and Scott on Lancet in 2004, the annual rate of global brain atrophy in healthy people is 0.2% - 0.5% compared with 2 - 3% in AD patients [11]. Not only the rate, but also the pattern of the cerebral atrophy is found to be qualitative and quantitative different from normal aging. In healthy aged brains, the frontal lobe, in particular the prefrontal cortex, is the first area loses volume followed by the temporal lobes [12]. On the contrary, the topographic pattern of the cortical atrophy occurring in AD brain correlates well with the appearance of the clinical symptoms related to the disease. The brain damage firstly occurs in the medial temporal lobe [13], where the hippocampus is located and new memories are formed. Several Magnetic Resonance Imaging (MRI) studies have reported that the most affected brain regions in AD pathology are the hippocampus and the enthorinal cortex, which volumes are smaller compared to the healthy condition [9], [10], [14], [15]. Longitudinal MRI scans of hippocampal atrophy can track, with the appropriate accuracy and reproducibility [16], [17], the progression of the disease from MCI to clinical AD as well as from normal ageing to cognitive decline [11]. The atrophy progression continues along a temporal-parietal-frontal trajectory causing both cortical thinning and lateral ventricles dilatation [18].

The massive reduction occurring in the AD-affected brain is only the ultimate stage of the disease. The severe mental disability is preceded by multiple

alterations of the brain homeostasis, which prepare to the onset of both intra- and extracellular lesions. The neurofibrillary tangles (NFTs) and the amyloid "senile" plaques are reported to be the hallmarks of the disease [19]. NFTs are primarily made by masses of paired helical filaments derived from the phosphorylation and the subsequent abnormal folding of Tau protein [20], [21], [22], [23], [24], an intracellular stabilizer of the microtubule filaments [25]. The tangle-bearing neurons show an aberrant axonal transport that may lead to a cascade of events resulting in neuronal dysfunction and death [26]; as a result, the cytoplasmic NFTs became extra-neuronal "ghost NFTs" [24]. Several studies support a stereotypical pattern of regional distribution of NFTs, based on Braak staging [13], which fits well with the cortical neurodegeneration occurring in AD-affected brains (for reviews [18]). Neurofibrillary changes can be distinguished in six stages in which NFT pathology is initially confined to the transenthorinal region (transentorhinal stages I and II) then involves the medial temporal lobe (limbic stages III and VI) and ultimately the associative cortex (isocortical stages V and VI) [27].

The abnormal oligomerization and accumulation of the amyloid β peptide (Aβ) induces the formation of another histopathological feature of AD, the so-called senile plaques [19], [28]. Unlike NFTs, the amyloid plaques are only present within the extra-neuronal space and they firstly spread in the associative isocortex and subsequently in the allocortex as well as basal ganglia and cerebellum [19]. By using the newly developed Positron Emission Tomography (PET) imaging agents able to bind tau protein, it has been shown that NFTs better tracks the cognitive decline of AD-affected brain [29]. The amyloid plaques thus appear to be weakly connected with the progressive cerebral dysfunction and degeneration that occurs in AD brains [30]. However, the dominant model of AD pathogenesis has become, and still remains, the "amyloid hypothesis" that establish Aβ as the main trigger of a cascade of pathological events that occurs in the brain and eventually leads to AD [31], [32], [33]. The NFTs formation has been found to be a downstream event to amyloid accumulation [33], clarifying the more closely correlation of tau pathology with cortex neurodegeneration compared to Aβ spreading.

AD is divided into several subtypes depending on: - the presence of familial determinants (familial AD, FAD and sporadic AD, SAD) - the patient's age when the symptoms are first exhibited, before the age of 60-65 (early onset AD, EOAD) or after the age of 60-65 (late-onset AD, LOAD) [34], [35]. The proportion of the genetically based AD cases have widely varied over time, from as low as 10% as high as 40% or 50% [36], but generally both EOAD and LOAD have a genetic predisposition. Approximately 60% of EOAD cases is familial and 13% are inherited in an autosomal dominant manner with at least three generations affected [37], [38]. LOAD is the most common form of AD, accounting for more than 90% of AD total cases [37], which appears as a very complex disease strongly influenced by genetic variants in combination with environmental factors and life exposure events [39]. Both LOAD and EOAD are associated to four genes which mutations or polymorphism result in the disease. In particular, three forms of EOAD have been reported to be associated with several mutations of APP [40], [41] presenilin 1 (PSEN1) [42] and presenilin 2 (PSEN2) [43], [44] (for review [35]). All these genes encode for proteins that are related to the metabolism of Aβ: PSEN1 ([45] and PSEN2 [43], [46] are two protein subunits of the γ-secretase enzymatic complex involved in the cleavage of APP, which is the transmembrane precursor of Aβ peptide [47]. Regarding LOAD, inheritance of one or two ε4 alleles of the apolipoprotein E gene (ApoE) is considered the most prevalent risk factor for this type of AD so far [48], [49]. ApoE ε4 encodes for the ApoE glycoprotein, which is highly expressed in the liver, as well as in the brain in particular in microglia and astrocytes. ApoE protein is reported to be involved in the transport of cholesterol and other lipids in plasma and the Central Nervous System (CNS) by binding to the cell surface apoE receptors and therefore plays a role in synaptic maintenance [50]. The allelic variant ApoE ε4 gained several toxic functions during the pathological condition of LOAD, these could be summarized into the following categories: inhibition of hippocampal neurogenesis [51], altered cholesterol transport [52], inverse correlation with dendritic spine density [53], altered formation of Aβ due to APP processing changing [54].

The original criteria for the diagnosis of AD were established by the National Institute of Neurological and Communicative Disorders and Stroke (NINCDS) and the Alzheimer's Disease and Related Disorders Association (ADRDA) workgroup

in 1984 [55]. However, by 2009, the NINCDS- ADRDA criteria were revised and update by the National Institute on Aging (NIA) and the Alzheimer's Association (AA), in order to incorporate more modern innovation in clinical, imaging and AD research. The NIA-AA guideline includes the criteria for all-cause dementia as well as core criteria to classify individuals with dementia caused by AD [56], [57]. The current terminology discriminates between 1) Probable AD and 2) Possible AD; it should be noted that a "definitive" stage of AD is not included into the diagnostic criteria. The accuracy of the diagnosis for "probable AD" or "possible AD" is generally low; sensitivity has been reported to range from 71% to 88% whereas specificity ranged from 44% to 71%, depending on the specific histopathologic diagnostic criteria used [58]. Thus the assessment of pathophysiologically proved AD dementia can only made at *post mortem* by histopathological and morphological analysis of the cerebral tissue, to identify the presence of Aβ containing-senile plaques and a regional distribution of NFTs [27]. As mentioned by Guy M. McKhann and colleagues: "AD is fundamentally a clinical diagnosis", which requires a complete clinical evaluation of the patient health condition - both mental and physical - to ensure that the core criteria are satisfied and the final diagnosis is correct as much as possible. The diagnosis of the disease starts with a detailed medical history followed by routine phyisical exams. Subsequently, the cognitive status of the patient is evaluated through diagnostic tests such as the Mini-mental state exam (MMSE) [59] and the Mini-cog exam [60]; other tests have also been designed to assess the daily abilities, quality of life and mood state of sufferers [61]. Besides the neurological examinations, advanced imaging techniques are now used in order to exclude other brain disorders and also to monitor the regional areas more vulnerable to degeneration. The National Institute for health and Care Excellence (NICE) has included in the current guideline (NICE 2017) a combination of several structural imaging tests for AD diagnosis such as MRI and the positron emission tomography (PET) in addition to the perfusion hexamethylpropyleneamine oxime (HMPAO) single-photon emission computed tomography (SPECT) and the F-fluorodeoxyglucose (FDG) PET. By measuring the glucose uptake of neurons and glial cells, a positive scan of FDG-PET is able to suggest AD pathology if the pattern is temporoparietal and posterior cingulate [62] discriminating between

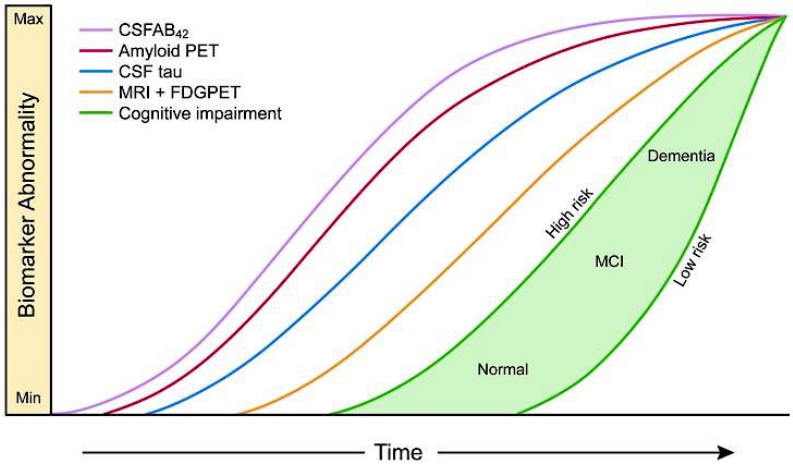

Figure 1.1 - Revised version of the dynamic biomarkers of the AD pathological cascade model.

Aβ deposition is measured by CSF Aβ42 (purple) or PET amyloid imaging (red). Tau pathology is measured by CSF total (t-tau) and phosphorylated (p-tau) tau (blue). Neurodegeneration is measured by MRI+FDGPET (orange). The green zone corresponds to the cognitive response of dementia sufferers with low and high risk boarders . X-axis shows the disease progression expressed as time. All biomarkers converge at the top right-hand corner of the plot that define the point of maximum abnormality. Image from C.R Jack et al. 2013.

AD and other subtypes of dementia. Depending on the result of the brain imaging analysis, it could be recommended the use of cerebrospinal fluid (CSF) biomarkers. Even though the CSF examination is not recommended as routine investigation for dementia, the International Working Group and the NIA-AA suggest that it may add scientific value to AD diagnosis [57], [63]. However, the pathobiological variance typical of AD precludes any biomarker to have a 100% diagnostic accuracy; for this reason the combination between AD biomarkers and imaging studies may help to make a diagnostic decision [64]. The most widely studied CSF biomarkers of AD are Aβ peptide, total Tau (t-Tau) and phosphorylated Tau (p-Tau) [65], [66]. These biomarkers, in addition to MRI, PET amyloid imaging and FDG-PET, were included in the hypothetical model of AD biomarkers proposed by C. R. Jack and colleagues in 2010 [67] and revised in 2013 [64]. The model is focused on the temporal ordering of amyloid biomarkers, identified by CSF Aβ and PET amyloid imaging, and the neurodegeneration markers, identified by CSF tau, MRI and FDG-PET, of AD pathology. As described by the model, the Aβ deposition is the first abnormality occurring before the onset

of tau pathology. It is followed by synaptic loss and brain atrophy, which proceed the clinical symptoms of the cognitive impairment occurring at the latest stage of the disease (Fig.1.1) [64]. In recent years, new AD biomarkers continue to be discovered, for example the dendritic protein Neurogramin whose CSF levels correlate well with cognitive decline and AD progression [68]. Nevertheless, the final goal would be the discovery of an AD biomarker with high sensitivity, specificity and safety that should be less invasive than those present in CSF, such as a blood biomarker [69].

Despite the progresses in the knowledge of AD pathophysiology, the disease is still incurable. So far, the medical treatment includes the cholinesterase inhibitors (such as donepezil, galantamine and rivastigmine) [3] and the *N*-Methyl-D-aspartate (NMDA) receptors blocker memantine [4]. Even if the standard therapy provides some cognitive benefits and symptomatic relief, especially at the beginning of the decline, they do not alter the progression of the disease. For this reason, new treatments are urgently needed to stop the spread of AD over the next few years, even though the cause of the disease till remain unclear and difficult to reveal.

2. Amyloid beta (Aβ)

Most of the AD clinical trials pursue the goal to recover or at least slow down the cognitive decline in dementia patients. To defeat AD, the main strategy works towards the reduction -or even elimination- of the Aβ peptide from the affected brain especially acting on its clearance [70].

Why Aβ is considered the keystone of AD pathophysiology?

Which are the toxic effects and the ways of action of Aβ?

The following section tries to answer the questions above by giving an in depth examination of Aβ peptide as causative factor in AD development.

2.1 Aβ discovery

AD research had remarkable progresses in the 1980s, thanks to the dedication of some scientists who tried to understand the biochemical nature of the amyloid deposits. One of those researchers was Dr. G.G. Glenner, who worked at the University of California in San Diego (UCSD). In 1982, his lab (which was actually the first to create an AD brain bank) opened a position for a job aimed to identify the protein(s) forming the senile plaques. That is how Dr. Wong joined the Glenner's lab and so their collaboration started; at first they examined meninges from human AD-affected brains because of the abundance of amyloid deposits in these membranes [71]. Two years later, their efforts and hopes were rewarded by the discovery of a protein specifically present in donated brains of AD patients compared to controls. They isolated a 4,2 KDa protein, which was fractionated by High Performance Liquid Chromatography (HPLC) into two peaks, β_1 and β_2, perhaps due to a proteolytic cleavage of the newly called β-protein. This protein had a β-pleated sheet structure established by polarization microscopy [28] and this conformation was very similar to that determined by X-ray diffraction in earlier studies [72]. The resulting protein was also sequenced as far as residue 24, thus obtaining the N-terminal sequence of β-protein [28]. In the same period Glenner and Wong found out a correlation between AD and Down Syndrome (DS); the amyloid plaques present in AD brains were the same to those included in DS affected brains, which is in line with the early sign of dementia in patients with trisomy 21. Thus, it has been speculated that the β protein-coding gene was located on chromosome 21 [73]; these findings were both confirmed

and improved in Masters et al. paper published in 1985 [74], paving the way for the future studies on Aβ.

2.2 Aβ overview

Nowadays the senile plaques-assembling protein is called Amyloid Beta or A-beta (Aβ). It is actually a peptide, rather than a protein, because of its variable length that changes from 38 to 43 residues [75]. No gene encodes for Aβ peptide, but it derives from the cleavage of the amyloid precursor protein (APP). The human gene of APP was cloned in 1987 by several labs independently [76]; [77]; [78]; [79]; it is highly expressed in the brain, as expected, but it is also ubiquitously expressed in many different tissues [32]. APP belongs to the APP family, which also includes the genes encoding others APP-like proteins (APLPs), such as APLP1 and APLP2. These APP proteins share a similar structure organization. In particular, APP is a type I single-pass trans-membrane protein characterized by a large extracellular domain and a short C-terminal tail. Among the APLPs, APP is the one with the Aβ domain that is localized in the trans-membrane portion of the protein interacting directly with cholesterol and sphingolipid-enriched microdomains within plasma membrane. The interplay between lipid rafts and APP is known to modulate the canonical APP processing, both non-amyloidogenic and amyloidogenic [80]. Indeed, APP undergoes to sequential cleavages by several proteases - named α- β- and γ-secretases - either preventing or allowing Aβ formation. The α-cleavage occurs within the amyloid region thus excluding Aβ peptide to the end products derived from the non-amyloidogenic pathway. Alternately the full length APP is cleaved by β-secretase (BACE1) into the soluble secreted APP (APPsβ) and C-terminal fragment-β (CTFβ); the latter undergoes γ-cleavage resulting in the release of both APP intracellular domain (AICD) and Aβ peptide in the extracellular space (amyloidogenic pathway) [47].

Since the Aβ deposition drives the formation of the extracellular senile plaques, it is believed for a long time that the peptide was exclusively released outside neurons. Even though the extracellular cleavage of APP is the most frequent mechanism driving the Aβ formation, recent studies on transgenic mouse and human AD/DS-affected brains have highlighted an unusual intraneuronal way of Aβ release [81]. It

seems that the deposition of the peptide inside the cells is the primary steps towards Aβ plaques deposition. As both APP and BACE1 are integral membrane proteins, they are usually secreted along the classical ER-Golgi pathway. Although APP and BACE1 are sorted into distinct organelles, it has actually been described an interaction between APP and BACE1 that takes place in Golgi and/or endosomes, depending on which neuronal part (dendrites, axon or soma) is considered [82] [83]. Further studies have also pointed out the reuptake of extracellular Aβ through alpha7 nicotinic acetylcholine receptors as an additional mechanism implicated in the deposition of Aβ inside the cells [84].
Despite its different release sites, Aβ is always produced as monomer by the proteolytic cleavage of APP. Thus, the amyloid plaques formation is a multi-step process involving several levels of aggregation that leads to various Aβ species.

2.3 Aβ structure & assembly

The most common forms of Aβ peptides released from neurons are $A\beta_{1-42}$ and $A\beta_{1-40}$ that differ in the absence or presence of two extra C-terminal residues (Ile41-Ala42) [85]. Normally, both forms are present in brain parenchyma with $A\beta_{1-40}$ in excess than $A\beta_{1-42}$ (9:1) [86]. The latter seems to be more prone to aggregate in vitro [87] as well as in vivo, confirmed by the fact that the amyloid plaques found in AD patients are mostly constituted by this form of the peptide [88], [89]. However, all the Aβ isoforms share a common structure that makes the peptide unstable and prone to aggregate [90] [91]. Aβ belongs to a class of proteins called “naturally unfolded” that lack of a determined secondary and tertiary structure under physiological conditions [91]. In fact, NMR studies have shown that monomers of $A\beta_{1-42}$ or $A\beta_{1-40}$ possess no α-helical or β- sheet structures and they exist predominately as random extended chains [92]. The Aβ dynamics relies on these structural features that eventually lead to an altered conformation of the peptide resulting in the formation of aggregates [91]. Aβ aggregation and fibrillation are processes that are commonly related to AD pathogenesis [93]. As all the “naturally unstructured” proteins, aggregation of Aβ monomers proceeds through the formation of a partially unfolded intermediate. This species can contain different amounts of ordered structures representing the first

steps of the aggregation process. The second step is the formation of oligomers including soluble oligomers, protofibrils and proto-aggregates. A “nucleation-dependent polymerization” drives the subsequent aggregation of Aβ starting from a kinetically disfavored nucleus. Once a critical nucleus size has been generated, the conditions change in favor of a progressively addition of small oligomers to the seed leading to fibril generation [94], [95]. Thus, some transition species such as dimers, trimers and small aggregate are formed before plaques generation. These oligomeric form of Aβ is reported to be the primary toxic specie for neurons [96]–[98], [99]. The cytotoxicity seems to rely on its structures, which is rich in beta-strands making the oligomers highly hydrophobic and able to interact with different cellular components [100].

3. Aβ neurotoxicity

A plethora of experimental evidences have showed the cytotoxic effects induced by Aβ on single neuronal cells as well as on network circuits. To study the several ways of action by which Aβ triggers AD pathology, many culture systems and transgenic mouse models have been used so far. Since the Aβ sequence differs by three amminoacids between human and rodent, the latter lacks of senile plaques during its normal aging [101]. Thus, the murine amyloidopathy is usually achieved by the overexpression of familial AD (FAD)-associated mutant form of human APP (hAPP) [102]. In Aβ overexpressing transgenic mice, an age-dependent Aβ-overproduction and the resulting plaques maturation are commonly detected. Besides the over 50 hAPP transgenic mice currently in use, other mouse models have been generated to elucidate the pathogenic mechanism of AD; these include mutant PS1, PS2 and Tau transgenic mice and mouse models generated to developed both Aβ-and Tau-pathologies [103]. Although synaptic impairment followed by neuronal loss are present, the overall pathological hallmarks of AD could not be simply recapitulated by the overexpression of human mutated genes implicated in the pathogenesis of the disease. However, much of what we know about the development and progression of AD comes from the study of these mouse models.

I*n vitro* model systems of Aβ-overproduction are also achieved by the exogenous application of Aβ (synthetic or natural secreted form) on acute brain slices preparations or cultures of neuronal cells. The overexpression of APP, β- and γ-secretases is another way to overproduce the amyloid peptide in cell systems.

After the discovery of Aβ as the major component of senile plaques, genetic evidences led to the concept that Aβ itself is able to initiate the cascade of events involved in AD pathogenesis. This concept is well explained by the so called “amyloid hypothesis” which was firstly proposed by Hardy [31],[33] and contemporaneously by Selkoe [32] in 1991. This Aβ-centric philosophy has become the driving force into AD research and therapies development until now. The “amyloid cascade hypothesis” is structured around a sequence of pathogenic and neurotoxic events that eventually lead to AD (Fig. 3.1).

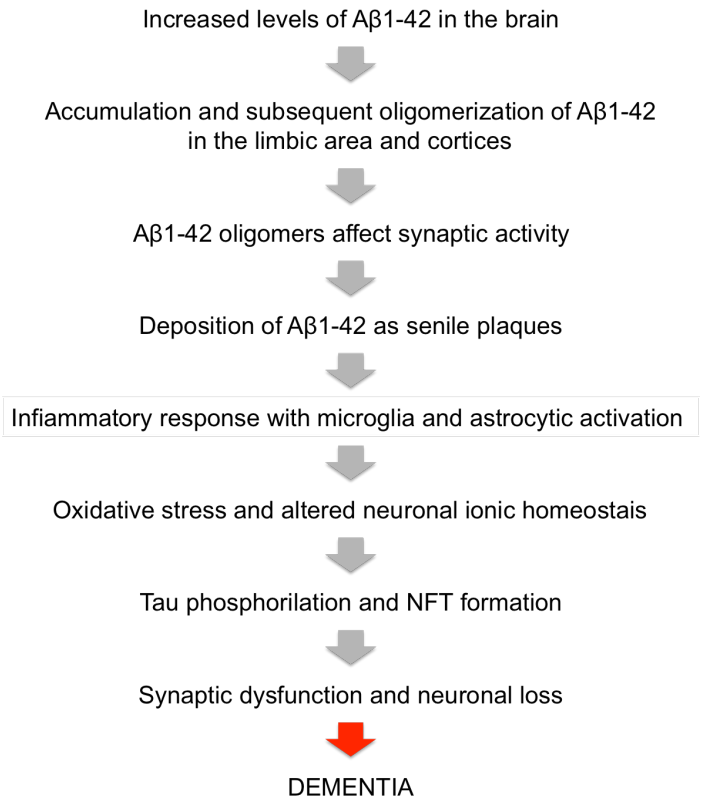

Figure 3.1 - The Amyloid Cascade Hypotesis

Flow chart summarising the Amyloid Cascade Hypothesis, where the formation of Aβ oligomers are the initiating event in Alzheimer's Disease pathology. Modified from Selkoe and Hardy (2016).

Aβ-overproduction and accumulation in the brain parenchyma are the trigger events proposed by Hardy and Selkoe [104]. The increase of the extracellular release of Aβ could be explained in patients with familial or late-onset AD, in which missense mutations occur in genes (PS1, PS2, APP) that are crucial for Aβ production [105]. However, the causes underlying the onset of the sporadic form of the disease are not yet fully understood. Although it involves a strong genetic predispositions [106] sporadic AD is still considered a multifactorial disease. It has been hypothesized that the pathological rise of Aβ in certain cerebral areas may be due to an imbalance between production and clearance processes of Aβ [70], [107]. The peptide has been found not only in the brain interstitial fluid (ISF) [108] but also in plasma and CSF of healthy people and AD patients [109]. However, by measuring the CSF concentration of labeled $A\beta_{1\text{-}40}$ and $A\beta_{1\text{-}42}$, Mawuenyega and colleagues were able to measure both Aβ production and clearance rate in AD sufferers compared with age-

matched controls. As a result of a stable production but a decreased clearance of Aβ, the clearance process is impaired during the disease [107]. This may be related to the dependence of Aβ clearance process from the ApoE isoforms in particular from the ApoE ε4, which is the major genetic risk for sporadic AD [110]. Also, the half-life of Aβ within the ISF is doubled in PDAPP older mice compared to younger, revealing that the ability of the brain to clear Aβ decreases with age [111]. Whatever the mode by which the amyloid homeostasis will become unstable, the pathological result is an increased level of the peptide over the picomolar concentration found in physiological conditions [111], [112]. According to the "amyloid hypothesis" and data from oligomerization studies, increased Aβ brain concentration triggers the accumulation of higher order forms of the peptide derived from monomers aggregation. This process is crucial for the cell damaging effects caused by the peptide. Indeed, among the several isoforms of the peptide, ranging from endogenous monomers to fibrillar elements, oligomers are reported to be the Aβ species with the higher grade of toxicity [113]. The Aβ active pool with toxic potential is mainly composed by small oligomers such as dimers and trimers [98]. It has been described that the application of fibril free-synthetic preparation of Aβ [97], oligomers derived from cells expressing human APP [99] or directly extracted from AD brains [114] induce cell viability impairment and synaptic transmission depression both *in vivo* and *in vitro*. In 2002, Selkoe described AD as "a synaptic failure", pointing out the role of Aβ as a synaptotoxic element in pathological conditions. Indeed, synaptic dysfunction and loss of dendritic spines have been described as the early symptoms that lead to neuronal death and cerebral atrophy typical of AD-affected brains. The mechanism by which Aβ would exert this action is not yet fully understood, however numerous evidences indicate that pathologically Aβ levels may indirectly cause a partial block of NMDA receptors (NMDAR) and induce Long-Term Depression (LTD). The magnitude of the NMDAR activation is fundamental for the regulation of the excitatory synaptic transmission, as it can induce either Long Term Potentiation (LTP) or LTD. The outcome varies depending from the extent of the intracellular calcium rise in the dendritic spines and the downstream activation of specific signaling pathways [115].

LTP is defined as the long-lasting strengthening of synapses following high-frequency stimulation (tetanus) of afferent fibers. It is characterized by a strong activation of NMDAR that mediated an intracellular calcium flux responsible for AMPA insertion

at post-synapses and growth of dendritic spines (called synaptic potentiation). Conversely, LTD requires a long low-frequency synaptic signal that leads to spine shrinkage and synaptic loss. This is fundamental to counteract the excitotoxicity caused by a persistent LTP. Oligomeric Aβ depress the hippocampal synaptic activity by enhancing LTD [116] and impairing LTP [99], [114]. The mechanism by which LTD would be facilitated by Aβ is still unclear, however it may involve different ways of action: desensitization of NMDAR caused by the block of glutamate uptake at synapses and the resulting increase of glutamate levels at the synaptic cleft, activation of extrasynaptic NMDAR or endocytosis of NMDAR through the activation of the α-7 nicotinic receptor and PP2B, a calcium sensitive enzyme that regulates NMDA receptor transmission and synaptic plasticity [116].

Although the effects of Aβ on excitatory synaptic transmission have been extensively studied, fewer investigations have focused on the effects of the peptide on more complex networks. Neuronal circuits are formed by synaptic interactions among excitatory, inhibitory and modulatory cells that cooperate to maintain a balanced activity. . Recent studies pointed out that amyloid depositions begin to form in specific brain cortical and subcortical regions involved in learning, memory and emotional behavior. These areas are anatomically and functionally connected and represent the brain system called “default network”. It includes areas associated with the medial temporal lobe memory system, such as entorhinal cortex and hippocampus, which are reported to be impaired in AD patients. Cognitive active tasks do not engage the default mode, which is most active during passive state and cognitive baseline tasks that direct attention away from external stimuli. Peculiar metabolic properties set the default network apart from other cerebral regions; it is characterized by high glucose metabolism and high regional blood flow. Functional MRI (fMRI) analysis of patients with early mild-to-mild AD showed reduced network activity compared to healthy conditions [117], [118] in line with the brain hypometabolism found in AD sufferers that correlates well with the progression of the disease [119]. Aβ oligomers alter the excitatory transmission via several NMDAR-dependent processes, however it has also been described a GABAergic dysfunction in hAPP and PS1 double transgenic mice (hAPP/PS1) that induces an alteration in synaptic inhibition of neurons situated in the vicinity of amyloid plaques. In the same study, calcium imaging experiments performed on cortical circuits also showed an

imbalance between hypoactive and hyperactive neurons than non-transgenic controls [120]. In addition, reduced expression of the Nav1.1 voltage gated sodium channels subunit (SNC1) in human amyloid precursor protein (hAPP) transgenic mice prevents the action potential propagation in parvalbumin interneurons leading to a GABA deficit release [121]. Thus, both excitatory transmission and synaptic inhibition would be modified by high Aβ levels causing the shift from NMDAR-dependent signaling cascades, which include synaptic potentiation, towards the induction of LTD and synaptic loss. These evidences sustain the hypothesis that Aβ may cause network instability promoting the disruption of neuronal synchrony, which in turn leads to an epileptiform activity. AD sufferers have indeed a higher risk to develop clinical seizures during the course of their illness [122]; this epileptiform behavior also occurs in mice models of amyloidopathy which show non-convulsive seizure activity [123], [124], [125], [126]. Data obtained from Aβ-overexpressing mice have recently reported alterations in the intrinsic properties of excitable cells that point towards an Aβ-dependent neuronal hyper-excitability [127], [128], [129], [130], [131], [132], [133], [134]. The increase in the action potential firing rate has been reported to be the main change found in AD-mouse models [127],[129],[131],[132]. A depolarization of the membrane potential by about 10 mV has been suggested to be one of the possible mechanisms of the increased cellular hyper-excitability found in APdE9 mice, which also display seizures during EEG-video recordings [126]. Amyloidopathy seem related to a decrease in the width of action potentials; patch-clamp recordings performed by isolating nucleated outside-out macropatches from the cell bodies of CA1 pyramidal cells of PSAPP mice have shown that the action potential (AP) narrowing correlates with a 50% decrease in sodium voltage-gated currents related to control condition [127]. Narrower AP has also been observed in CA1 pyramidal hippocampal neurons of Tg+ CNRD8 mouse; in this study authors suggest that the alteration of the AP waveform is mainly due to an increased expression of Kv3 channel, which are responsible for the repolarization phase of the action potential [129]. Decreased width of action potentials was also identified in PDAPP mice aged 9-10 months; conversely older PDAPP mice (20-23 months) display a normal firing activity but a narrower AP and reduce peak compared to age-matched wild-type control mice. Moreover, an increase of the amplitude of the fast spike after-hyperpolarization (AHP) might explain the lack of an altered firing activity in these

mouse models of AD [134]. Furtermore, pre-treatment (2-5 hours) with 500 nM of oligomeric Aβ in CA1 hippocampal slices of wild type mice aged 4-5 weeks alters the action potential subtreshold, which is more hyperpolarized, but depress AHP leading to a net hyper-excitability of cells without affecting the firing rate of neurons [133]. In the majority of these studies CA1 hippocampal region is the main brain area studied, as implicated in memory formation and plasticity. However, hippocampus exchanges information through the enthorinal cortex, which is the input-output structure that connects neocortex with the perforant pathway of the hippocampus. Analyzing two different cell-types of the enthorinal cortex in Tg2576 transgenic mice, Stellate Cells (SCs) and Fan cells (FCs), Marcantoni and colleagues described a hyper-excitability behavior of FCs with an enhanced AHP and shorter action potential width compared to wild-type mice. Tg2576-FCs also exhibited a decreased firing frequency during mild and higher depolarizations whereas SCs display a normal excitability when stimulated with increasing current injections [135].

All the above evidences support a toxic role of Aβ on nervous system that is composed by billion of synaptic connections between different types of cells whose outputs may be excitatory or inhibitory. The neuronal network physiology relies on the synaptic integration of signals that must be constant and efficient. Aβ appears to be a disruptive element of the network homeostasis in pathological conditions by altering the degree to which neuronal activities are correlated.

4. Targeting Aβ

In the last two decades Aβ has been the primary focus for the scientific community regarding AD research and treatment. Indeed, among 105 agents included in the Alzheimer's drug development pipeline, half of them specifically targets Aβ as both antibodies directed at different forms of the peptide (monomers, oligomers, fibrils) and as β-secretase inhibitors. So far, the key factors involved in AD development - including Aβ - have been partially highlighted. There is currently an urgent need to understand how these factors temporally and functionally cooperate to cause the disorder in order to design a successful therapy.

Even though AD is an incurable disease, some medications and alternative-approved therapies are commonly used to treat dementia patients. Below there is a summary of the prescription drugs and other interventions used for helping AD people as well as a summary of the current AD-clinical trials and their outcomes.

4.1 AD Approved Therapies

Although there are different parameters to identify the multiple cognitive decline levels in AD patients, the disease progression is well represented by three principal stages: mild cognitive impairment (MCI), moderate AD and severe cognitive decline (or late dementia[136]; [137]. The commonly used medications are usually more suitable for one of the many progression stages of the disease. Due to the low levels of acetylcholine (ACh) detected in AD affected brains, the first drugs developed were the cholinesterase inhibitors, which aim to raise the ACh levels in the brain by blocking the cholinesterase activity. These medications are usually prescribed for patients with beginning AD, since they help to delay the worsening symptoms by stabilizing the cognitive functions [3].

A drug known as memantine, a NMDA receptor antagonist, is specifically used for the treatment of moderate to severe AD. Blocking the pathological activation of NMDA mainly improves the day-by-day functions thereby delaying the onset of care dependency, a benefit for both patients and caregivers [4], [68].

Many dementia patients also show behavioral disturbances such as aggressiveness, depression, agitation, wandering, anxiety and sleeplessness that could be managed by several prescription drugs. However, unwanted side effects can be caused by these medicines that accelerate cognitive decline and become consequently not effective. Thus, non-pharmacological approaches are emerging as complementary therapy in order to improve the quality of life of AD patients. Randomized controlled trials have shown strong effects of psychosocial interventions on dementia patients treated for agitation. Music therapy, meaningful and pleasant activities as well as social interaction (both real social life and doll-therapy) are useful alternative-therapies for agitation with short- and long-term positive effects. The idea behind the complementary therapies is to reconnect patients to their physical and social

behavior and also to slow down the distress and anxiety due to an uncertain and unfamiliar environment. Indeed, many people with dementia eventually move into care homes or hospitals when caregivers cannot manage anymore the growing need of these individuals. Also, due to the progressive brain impairment, AD patients may not recognize family members causing insecurity and anxiety feelings. These manifestations, including depression, could be managed by a variety of non-pharmacological measures together with the psychological support such as the cognitive stimulation therapy or the cognitive training, as the drug treatment is almost ineffective [138], [139].

All these interventions are very useful to increase the quality of life of AD sufferers and also to manage their feelings about the real world. Even so the final goal would be to stop the disease progression before the neurodegeneration becomes irreversible but unfortunately there is still no cure for AD. Despite this, more than 400 clinical trials are currently active looking for new compounds able to effectively manage AD.

4.2 Current Clinical Trials (2017)

Because of the growing worldwide cases of dementia and the high costs for AD health care, a large number of AD clinical trials start every year in the world. They evaluate new medications and non-pharmacological therapeutic approaches to recover the cognitive abilities or even to stop the neurodegeneration in affected brains. In 2017, there are 105 drug candidates in the AD pipeline divided into three phases (I, II, II) of drug development. Aβ is the primary target of these agents since they aim to reduce the peptide amount in the brain by different mechanisms [2]. The most developed strategies consist in targeting Aβ by blocking either β- or γ-secretases activity or by using antibodies against Aβ. So far, studies regarding the development of proteases inhibitors have been hampered due to the substrate promiscuity of both β- or γ-secretases. Blockage of BACE1 activity leads to very toxic effects due to the important physiological roles of its substrates, including its role in the regulation of axon myelination in the peripheral nervous system (PNS) by the proteolytic processing of Neuregulin-1 (NRG1) and its involvement in the regulation of axonal guidance [140]. In the same way, it has been demonstrated that Notch is one of the targets of γ-secretases [141]. Notch is a master gene involved in embryonic and adult

development; it regulates Neural Stem Cells (NSC) proliferation, neuronal differentiation as well as synaptic plasticity and dendritic arborization [142].

Recently, passive and active immunization are the most pursued AD approaches with the higher number of drug candidates in phase III (50% of the total agents). Passive immunotherapy uses human monoclonal/polyclonal antibodies against Aβ that bind specific sub-regions of the peptide to avoid the oligomerization. The antibody could be directed at soluble monomers or more aggregated species of Aβ (soluble or non-soluble). Induction of immunity after the exposure to Aβ peptide (full-length or a segment) by injection is instead called active immunization. Even if this procedure provides a prolonged antibody response, it has preceded more slowly than passive therapy due to the adverse effects and responses in elderly patients [143]. Nevertheless part of these studies is ongoing; some of the pipeline vaccines are able to induce an appropriate immune response to Aβ peptide with good tolerability and without dangerous side effects [141], [2].

Neurotrasmitter regulation is another relevant mechanism of action of the developing drugs. 30% of phase III- and 20% of phase II-agents [2] aim to either activate or inhibit some neuronal receptors implicated in AD pathogenesis and progression. Muscarinic and nicotinic receptors agonists as well as serotonin and histamine receptors antagonists are those currently under examination for their therapeutic potential [141].

Together with amyloid plaques, NFTs are the other pathological hallmark of AD affected-brains thus several approaches to target tau pathology have been developed in recent years. The adopted strategies work towards improvement in Tau protein homeostasis: inhibition of Tau aggregation, microtubule stabilization, reduction of Tau-phosphorylation and accumulation to avoid NFTs formation. Despite that, due to the essential role of microtubule dynamics in neuronal functioning, therapeutic Tau-targeting therapies are usually bound to fail [144], [145].

AD-affected brains are characterized by an altered cerebral functioning, where multiple molecular processes are compromised, such as neurotransmitter transmission, caspases activation, ROS production ect. New approaches that confer neuroprotection against the deleterious mechanisms prompting neuronal dysfunction are recently emerging. Multiple studies have revealed a decrease in Brain-derived neurotrophic factor (BDNF) levels in AD patients ([146] in addition to a drop in

Nerve growth factor (NGF) levels in mouse model of ageing [147] [148]. Both BDNF and NGF belong to the neurotrophins family, a group of growth factors and secreted proteins implicated in neuronal surviving, proliferation and differentiation. In addition NGF plays an important role in the maintenance of cholinergic neurons. Thus, the activation of BDNF signaling or the ex vivo NGF-gene delivery to AD patients are some examples of the more recent neuroprotective strategies adopted for dementia treatment [141], [149]. It is also well documented the association between oxidative stress and AD which have led to the introduction into the AD pipeline of therapies focused on the administration of antioxidants such as Vitamin A, C, B12, omega3 ect [150].
(for further information please visit clinicaltrials.gov)

4.3 Outcomes from Aβ-trials

Targeting Aβ is the most supported strategy to treat AD due to the centrality of the peptide in the initiation and progression of the neurodegeneration. Currently, the amyloid hypothesis addresses half of the agents currently in phase III. These drug-candidates should be either approved or rejected between 2016 and 2020; here's a summary of the Aβ-phase III outcomes that have already been published.
As mentioned before, Aβ-targeting therapies attempt to decrease the amyloid peptide levels in the brain by blocking the proteases activity involved in the APP-processing or by using passive or active immunization. The antibodies used to trigger an appropriate Aβ IgG response have recently been improved and newly tested as second generation vaccines. The goal has been to avoid the serious side reactions of the first generation vaccines, thus it has been designed a shorter Aβ peptide segments directed at the N-terminal end of the Aβ protein, which was supposed to contain a B-cell epitope while avoiding the T-cell activation so meningoencephalitis. Currently developing vaccines seem to have acceptable safety and tolerability, only one in nine agents is undergoing phase III study; it has reported to have good Aβ IgG response and no side effects.
As for the developing therapies based on passive immunization, there are currently three monoclonal antibodies against Aβ in phase III. The higher expectations were for the Eli Lilly & Co. EXPEDITION3 program, the phase III study designed to assess

the effect of the developing drug LY2062430 called solanezumab. It is the humanized analog of the murine antibody m266.2, whose mechanism of action differs from others N-terminal antibodies since it favors the peripheral Aβ clearance by altering the equilibrium of the native peptide between the central nervous system and periphery [151]. Solanezumab is a humanized monoclonal antibody that specifically binds soluble Aβ, in particular monomers. Phase I and II randomized, placebo-controlled studies confirmed its safety and tolerability in patients with mild to moderate AD. Magnetic resonance images and analysis on cerebrospinal fluids of AD sufferers did not show any abnormalities. However, 2 of the 4 subjects to whom was given given the highest concentration (10-mg/kg) of solanezumab reported asthenia. Previous AD-clinical trials - γ-secretases-targeting therapy and passive immunotherapies - have also reported asthenia as side effect. These symptoms could be related to a decreased concentration of the endogenous Aβ suggesting a putative physiological role of the native peptide. In phase III EXPEDITION 1 and 2 studies, 2052 people affected of mild to severe AD were recruited. Although the drug has continued to be safe, the overall EXPEDITION showed no improvement on the primary outcome measures ADAS-Cog11 and ADCS-ADL (Alzheimer's Disease Assessment Scale–Cognitive subscale (ADAS-Cog11) and Alzheimer's Disease Cooperative Study - Activities Of Daily Living (ADCS-ADL)). However, a subgroup of patient with mild AD displayed reduced cognitive decline after infusions of 400 mg of solanezumab once a month for 80 weeks [151]. Thus, the third phase of the EXPEDITION study started at July 2013 aiming to analyze the effect of the drug only in the group of mild AD. Unfortunately, in November 2016 Eli Lilli announced that Solanezumab missed primary endpoints of the trial leading to the withdrawal of the study. However, the Phase III study of the drug sponsored by Biogen is still ongoing. Aducanumab is a human monoclonal antibody against Aβ aggregates, including oligomers and fibrils. The drug was originally derived by the Neurimmune company (Switzerland) from healthy donor with good cognitive functions. A double-blind, placebo-controlled phase I randomized trial (PRIME) started in 2012 and 165 patients with prodromal or mild AD (Aβ positive to PET scan) were randomized and treated with increasing concentrations of aducanumab by intravenous infusions. The outcomes were positive: the drug is able to penetrate into the brain and reduce Aβ aggregates in a dose- and time-dependent fashion as measured by PET-scan. It has

good safety and tolerability with some side effects such as amyloid-related imaging abnormalities (ARIA), headache, urinary tract infection and upper respiratory tract infection [152]. Phase III began in August 2015 and it set to run until 2022.

Another promising phase III drug was a BACE inhibitor designed by Merck Company named Verubecestat (BIIB037). It is a small-molecule BACE1 inhibitor that have shown positive effects in reducing the celebrospinal fluid, plasma and brain concentrations of different isoform of Aβ, such as $A\beta_{1-40}$ and $A\beta_{1-42}$, in rats and monkeys after both acute and chronic treatment of the drug. Phase I study started in 2011, 78 patients with mild to moderate AD were recruited in order to test the safety and tolerability of the drug. Verubecestat was reported to have been generally safe and to have reduced the brain Aβ concentrations of AD sufferers. Phase II/III EPOCH study started in November 2012 with an initial recruitment of 200 mild-to-moderate AD patient then expanded to phase III with a total of more than 2000 participants. In February 2017, few months later the Eli Lilli announcement, Merck Company halted the EPOCH study for lack of efficacy. As reported by the website of the company: "Merck is stopping the study following the recommendation of the external Data Monitoring Committee (eDMC), which assessed overall benefit/risk during a recent interim safety analysis, and determined that there was virtually no chance of finding a positive clinical effect."

Recently, Axovant Company announced negative topline result of its Phase III MINDSET clinical trial. MINDSET study tested the therapeutic potential of the investigational drug intepirdine. It is a potent antagonist of the 5-HT receptor that promotes the release of acetylcholine in the brain. Despite the well tolerability, intepirdine do not improve the cognitive impairment of AD patients (http://investors.axovant.com/news-releases/news-release-details/axovant-announces-negative-topline-results-intepirdine-phase-3)

The failure of these three major clinical trials, together with the halting of past studies, adds the growing concern in the scientific community that the amyloid hypothesis may not be true, highlighting the necessity to reassess the centrality of Aβ in AD pathogenesis.

5. Reassessment of the amyloid hypothesis …or reconsideration of the Aβ role?

The amyloid hypothesis is the subject of the modern scientific debate because of the failures of Aβ-targeting therapies as well as some evidences that appear to undercut the centrality of the peptide in AD pathogenesis. As described before, the reduction or the tout court elimination of Aβ from AD-affected brains not only is ineffective to recover the cognitive impairment caused by the disease but also causes numerous side effects that led to the clinical-trials termination before the planned completion. The reasons underlying the lack of a successful therapy able to manage AD are likely due to the complexity of the disease that manifests itself at stages too far advanced to be able to restore the neurodegeneration. Indeed, some suggest that the disease is not targeted early enough, thus some clinical interventions are currently testing anti-Aβ drugs on elderly people who do not yet show symptoms of AD, such as cognitive impairment or dementia. The A4 study sponsored by Eli Lilly Company is an anti-Aβ AD trial that aim to test whether solanezumab can slow the progression of the disease in elderly people positive to amyloid pathology, measured by positron emission tomography (PET) imaging, but still asymptomatic. (ClinicalTrials.gov Identifier: NCT02008357). In addition, The DIAN and the API Colombia study have the purpose to analyze the effects of anti-Aβ treatments on pre-symptomatic elderly people at risk for familial AD [153]. Positive outcomes of these studies will validate the amyloid hypothesis; if they are not successful it will be necessary to rethink our approaches to the disease.

The key factor of the amyloid hypothesis is surely the Aβ peptide described as the primary trigger of the subsequent pathogenic events occurring in AD development, including Tau pathology. However, it is still unknown the biochemical pathway that links amyloid plaques to neurofibrillary tangles (NFTs) formation and how they are temporally involved in the disease progression. Tau pathology appears to be well correlated, both temporally and spatially, with neuronal loss and AD symptoms development than amyloid plaques [154]. Also, mutant tau transgenic mice display NFT-like neuropathology in absence of amyloid pathology. However, tau deposition is enhanced in double mutant (APP/Tau) transgenic mice whereas the development of amyloid deposition takes place at the same age of the parental strain (Tg2576

hAPP transgenic mice) [155]. Moreover, injection of a synthetic Aβ preparation into the brain of mutant human Tau–expressing mice led to a marked increase in neurofibrillar tangles [144]. Although the spreading of amyloid plaques does not precisely correlate with the neurodegenerative symptoms of AD, the genetic evidences strongly support Aβ as a fundamental toxic element in the disease initiation. The familial form of the disease is caused by mutations in genes involved in Aβ production, such as APP, PS1 and PS2 [156]; moreover Down syndrome patients with an extra copy of the APP gene develop age-related dementia and plaques deposition [157]. An assumption of the amyloid hypothesis is that Aβ is just an accident of APP metabolism and its production is a pathological process, not physiological. So far the scientific community has been focused on the toxicity of the amyloid peptide, discarding the idea that Aβ may have a potential biological function(s) during normal conditions. APP is early expressed during development [158] and Aβ is also physiologically produced by the brain since the very beginning of embryonic life in mammals and continues for the whole life of the organism [159]. Taking advantage from the microdialysis technique, it has been possible to measure the *in vivo* levels of Aβ; it is found to be at picomolar concentrations in human healthy brain as well as in the interstitial fluids (ISF) of wild-type mice [160], [112]. Interestingly, by simultaneously measuring the electroencephalographic (EEG) activity and ISF Aβ levels in the hippocampus of Tg2576 mice, Cirrito and colleagues were able to demonstrate a correlation between Aβ brain concentration and synaptic activity [160]. The amyloid levels in ISF are dynamically regulated indirectly by neuronal activity, that control the APP cleavage operated by BACE enzyme [161] and directly by synaptic activity, which also mediates the APP endocytosis [162]. Thus, brain activity physiologically regulates the level of the peptide in the ISF allowing an overall low Aβ concentration that is maintained over time and may be involved in normal brain physiology. Aβ synaptic modulation might be interpreted as a defense mechanism by which neurons prevent the toxic effects caused by the oligomeric form of the peptide at high concentrations. This is likely true in the light of the dose-dependent effects induce by Aβ. It is indeed proposed a negative feedback regulation of neuronal activity that rely on Aβ production and that could have a role in brain homeostasis maintenance [161]. This suggestion supports a biological function of

endogenous Aβ that could clarify why the absence or the reduction of native Aβ causes abnormalities and side effects both in humans and rodent [159].
It is therefore essential to reassess the role of endogenous Aβ in light of the evidences towards a possible physiological function of the peptide. This may help to clarify the sequence of the major pathological events involved in AD development and so to design successful treatments able to manage the disease.

6. Aβ trophic effects

Since Aβ is physiologically produced and released in the brain ISF during development, adulthood and aging [163], it may play a biological function in healthy conditions. Growing evidences push towards a modulatory role of Aβ at low concentrations on synaptic plasticity acting as a negative feedback signal to maintain the brain activity within a normal range. Kamenetz and colleagues were the first to propose a feedback loop regulation between neuronal activity and APP processing. By using organotypic hippocampal slices from APP-transgenic mice, they demonstrated that neuronal activity regulates Aβ production by controlling the level of BACE cleavage. Moreover, Aβ synthetized by APP overexpressing neurons depresses the synaptic activity of neighboring cells. Thus, increased neuronal activity produces more Aβ enhancing the APP-endocytosis [160] or APP-processing through BACE1 cleavage. High level of Aβ depresses the synaptic function leading to a drop in neuronal activity [161]. The impairment of synaptic functions caused by high levels of Aβ is well known and characterized, both *in vivo* and *in vitro* [93]. However, recent works suggest that low concentrations of Aβ could act as a positive regulator at synaptic level. Indeed, wild-type hippocampal slices perfused with 200 pM of $A\beta_{42}$ for 20 minutes show an enhancement of LTP that is reported to be dependent on the increase of transmitter release during tetanus [164]. Also, addition of 200 pM $A\beta_{42}$ rescue the LTP depression caused after APP suppression by siRNA or using anti-Aβ antibody suggesting a fundamental role of Aβ in LTP induction [165]. The Aβ-dependent enhancement of synaptic plasticity and memory [166] appears to be mediated by α7-containing nicotinic acetylcholine receptors (α7-nAchRs) [164], [165] which is in line with the finding that Aβ might directly bind α7-nAchRs with picomolar affinity [167]. Thus, controlling the concentration of Aβ is essential to modulate the effects triggered by the peptide on neuronal activity. Aβ aggregation is a concentration-dependent process that might be avoided decreasing the neuronal activity responsible for its production. Indeed, the brain ISF levels of Aβ are modulated not only during pathological conditions such as following hippocampus electrical stimulation [159] but also during physiological conditions, such as sleep-wake cycle [108]. It has been reported an increase of ISF Aβ levels following sleep deprivation in human APP transgenic mice; furthermore individuals with sleep

fragmentation have higher risk to develop AD compared to individuals with regular sleep [168]. Periods of wakefulness are usually associated with an increase in synaptic strength whereas periods of sleep are associated to a decrease in synaptic strength [169]. Aβ fluctuations might have a role in this phenomenon since relatively small increases in endogenous Aβ amount, enhanced the release probability of synaptic vesicles and increased neuronal activity in neuronal cultures [170].

Depletion of endogenous Aβ significantly reduced the cell viability of rat cortical neurons treated with secretase inhibitors or antibody against Aβ; however low concentrations of Aβ, ranging from 10 pM to 1 nM, rescue the toxic condition in a concentration dependent manner suggesting a crucial role of the peptide in neuronal survival [171]. In the same way, it has been demonstrated a neuroprotective role of monomeric Aβ under conditions of trophic deprivation as well as during excitotoxicity. This neuroprotective action was mediated by the activation of the PI-3-K (phosphatidylinositol-3-kinase) pathway, and involved the stimulation of IGF-1 (insulin-like growth factor-1) receptors [172].

Some recent studies underlie a role of Aβ in neurogenic processes both in the embryo and in the adult brain. Both $A\beta_{1-40}$ and $A\beta_{1-42}$ seem to have a trophic function on neural stem cells (NSCs). NSCs are present in the adult human brain only in two regions: the subventricular zone (SVZ) and the subgranular layer of the dentate gyrus in the hippocampus. In vitro experiments performed on rat NSCs show that $A\beta_{1-42}$ can directly induce neuronal differentiation without affecting cell viability or proliferation [173]. Another work was published asserting that Aβ can lead mouse NSCs differentiation and proliferation, but only in its oligomeric form [174]. Thus, the precise effects of Aβ on NSC are not yet clear as the experimental conditions vary too much between studies. It is possible that both the isoform of the peptide -monomers and oligomers- act as pro-differentiating elements but during different conditions, physiological or pathological, in order to allow the insertion of newborn neurons into the network. In light of this, amyloid plaques formation might be a compensatory mechanism of the brain by which Aβ would be trapped into aggregates in order to decrease its concentration. This might explain the presence of amyloid plaques in brains of older people with no signs of cognitive impairment or dementia symptoms [159].

Based on these data, Aβ appears to be a physiological peptide normally produced by the brain. It may induce negative or positive effects depending on its concentration, which is finely regulated by neuronal activity and follows circadian rhythms. Although the oligomeric form is well known to have neurotoxic effects, it is suggested that low concentrations of Aβ could modulate neuronal homeostasis in healthy conditions acting on synaptic functions as well as neuronal survival.

Aims of the work

So far the amyloid hypothesis has mainly driven the AD drugs development; however most of the anti Aβ-clinical trials have been suspended due to the lack of significant cognitive improvements as well as to the side effects caused in AD patients in some studies. Although the negative outcomes of β- and γ-secretases targeting therapies are reasonable explained by the significant biological functions covered by such proteases, the reason Aβ-centric therapies fail is still unclear. Thus, to design a successful therapy for AD it is therefore crucial to uncover the role of soluble endogenous Aβ in the healthy brain. Even though the amyloid peptide has been extensively studied because of its association to AD, its physiological function(s) is now being studied in much more detail (see paragraph "Aβ trophic effects" for details).

My thesis work is part of the recently emerging idea that Aβ – at low concentrations - is not just a toxic waste product of the brain but it might be a relevant element involved in the maintenance of neuronal network homeostasis.

Our final goal is therefore to explore the effects of the monomeric $A\beta_{1\text{-}42}$ peptide on excitable cells.

First, we aim to assess the effects of monomeric Aβ on the excitability of immature cortical neurons. Starting from a preparation of pure monomers, the aggregation of the peptide as well as its impact on neuronal functioning is dependent on the monomers concentration. We intend to evaluate the effects of different concentrations of Aβ on neuronal activity, looking for a concentration threshold at which the peptide switches from being trophic to toxic.

Among its several actions, it has been found a pro-differentiating role of Aβ on Neuronal Stem Cells (NSC). Since we use immature neurons as model system, we subsequently aim to analyze whether monomeric Aβ affects the developing process of these cells, in particular the electrical maturation and how it affects the neuronal morphology.

Whether they are toxic or trophic, the overall Aβ effects converge towards an altered communication among nerve cells. Indeed, it is well described a toxic effect of Aβ at synaptic terminals but little is still known about the effects of monomers. It is

intriguing to think that also the monomeric form of the peptide may have a role at synapses as modulators of the communication among neurons. Thus, we finally plan to investigate the synaptic alterations induced by the monomeric form of Aβ on juvenile neurons focusing on excitatory synapses since they are more sensitive to Aβ levels than inhibitory synaptic connections.

Materials and Methods

Electrophysiology

Patch clamp recordings were collected using an Axopatch 200B amplifier (Molecular Device, CA, USA) and Digidata 1322 acquisition system. Analog-to-digital converter signals were digitized at 5 kHz and filtered at 1 kHz. Patch electrodes (GB150F-8P with filament, Science Products) were pulled from hard borosilicate glass on a Brown-Flaming P-87 puller (Sutter Instruments, Novato, CA, USA) and fire-polished to a final electrical resistance of 5-7 MΩ.

Whole-cell, patch-clamp recordings were performed at room temperature on primary cortical neurons ranging between 4 to 18 DIV. The composition of the extracellular solution was: (in mM) 138 NaCl; 4 KCl; 2 CaCl2; 1.2 MgCl2 ; 10 HEPES; 10 D-glucose (pH 7.4 – osmolarity adjusted to 300 mOsm with NaOH).

The composition of the intracellular solution was (in mM): 126 K-gluconate, 4 NaCl, 0.05 CaCl2 , 0.1 EGTA, 10 HEPES, 10 D-Glucose 1 MgCl2 , 3 mM ATP-Mg^{2+} , 0.1 mM GTP-Na^{+} (pH 7.2; osmolarity adjusted to 270 mOsm with KOH). After forming a tight seal (>1 GΩ) and entering the whole-cell configuration in voltage-clamp mode, the amplifier was switched to current clamp mode. The resting membrane potential (Vm) was first measured and only cells with Vm more negative of -50 mV were considered. In all data sets performed, pipette-capacity, whole-cell capacity and series resistance were compensated before each protocol whereas the liquid junction potential was not corrected.

Current-clamp recordings: To elicit action potentials (APs), neurons were held at -60 mV and stimulated with depolarizing current injections of 800 ms duration and amplitude ranging from 10 pA to 100 pA. To assess individual AP waveforms at 4 DIV, the first spike fired at 80 pA current injection was analyzed, as at 80 pA of current injection all cells fire. AP width was measured from the threshold as the width at half-amplitude. The half-width value was calculated considering the AP width measured at 50 % of the peak amplitude. AP threshold was determined by analyzing phase plots as the voltage (mV) at which dV/dt surpassed 5 mV. The criterion for spike threshold was set at 5 V/s because this is just above the maximal level of dV/dt obtained by our noise injection when action potentials were not

initiated. AP amplitude was calculated from the holding potential (Vh) of the cell to the peak of the AP.

Voltage-clamp recordings: Inward sodium currents (INa) were elicited by delivering a series of depolarizing voltage steps (from −80 to +60 mV in 20 mV increments, 800 ms duration) from an holding potential of −70 mV. INa^+ was estimated by analytical subtraction of ionic current after addition of Tetrodotoxin (TTX; 0.3 μM) (Tocris) from the total current of the cell. Potassium currents (fast transient K current named IK_A and delayed rectifier K current named IK_V) are evoked by voltage steps from different Vh (-80 mV or - 40 mV) to -5 mV; 2000 msec duration. Briefly, IK_V was evoked by a voltage step from – 40 mV (where IK_A channels are already inactivated) to - 5 mV. The total outward current (which is composed by both IK_A and IK_V) was recorded by a voltage step from -80 mV to -5 mV. IK_A was isolated by analytical subtraction of IK_V from the total potassium current (IK_A + IK_V) recorded in the same cell (Fig. 6A). IK_V was measured at the end of the waveform voltage step whereas IK_A was measured at the peak current of the test step. Both INa and IK values were reported as pA not normalized as

Spontaneous excitatory postsynaptic currents (sEPSCs) recordings were performed in voltage-clamp mode by adding Gabazine (5 μM, Tocris) to the extracellular solution. The Vh was kept at -70 mV and the each recording recordings lasted >1-5 minutes. The detection level for sEPSCs analysis was set at 5 pA. Analysis of sEPSC frequency, amplitude, rise/decay time and area was performed offline by Clampfit 9.2.

All data analysis was performed offline with Clampfit 9.2 (Molecular Device, CA, USA) or Origin 9.1.

$A\beta_{1\text{-}42}$ Depsi-peptide

$A\beta_{1\text{-}42}$ Depsi-peptide was kindly provided by IRCSS-Mario Negri Institute for Pharmacological Research, Milan. $A\beta_{1\text{-}42}$ Depsi-peptide is obtained through solid phase protein synthesis (SPPS) which allows the formation of an ester binding between the hydroxyl group of serine 26 and the subsequent glycine. The monomeric form of the peptide is maintained at acid pH and -80°C for several months preventing the self-aggregation. The $A\beta_{1\text{-}42}$ native form is obtained as pH is switched to neutral allowing a time and concentration-dependent aggregation of the peptide.

To properly obtain the native form of $A\beta_{1-42}$ we switched the pH of the suspension buffer (distilled H_2O) by diluting the Depsi-peptide solution (initial concentration depends from the synthesis process) in 1X DPBS w/o Mg^{2+} and Cl^- to a concentration of 100 μM and subsequently diluted in neuronal culture medium at the desired final concentration (10 nM, 100 nM, 500 nM). 4 DIV neurons were treated the day after the dissection (1 DIV) whereas 7 DIV neurons were treated at 4 DIV; in both cases neurons was treated with Depsi-peptide for 72 hours and the culture medium was not replaced during the treatment period.

Primary cultures of cortical neurons

Cultured cortical neurons were isolated by CNR - Institute of Neuroscience, Milan [175] and were prepared from rat embryos at gestational age 18 days (E18) and plated in 12-well at a density of 75'000 cells/well on glass cover slips treated with L-Polylysine (50 μg/ml). Cultures were grown at 37°C with 5% CO2 in Neurobasal Medium supplemented with 2% B27, 0,25% L-glutamine, 1% Penicillin/Streptomycin and 0,125% glutamate for 4 days. At the fourth day in vitro (4 DIV), 500 μl of culture medium was substituted with 400 μl of fresh medium without glutamate and cultures were grown until 7, 11 or 18 DIV.

Treatments

For experiments on 4 DIV neurons, cells were treated at 1 DIV with $A\beta_{1-42}$ at different concentrations (10 nM, 100 nM, 500 nM) for 72 hours. For experiments on 7 DIV neurons, cells were treated at 4 DIV for 72 hours with 10 nM $A\beta_{1-42}$. During the $A\beta_{1-42}$ treatment period the culture medium was not replaced. For sEPSC recordings, 1 μM TTX, 50 μM D-2-amino-5-phosphonovalerate (APV) or 1 mM Mg^{2+} were added to the medium of both control neurons and 10 nM $A\beta_{1-42}$- treated neurons at 4 DIV. Patch clamp recordings of sEPSC were done at 7 DIV. The regular extracellular solution was used to eliminate TTX, APV or Mg^{2+} from the culture, it was subsequently used with the addition of Gabazine to record sEPSC.

Cell viability assay

Neuronal viability was assessed using the 3-(4,5-dimethylthiazol-2-yl)-2,5-diphenyltetrazolium bromide (MTT) assay (Sigma Aldrich). Cortical neurons were cultured in 12-well at the density of 75'000 cells/well and incubated at 1 DIV with 10, 100 or 500 nM $A\beta_{1-42}$. 4 DIV untreated and $A\beta_{1-42}$-treated neurons were first washed with Phosphate Buffered Saline (PBS) 1x and then incubated with MTT 100 ng/ml (Sigma) dissolved in PBS 1x. The cells were then incubated for 90 minutes at 37°C. After MTT treatment, the supernatant was removed and the cells were lysed in DMSO. The absorbance was measured at 570 nm and 630 nm as a reference wavelengths (to measure cell debris) using Ultrospec 3000 (Pharmacia Biotech) spectrophotometer. All experiments were performed in duplicate. The cell viability of each treatment was expressed as percentage of the control.

Transfection

In order to obtain low-density fluorescent neurons for the analysis of the total dendritic length, neurons were transfected with an empty pLVTHM plasmid expressing EGFP using Lipofectamine 2000. To transfect 75'000 cells a mix of 1.5 µg DNA + 200 µl Neurobasal was prepared and vortexed. 3 µl Lipofectamine 2000 were added and the mix was stirred using vortex. After 15 minutes at room temperature, the mix was added to neuronal cultures and left for 45 minutes at 37°C. The culture medium was previously substituted with 1 ml fresh Neurobasal supplemented with conditioned medium (800 µl + 200 µl respectively). After 45 minutes, the entire medium was removed and 1 ml of conditionated medium was added to each well. Neurons were then kept at 37°C with 5% CO2. Cells was transfected at 3 DIV or 6 DIV then fixed at 4 DIV or 7 DIV respectively to make the total dendritic length analysis.

Immunocytochemistry

4 DIV and 7 DIV neurons were fixed with 2% paraformaldehyde plus 2% sucrose at room temperature for 8 minutes and washed in PBS three times. Then, samples were mounted on glass slides with Mowiol. Slides were observed under LSM510 META

confocal microscope (Carl Zeiss) using a x40 objective. Samples were excited at 488 nm and recorded at 515-550 nm wavelengths. Images were elaborated with Zeiss LSM 510 Image Examiner software. Dendritic length was measured by tracing dendrites from the soma center, which was set at zero. Sholl analysis was made to measure the total dendritic length for each neuron. Series of circles with increasing gradii centered at the soma were generated and the length of the dendrites within each subsequent radial bin at 10 μm increments was summed. The dendritic length analysis was performed using NeuronStudio (CNIC) software.

Western Blotting

Cells samples (12-well) at 7 DIV were lysed in ice-cold RIPA buffer (NaCl 150 mM, Tris 50 mM, EDTA 1 mM, NP40 1%, Triton 1%) plus protease inhibitors cocktail. After gently shake for 20 min at 4°C, samples were centrifuged at 13000 g for 2 min (RT). Lysates were kept at – 80°C until use. Protein concentration was assessed by Pierce BCA protein assay kit (Thermo Fisher). Complete lysis of the cells was obtained by 30 minutes of incubation in Lysis Buffer at 60°C. The same amount of proteins for each sample was loaded onto a 10% SDS-polyacrylamide gel electrophoresis (PAGE) under reducing conditions; resolved proteins were transferred onto Nitrocellulose membranes (GE Healthcare) of 0,2 μm pore size into a transfer buffer (glycin 1%, tris-base 0,02 M, methanol 20%) to which is applied a constant voltage.

Membranes were first incubated for 1 hour at RT with 5% milk in PBS-0,02% Tween (TBST) on the oscillator to block non-specific binding sites. Subsequently, proteins of interested were probed with the primary antibody (diluted in TBST) for 1 hour at RT and revealed by secondary antibody conjugated with infrared-emitting fluorophores. Signals were detected and quantified using an Odissey scanner (Li-Cor) controlled by the ImageStudio software (Li-Cor).

The primary antibodies used were: Spectrin, 1:500, α-rabbit (Cell Signaling), GAPDH, 1:10000, α-mouse (GeneTex Inc.). The secondary antibody used was α-rabbit and α-mouse Li-cor Odissey 1:7500.

Analysis

Data are reported as mean ± S.E.M (Standard error of the mean). Significance was taken at $p<0.05$ using unpaired two-tailed Student's t-test, one-way ANOVA, two-way ANOVA. Data for the total dendritic length (Fig.8; Fig.14) and sEPSC parameters comparison (Fig. 13; 16) were evaluated by two-way ANOVA (factors: DIV x $A\beta_{1-42}$ treatment for Fig.8; TTX x $A\beta_{1-42}$ treatment for Fig. 14 and 13; NMDA-deprived condition x $A\beta_{1-42}$ treatment for Fig.16). Cumulative probability distribution of sEPSC was tested for significance with a two-tailed Kolmogorov-Smirnov test and significance was defined as $p<0.0001$. Statistical analysis was performed using PRISM 4.0 software (Graph-Pad San Diego, USA).

Results

Accumulation of Aβ in the brain as soluble and insoluble aggregates is central to the pathogenesis of AD [33]. For this reason, most of the studies have mostly analyzed the pathological outcomes triggered by Aβ on neuronal transmission and synaptic plasticity. To date, little is known about the physiological role(s) of monomeric Aβ; however, emerging evidences have reported an activity-dependent production of Aβ [160] strongly supporting a biological function of the peptide [176]. The main purpose of my research thesis is to explore the effects induced by monomeric Aβ, in its physiological form and concentration, on neuronal excitability.

$A\beta_{1-42}$ Depsi-Peptide assembly under culturing conditions

As previously described, Aβ is found in human and murine brains (both healthy and AD suffering) at low concentrations ranging from picomolar to nanomolar [111], [112], [113], [177]. Due to the instability of its "intrinsically unfolded" structure, the monomeric form of Aβ tends to aggregate at high temperatures in a concentration-dependent manner [178]. Thus, the main problem using synthetic amyloids is to control the conformational state of the peptide during the study. In our investigations, we used the $A\beta_{1-42}$ Depsi-peptide which is a synthetic peptide designed to obtain pure solutions of monomers, in their native structure, or oligomers. After switching the pH of the buffer where the peptide is suspended, it is possible to choose the conformational state of Aβ by setting its incubation time (see methods). The suspension buffer of $A\beta_{1-42}$-Despsi peptide is distilled water subsequently diluted in PBS 1X solution, thereby avoiding possible toxic effects on neuronal properties caused by others commonly used solvents such as DMSO. Furthermore, the low propensity to aggregate due to its high solubility [179], make the $A\beta_{1-42}$ Depsi-peptide an ideal tool to study the monomeric form of Aβ. We are currently running experiments to test the conformational state of our $A\beta_{1-42}$ Depsi-peptide monomeric preparation by Surface Plasmon Resonance (SPR) experiments. Increasing concentrations of monomeric $A\beta_{1-42}$ Depsi-peptide (10 – 100 – 500 nM) were incubated for 72 hours at 37°C, the proper growth temperature for cells, and SPR analysis was made on these samples. Preliminary experiments suggested that

monomeric amyloid solution, diluted in Neurobasal medium, does not aggregate after 72 hours of incubation at 37°C (data not shown). Using the Atomic Force Microscopy technique, we are planning to assess more accurately if there is a population of oligomers in our solution that cannot be detected by SPR.

Monomers of $A\beta_{1-42}$ Depsi-petide are not toxic for primary cortical neurons

Aβ production and accumulation is mostly restricted in the "default-mode network", a set of highly active brain regions that also include several cortical areas. As model system we therefore used cortical neurons from 18 days rat embryos. We tested the monomeric preparation of Aβ 1-42 Depsi-petide on neurons at 4 DIV, a very early stage of neuronal maturation. These cells have not yet formed an interconnected network and display immature electrical properties. Moreover, no signs of neuritogenesis or neuritic spines are evident at this stage of maturation as previously demonstrated [180]**.** Thus, 4 DIV neurons are a suitable model to examine a direct effect of the monomeric solution of $A\beta_{1-42}$ Depsi-petide ($A\beta_M$) on the electrical properties of isolate neuronal cells. The levels of monomeric Aβ are dynamically regulated by spontaneous activity, varying along brain areas [160]. Since Aβ aggregation is a concentration-dependent process and oligomers have been reported to be toxic for neurons [97]–[99], [181], the effects elicited by the Aβ peptide are

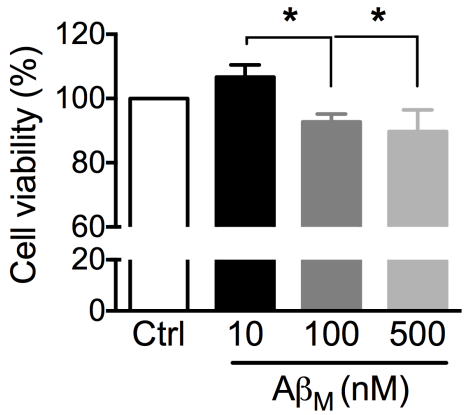

Figure 1 - Slight alteration of neuronal viability following $A\beta_M$ treatment at 4 DIV

Rat cortical neurons were incubated with 10 nM, 100 nM and 500 nM of $A\beta_M$ for 72 hours. Monomeric Aβ was added to the medium at 1 DIV. After 72 hours, cell viability tends to increase in neurons incubated with 10 nM $A\beta_M$. Data are expressed in percentage of control and represent the mean percentage of basal viability ± standard error of three independent experiments, with duplicate samples. $A\beta_M$ 10 nM 106.6 ± 3.79; Aβ 100 nM 92.76 ± 2.38; $A\beta_M$ 500 nM 89.71 ± 6.75. *P<0.05 one-way ANOVA ($F(3,8)=3.504$, $p=0.0693$ followed by Fisher's post hoc test (10 nM vs 100 nM P=0.0418, 10 nM vs 500 nM P= 0.0184)

therefore dependent on its amount in the brain ISF. We therefore decided to test different concentrations of the peptide based on previous in vitro studies on brain slices and dissociated cells in which Aβ level ranges from pM to μM concentrations. In our experiments, the lowest $A\beta_M$ concentration used was 10 nM, a value close to that measured in normal and AD-affected brains [111], [112], [113], [177] whereas the highest concentration used was 500 nM that resemble the Aβ concentrations commonly used in most of the scientific works focused on AD. To assess whether the $A\beta_M$ solution was neurotoxic, we first treated 4 DIV neurons with serial dilutions of $A\beta_M$ (10, 100, 500 nM) for 72 hours and determined the cell viability by MTT assay (Fig.1). Treatment with the lowest $A\beta_M$ concentration tested, 10 nM, has slightly increased cell viability compared to control group and it is significantly different from the viability of cells treated with highest concentrations of $A\beta_M$ (*$P<0.05$, One-way ANOVA). Consistent with previously finding [182], no significant toxic effect on neuronal viability was seen in neurons treated with both 100 nM and 500 nM $A\beta_M$ (Fig. 1).

Concentration-dependent effects of $A\beta_M$ on neuronal excitability of 4 DIV immature neurons

Next, we monitored the neuronal excitability of 4 DIV control and $A\beta_M$ -treated cells by whole-cell patch-clamp recordings. To measure the firing rate, the resting membrane potential of the cells were held (Vh) at -60 mV and increasing pulses of depolarizing current (from 10 to 100 pA, 800 ms duration) were delivered. This protocol allow us to elicit the first action potential (AP) as well as the maximal activity achievable by the cells. Fig. 2A shows the electrical activity achievable by example

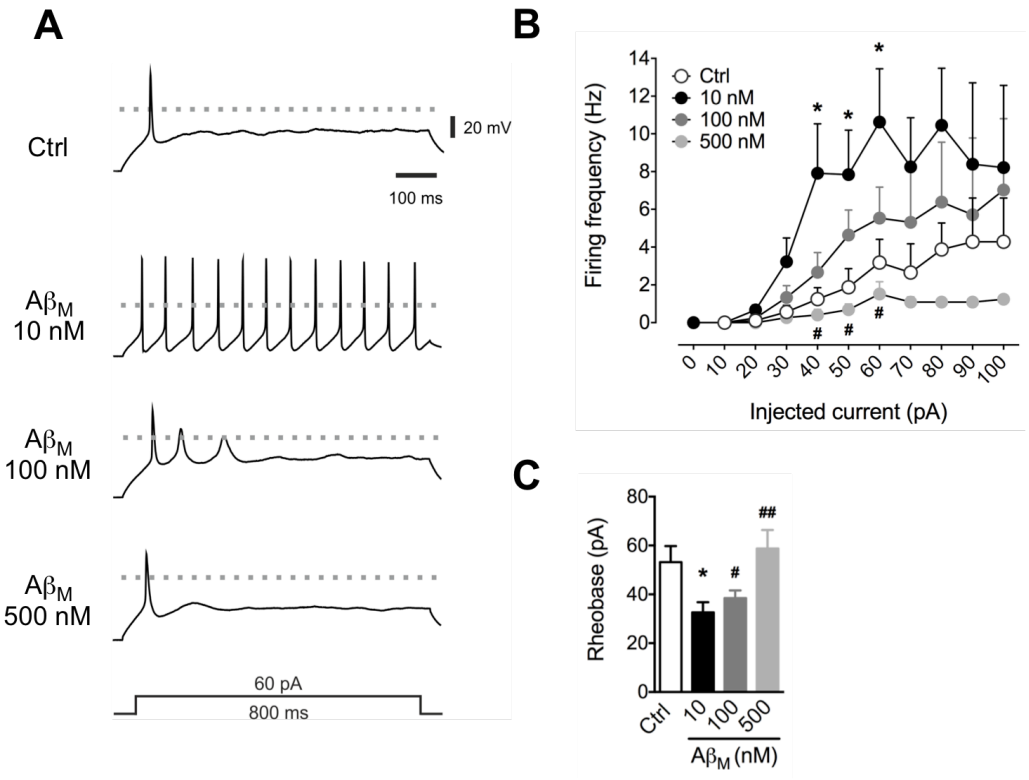

Figure 2 - $A\beta_M$ alters the electrical activity of primary cortical neurons at 4 DIV

The electrical activity of 4 DIV untreated and $A\beta_M$-treated neurons was monitored by whole-cell patch-clamp technique in current-clamp mode. **A.** Representative traces recorded from 4 DIV untreated and $A\beta_M$-(10 nM, 100 nM, 500 nM) treated neurons showing their evoked firing activity in response to 60 pA current injection. Dashed lines represent 0 mV **B.** Firing frequency as a function of injected current in untreated cells (white) and neurons treated with increasing concentrations of $A\beta_M$ (10 nM black; 100 nM dark grey, 500 nM light grey). *P<0.05 vs Ctrl $^{\#}$P<0.05 vs 10 nM; unpaired t-test for the individual steps of current. **C.** Rheobase values are significantly lower in neurons treated with 10 nM $A\beta_M$ compared to those treated with 100 nM and 500 nM $A\beta_M$ as well as to untreated neurons (*P<0.05 vs Ctrl; $^{\#}$P<0.05 vs 10 nM unpaired t-test)

cells from the four groups analyzed at 60 pA of current injection. Control cells at 4 DIV were limited in their ability to generate APs displaying an immature firing pattern with a low frequency. Conversely, cells treated with 10 nM $A\beta_M$ fire much more rapidly compared to untreated neurons. However, treatment with 500 nM $A\beta_M$ did not increase the excitability of the cells, which display instead an electrical behavior comparable to that of control neurons. Treatment with 100 nM $A\beta_M$ has raised the firing frequency compared to control values but the effect was less pronounced than in neurons treated with 10 nM $A\beta_M$. Despite the Rm was equal in all groups analyzed (see Table 1), we observe that the rheobase value, which is the minimum current for infinite duration at which the cell generates an AP, was significantly lower in neurons treated with 10 nM $A\beta_M$ compared to untreated cells (*$p<0.05$) (Fig. 2C). In fact, the current that must be injected to the cells in order to generate the first AP increases with increasing concentration of $A\beta_M$ (Fig.2B). This result suggests that 72 hours treatment with 10 nM $A\beta_M$ makes neurons more excitable than both control cells and neurons cultured with higher concentrations of $A\beta_M$ peptide. Indeed, during step depolarizations (Fig. 2B), the firing frequency of 10 nM $A\beta_M$-treated neurons increased markedly relative to the firing rest of control cells, but only at current values near to the rheobase (from 40 to 60 pA) (Fig.2B). The firing frequency of the

four groups was identical up to 30 pA and started to increase in 10 nM $A\beta_M$-treated neurons above 40 pA. At 60 pA, untreated cells (n=11) had a mean maximal frequency of 3.18 ± 1.23 Hz compared to 10.62 ± 2.83 Hz in neurons cultured with 10 nM $A\beta_M$ (n=12) (*$P<0.05$ vs Ctrl). As suggested by rheobase values, there is an inverse correlation between $A\beta_M$ concentration and excitability. The firing frequency reached maximal values (from 8 to ~10 Hz) in 10 nM $A\beta_M$-treated neurons and decreased when neurons were cultured with higher concentrations of the Aβ peptide. At 60 pA, the firing frequency varies between 5.53 ± 1.65 Hz in 100 nM $A\beta_M$ neurons and 1.53 ± 0.651 Hz in 500 nM $A\beta_M$ neurons (#$p<0.05$ vs 10 nM $A\beta_M$), which is very close to the basal frequency of 4 DIV control neurons (3.18 ± 1.23 Hz) (Fig. 2B). By analyzing the cells able to generate a burst of APs, we observed an increase in the number of spiking neurons treated with both 10 nM and 100 nM $A\beta_M$ with respect to control cells and this phenomenon did not occur at 500 nM $A\beta_M$ (Percentage of

spiking neurons: Control cells 25% n=24; treated with ($A\beta_M$) 10 nM 55% n=20, 100 nM 53% n=17, 500 nM 22% n=9, data not shown).

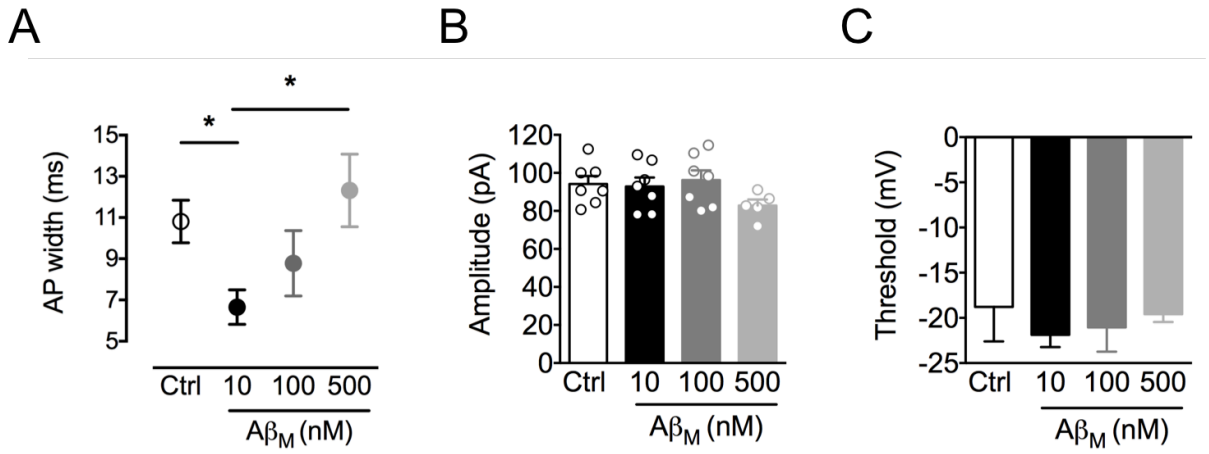

Figure 3 - $A\beta_M$ alters AP waveform in 4 DIV neurons

A. The width of the first AP elicited with 80 pA current injections was measured in 4 DIV untreated and treated neurons with 10, 100, 500 nM $A\beta_M$. The plot shows a direct correlation between AP width and $A\beta_M$ concentration. Control 10.8 ± 1.03 ms n=17; 10 nM $A\beta_M$ 6.6 ± 0.84 ms n=10; 100 nM $A\beta_M$ 8.8 ± 1.6 ms n=7; 500 nM $A\beta_M$ 12.3 ± 1.7 n=10 *$p<0.05$; one-way ANOVA followed by Fisher post hoc test. Circles indicate average values of AP width, bars indicate SEM **B.** AP amplitude was measured from the Vh to the peak of the AP, no significant differences were observed between the four conditions. **C.** Mean values of the spike threshold measured in the phase/plot. Values were taken as when dV/dt surpassed 5 mV/ms.

$A\beta_M$ treatment of immature cortical neurons results in the reduction of the AP width.

The increased excitability of cortical or hippocampal circuits of Aβ overexpressing mice is a well reported phenomenon [127], [134], [131], [126]. These studies has been carried out on brain slices of young (from 5–7 [127] weeks old to 8–9 month old mice [131]) or adult (20–23 month old [126], [134]) transgenic mice in order to explore possible alterations in the intrinsic excitability properties. However, in rodent, an overall maturation of the brain structures and synaptic density is completely achieved at the end of the first month after birth (for review [183]). The increase in the firing activity observed in Aβ overexpressing mice [127], [131], [132] points towards hyperexcitability and correlates with the high incidence of seizures in AD sufferers

Table 1 - Summary of RMPs and AP parameters measured in untreated and $A\beta_M$-treated neurons at 4DIV

	Ctrl	10 nM $A\beta_M$	100 nM $A\beta_M$	500 nM $A\beta_M$	F	P value
RMP (mV)	- 60.57 ± 1.06 n= 23	- 63.2 ± 0.98 n= 19	- 60.2 ± 1.04 n= 9	- 63.67 ± 1 n= 9	(3,56) 2.25	0.092
AP width (ms)	10.81 ± 1.03 n= 10	6.66 ± 20.84 n= 17	8.78 ± 1.58 n= 7	12.32 ± 1.76 n= 10	(3,40) 4.65	0.007
Amplitude (pA)	94.19 ± 4.12 n= 7	92.82 ± 4.72 n= 7	96.21 ± 5.14 n= 7	82.83 ± 3.15 n= 5	(3,22) 1.44	0.257
Treshold (mV)	- 18.79 ± 3.82 n= 7	- 21.87 ± 1.36 n= 7	- 21.06 ± 2.68 n= 7	- 19.6 ± 0.86 n= 5	(3,22) 0.29	0.833

RMP and AP parameters were calculated for untreated and neurons treated with 10 nM $A\beta_M$, 100 nM $A\beta_M$, 500 nM $A\beta_M$ at 4 DIV. Values are expressed as mean ± SEM. *p<0.05, one-way ANOVA

[122], [184]. Conversely, the cortical neurons used in our experiment were obtained from rat embryos at E18, a stage of development in which the membrane properties are still immature [185]; in fact the cells begin to mature electrically in the very early postnatal period instead embryonically [183]. Thus, the increased firing activity resulting in 10 nM $A\beta_M$ treatment might be an early sign of the electrical maturation of the neurons. To better explore how the electrical properties of the cells were altered, we analyzed some basic characteristics (duration, amplitude and threshold) of the first AP generated in response to 80 pA of current injection (Table 1). As shown in Fig. 3A, cells cultured with 10 nM $A\beta_M$ showed narrower APs with decreased width values relative to control cell. On the contrary, higher concentrations of the peptide (100 nM, 500 nM) did not significantly reduce the AP duration compared to that recorded in untreated neurons (Fig.3A). The amplitude of the first AP was also measured. As shown in Fig.3B, the mean AP amplitude was between 80 and 95 mV in all groups and did not show any changes after $A\beta_M$ treatment at different concentrations (10, 100, 500 nM). There was also no significant difference in AP threshold between untreated cells and neurons treated with increasing concentrations of $A\beta_M$ (Fig.3c). In addition, changes induced by $A\beta_M$ on neuronal excitability were not associated with modification of the resting membrane potential (RMP), which was unaffected in all the conditions analyzed (Table 1).

Firing pattern maturation of 4 DIV neurons treated with 10 nM $A\beta_M$

We observed a concentration-dependent effect induced by $A\beta_M$ treatment on neuronal excitability of immature neurons at 4 DIV (Fig.2). Neurons cultured with 500 nM $A\beta_M$ displayed a discharged firing pattern that was very similar to that recorded in 4 DIV control neurons. This is possibly due to an early aggregation of $A\beta_M$ in oligomers that are known to impair neuronal functioning [97]. Conversely, the chronic presence of 10 nM $A\beta_M$ for 72 hours is able to elevate the neuronal firing frequency (Fig.2B) by reducing the duration (Fig.3A) of individual APs. These changes in the electrical activity induced by 10 nM $A\beta_M$ recapitulate a physiological process of electrical maturation typical of neuronal cells [185]. Moreover, the viability of treated neurons was not affected by 10 nM $A\beta_M$ treatment, which instead caused a slight increase in the cell metabolism (Fig. 1). Our final goal has been to elucidate a potential physiological role of $A\beta_M$ by using a concentration as close as possible to those found in both normal and AD brains, which range between pM to nM concentrations [111], [113], [108], [177]. Among the overall concentrations we tested, 10 nM $A\beta_M$ was the minimum amount with the clearest biological effect on neurons. Therefore we only focused on this concentration for the subsequent experiments.

Neurons cultured with 10 nM $A\beta_M$ for 72 hours showed a firing frequency as well as some APs duration similar to those commonly found in cells at more mature stages of development. Over time, developing neurons spontaneously display an increment in the firing rate that stabilizes at mature age (Fig.4A) [186]. Accordingly, we used the duration of the first-elicited action potential as a parameter to compare the electrical activity of both 4 DIV untreated and 10 nM $A\beta_M$-treated cells to that assessed at higher *in vitro* stages of maturation, such as 11 DIV and 18 DIV (Fig.4B). Neurons cultured with 10 nM $A\beta_M$ showed an AP width lower than immature 4 DIV but still higher than 11 DIV and 18 DIV control neurons suggesting a possible implication of $A\beta_M$ in neuronal electrical maturation (Fig. 4B)

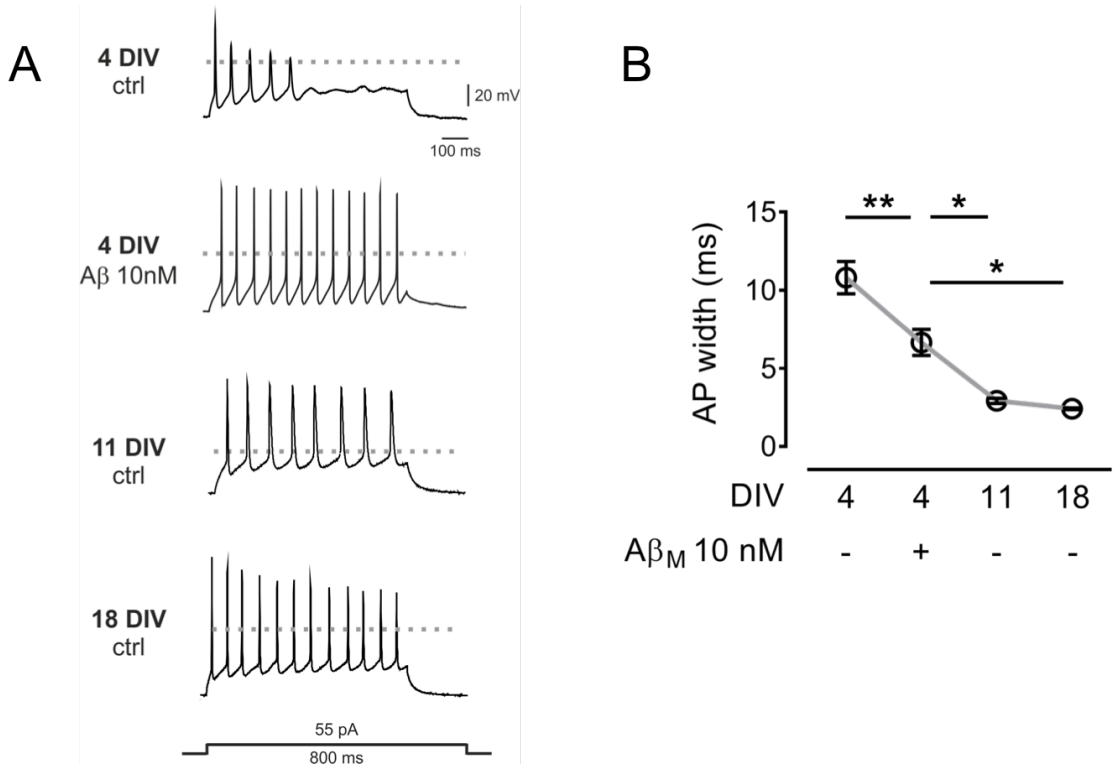

Figure 4 - Treatment with 10 nM $A\beta_M$ induces electrical changes toward an advanced stage of maturation.

A. Representative recordings of neurons at different stages of maturation and in 4 DIV treated with 10 nM $A\beta_M$. Current clamp recordings of firing activity elicited by a current step of 55 pA, 800 ms duration. Dashed lines represent 0 mV **B.** AP width values were plotted for all the conditions analyzed (4 DIV untreated, 4 DIV 10 nM $A\beta_M$, 11 DIV untreated, 18 DIV untreated). 4 DIV untreated 10.8 ± 1.04 ms n=10; 4 DIV 10 nM $A\beta_M$ 6.65 ± 0.84 ms n=17; 11 DIV untreated 2,91 ± 0.17 ms n=7; 18 DIV untreated 2.4 ± 0.05 ms n=4 *p<0.05; one-way ANOVA followed by Fisher post hoc test.

Analysis of ionic conductances on 10 nM $A\beta_M$ -treated cells at 4 DIV

Any modifications in passive properties of neurons could lead to an alteration in the electrical activity of excitable cells, thus we analyzed these biophysical parameters in both untreated and 10 nM AβM-treated neurons. As summarized in Table 2, RMP, input resistance (R_{in}) and membrane capacitance (C_m) were comparable in the two conditions analyzed (Table 2).

Table 2 - Summary of passive properties of untreated and 10 nM $A\beta_M$-treated neurons at 4 DIV

	Ctrl	10 nM $A\beta_M$	P value
RMP (mV)	-60.57 ± 1.06 n= 23	-63.21 ± 0.98 n= 19	0.079
R_{in} (MΩ)	1454 ± 299 n=11	1192 ± 126 n= 10	0.445
Cm (pF)	19.55 ± 2 n= 11	23.64 ± 1.9 n= 10	0.153

Passive properties calculated for untreated and 10 nM $A\beta_M$ - treated neurons at 4 DIV. Values are expressed as mean ± SEM. *p<0.05, unpaired t-test.

We then analyzed the ionic conductances mainly involved in the generation of AP. We firstly measured the voltage-dependent sodium currents (INa) of both untreated and 10 nM $A\beta_M$-treated neurons. A voltage step protocol (from – 80 to +60 mV, 20 mV increment, 800 ms duration) was applied to single voltage clamped neuron. After recording of stable whole-cell current, the protocol was then repeated after bath-applied 300 nM TTX to isolate INa. Pure TTX-sensitive current was obtained subtracting the membrane current left after the selective block of INa from whole cell current. As shown in Fig 5, the average amplitude of the inward INa was unchanged

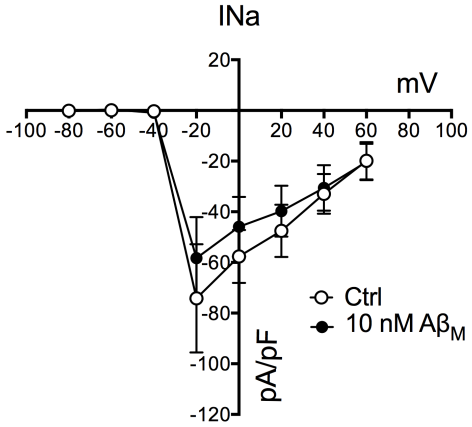

Figure 5 - Sodium current is not altered following 10 nM $A\beta_M$ treatment

Current-voltage relationship plot of INa recorded in 4 DIV untreated (blank circles) and 10 nM $A\beta_M$ treated neurons (black circles). INa was normalized on cell capacitance.

in 10 nM $A\beta_M$ treated-neurons compared to untreated cells. Furthermore, the involvement of INa to spike generation was also derived by the phase plot (obtained by drawing the first time derivative of voltage (dV/dt) vs. voltage) analysis of the spike threshold potentials. The threshold values were comparable between the two groups (control -23.2 ± 0.97 pA; 10 nM $A\beta_M$ -21.01 ± 1.6 pA, unpaired t-test *p < 0.05). We therefore conclude that the Na^+ channels responsible for AP generation

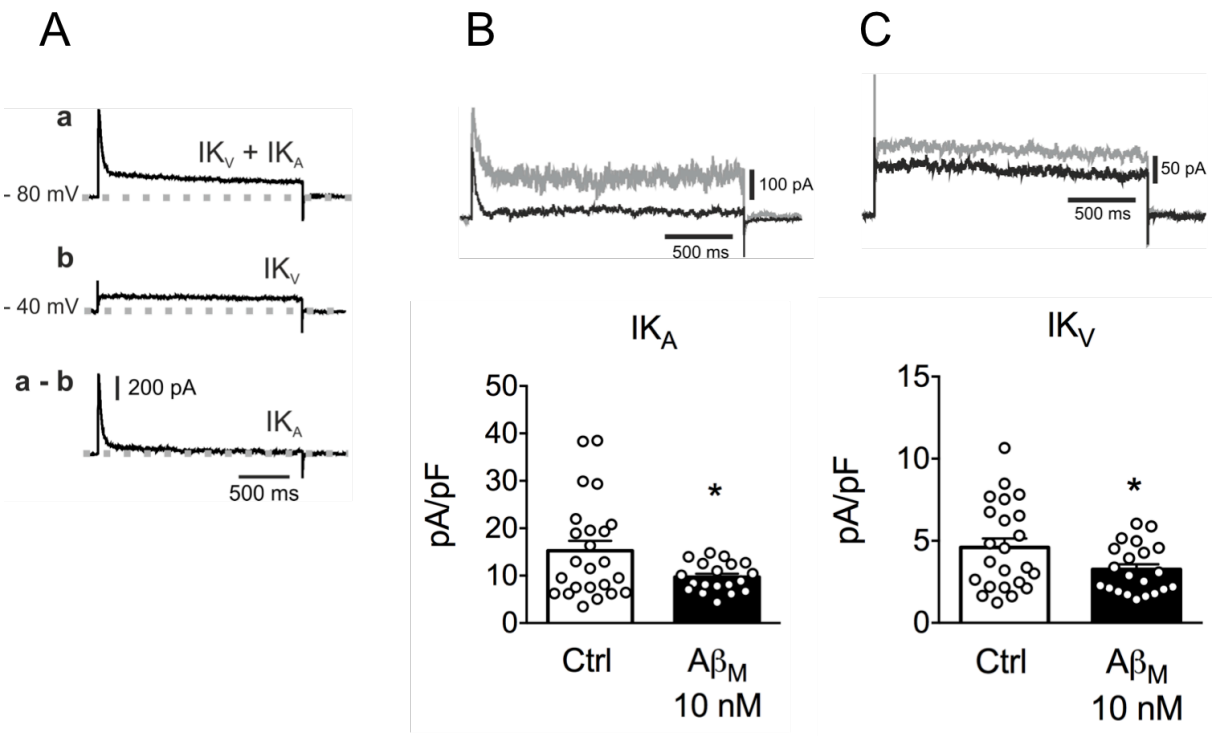

Figure 6 - Slight alterations of IK_V and IK_A induced by 10 nM $A\beta_M$

A. Graphical representation of the protocol used to obtain IK_V and IK_A. Briefly (a) The total outward current (which is composed by IK_A and IK_V) was recorded by a voltage step from -80 mV to -5 mV. (b) IK_V was evoked by a voltage step from – 40 mV to -5 mV. (c) IK_A was isolated by analytical subtraction of IK_V from the total potassium current (a) (IK_A + IK_V) recorded in the same cell. Currents were normalized on cell capacitance **B.** At the bottom, the plot represents the values of IK_A density of untreated cells (white, untreated neurons 351.2 ± 58.14 pA n=19) and 10 nM $A\beta_M$ treated neurons (black, 211.8 ± 18.52 pA n=24) (t-test, *p<0.05). At the top, representative IK_A patch-clamp recording of untreated cells (grey) and $A\beta_M$ treated neurons (black). **C.** At the bottom, the plot represents the values of IK_v density of untreated cells (white, untreated 103.2 ± 13.85 pA n=24) and 10 nM $A\beta_M$ (black, 70.13 ± 7.39 pA n=21) (student t-test, *p<0.05). At the top, representative IK_A patch-clamp recording of untreated cells (grey) and $A\beta_M$ treated neurons (black).

are not the main causes of the different firing pattern observed in $A\beta_M$ treated-neurons.

If INa regulate the rising phase of APs, then potassium currents (IK) are responsible for the repolarization of the membrane potential. The delayed rectifier K-current (IK_V) and A-type current (IK_A) are two of the potassium currents that mainly compose the total outward current of cortical neurons and also contribute to spike repolarization [187], [188]. We therefore measured these outward currents in neurons at 4 DIV. IK_V is mainly sensitive to Tetraethylammonium (TEA) and slowly inactivating, whereas IK_A is fast inactivating and mainly sensitive to 4-aminopyridine (4-AP). These two types of potassium current are usually pharmacologically isolated from the total whole cell current. However, both IK_V and IK_A are sensitive to both TEA and 4-AP making their separation from the total outward current not accurate,

even at low concentration of the blockers [189]. Thus, we isolated IK_V and IK_A by applying a voltage-step protocol from two different holding potentials (-80 mV or -40 mV) to – 5 mV (2000 ms duration) (Fig. 6A). The current recorded by holding the cells at -80 mV is mainly composed by both IK_V and IK_A (Fig.6Aa), whereas the inactivation of the A-type potassium channels at -40 mV allows the isolation of IK_V (Fig.6Ab). Thus, IK_A was obtained by analytically subtracting the IK_V from the total outward current (IK_V + IK_A) recorded [189] (Fig. 6Ac). IK_A significantly decreased from 351.2 ± 58.14 pA (n=19) in control cells to 211.8 ± 18.52 pA (n=24) (* $p<0.05$, unpaired t-test) in $A\beta_M$-treated cells (Fig. 6B). The slowly inactivating K-current - IK_V - has slightly, but significantly, decreased in neurons treated with 10 nM $A\beta_M$ (control 103.2 ± 13.85 pA n=24; 10 nM $A\beta_M$ 70.13 ± 7.399 pA n=21) (* $p<0.05$, unpaired t-test) (Fig. 6C). A reduction in the outward current could be implicated in the increased excitability displayed by neurons cultured with 10 nM $A\beta_M$. However, we do not know whether the decrease in IK_V and IK_A is due to a decrease in the number of active channels or to modifications in their properties.

Effects of 10 nM $A\beta_M$ treatment on the total dendritic length in 4 DIV neurons

We found that 10 nM $A\beta_M$ - treatment alters the waveform of the first AP decreasing its duration (Fig. 3). These alterations are likely due to a decrease in the outward currents of the cells (Fig. 6), both IK_V and IK_A. The final effect was an increase in the rate of the firing pattern displayed by immature neurons that resembles the spiking activity of cells at more mature stage of development (Fig. 4A).

In developing neurons excitability goes with the spreading of the dendritic processes that are prompted to growth by the afferent electrical activity [190]. Thus, the total dendritic length of 4 DIV control cells was compared to that measured in 10 nM $A\beta_M$ - treated neurons (Fig.8). As the excitability increased, even the total dendritic length raised by 20% increment in cells exposed to 10 nM $A\beta_M$ relative to control neurons (Fig. 7).

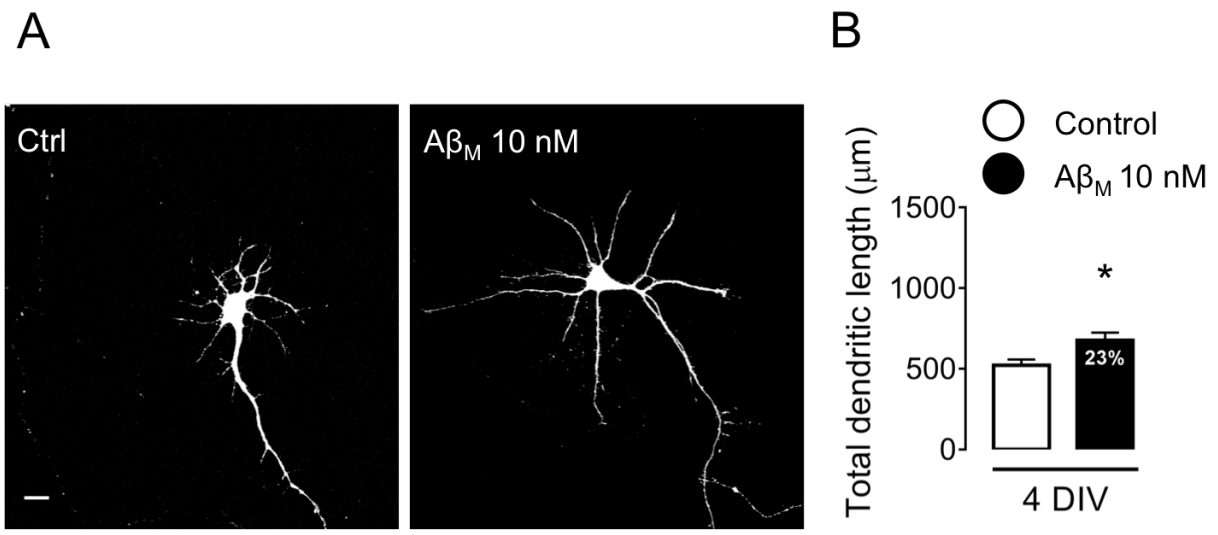

Figure 7 - The dendritic arbor growth increases after treatment with 10 nM Aβ$_M$ in 4 DIV neurons.

Analysis of total dendritic length in 4 DIV untreated and 10 nM Aβ$_M$-treated neurons. Neurons were treated at 1 DIV, transfected with GFP at 3 DIV and fixed at 4 DIV. Images were acquired at the confocal microscope, from 3 different culture preparations, minimum 5 cells for each conditions were analyzed. **A.** Representative images of control cells and 10 nM Aβ$_M$-treated neurons at 4 DIV. Scale bar= 20 µm **B.** Treatment with 10 nM Aβ$_M$ results in a significant increase in the average length of dendrites (Control 520.5 ± 37.62 µm n=26; 10 nM Aβ$_M$ 676.3 ± 48.32 µm n=23) (unpaired t-test, *p<0.05).

Since modifications in cell morphology correlate well with functional synaptogenesis, we next wondered whether synaptic currents of immature neurons were affected by treatment with 10 nM Aβ$_M$. However, neurons at 4 DIV display undeveloped synapses which spontaneous activity is awkward to record and analyze; synaptic currents are thus undetectable in most of the cells. For this reason, we still used immature neurons though at a more advanced stage of *in vitro* development. We shifted the experimental window forward, keeping the duration of the treatment unchanged: 4 DIV neurons were cultured with 10 nM Aβ$_M$ for 72 hours and the experiments were performed at 7 DIV. We therefore wanted to reproduce the results obtained in 4 DIV immature neurons also in 7 DIV cells. That is, we observed whether Aβ$_M$-treated neurons at 7 DIV displayed an augmented dendritic arborization and an increased excitability as seen at 4 DIV. Thus, before studying the effects of 10 nM Aβ$_M$ on 7 DIV synaptic activity, we did an immunocytochemistry analysis to measure the total dendritic length of 7 DIV control and 10 nM Aβ$_M$-treated neurons.

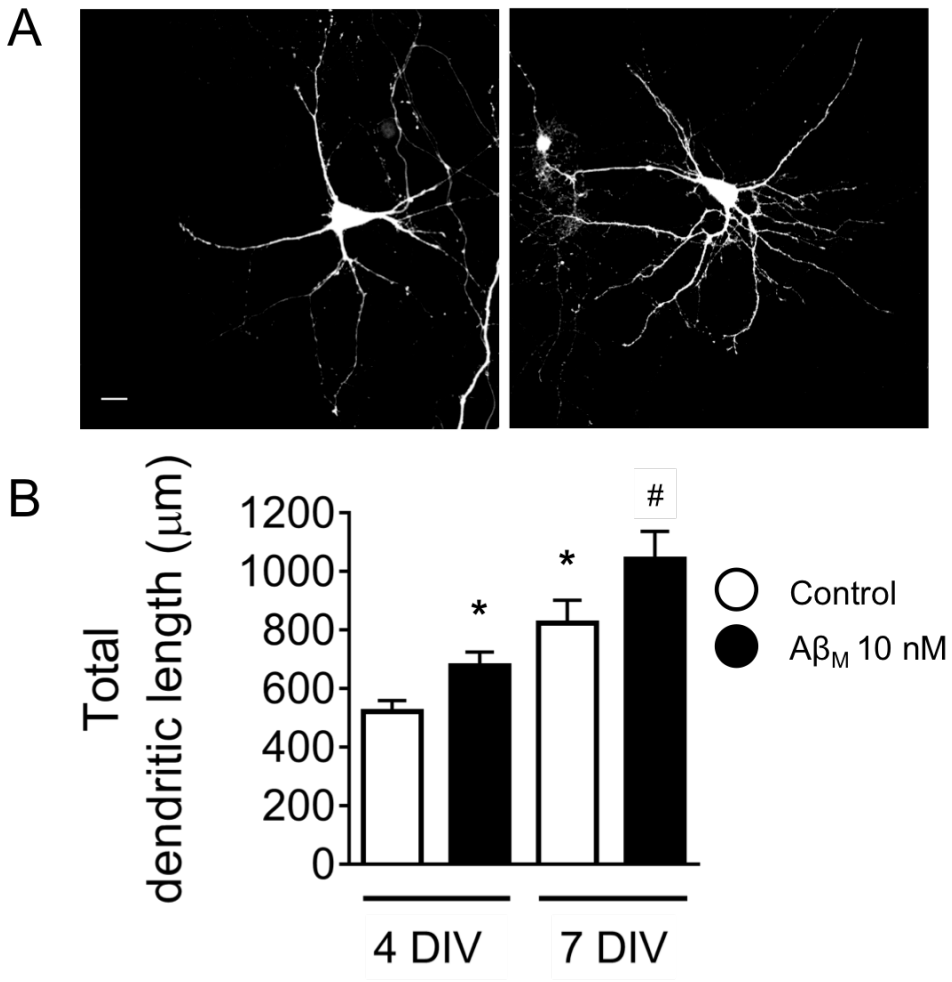

Figure 8 - Treatment with 10 nM $A\beta_M$ causes the growth of the dendritic arbor in immature neurons at 4 DIV as well as 7 DIV.

Cells were treated at 4 DIV, transfected with GFP at 6 DIV and fixed at 7 DIV. Images were acquired at the confocal microscope, from 2 different culture preparations. Minimum 5 cells for each conditions were analyzed **A.** Representative images of control cells and 10 nM $A\beta_M$-treated neurons at 7 DIV. Scale bar= 20 µm **B.** The total dendritic length of 4 DIV neurons were compared to that measured in 7 DIV neurons in normal condition or after treatment with $A\beta_M$. (4 DIV Control 520.5 ± 37.62 µm ; 10 nM $A\beta_M$ 676.3 ± 48.32 µm; 7 DIV Control 823 ± 78.8 µm; 10 nM $A\beta_M$ 1040 ± 96.1 µm, two-way ANOVA followed by Tukes post hoc test, *$p<0.05$)

Low concentrations of $A\beta_M$, 10 nM, caused an increase in the total length of the dendritic arbor by about 20% compared to control condition. The increment of the dendritic arbor growth in $A\beta_M$-treated cells is not statistically significant compared to control neurons (note that only 2 culture preparations were analyzed), but it maintains the same trend obtained at 4 DIV (Fig.8). Since the main effect of 10 nM $A\beta_M$ was to increase the excitability of 4 DIV silent cells (Fig.2), we also stimulated 7 DIV neurons with increasing current injections to assess any modification in the electrical behavior after treatment with 10 nM $A\beta_M$. Whole-cell patch-clamp experiments in current clamp mode were carried out on control and treated-cells. As shown in Fig. 9, at the same value of current injection, treated neurons elicit a train of APs at higher frequency than control cells, thus appearing more excitable. To confirm this idea, we looked at the rheobase values, that represent a measurement of neuronal excitability. The rheobase values decreased from 54.66 ± 6.819 pA (n=13) for control cells to 37.40 ± 4.309 pA (n=12) for 10 nM $A\beta_M$-treated neurons (*P<0.05, unpaired t-test) (Fig.10A). Note that, as shown in Fig. 10B, around the threshold level (40 pA) of current injection, 7 DIV treated cells triggered APs firing at lower injected current than control neurons whereas both conditions reach the firing-saturation at high current values.

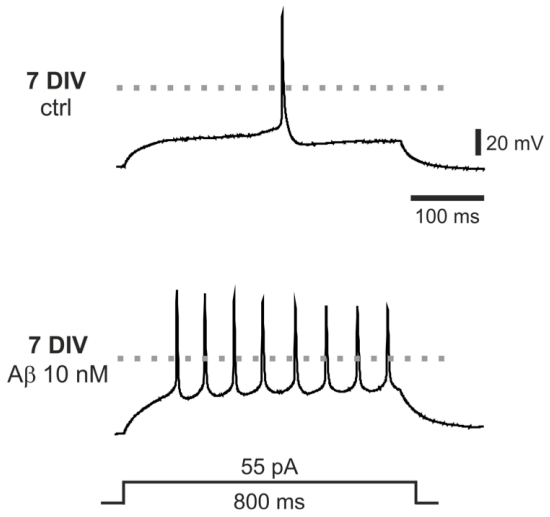

Figure 9 - Electrical activity of 7 DIV neurons treated with 10 nM $A\beta_M$

Representative traces of 7 DIV untreated and 10 nM $A\beta_M$ -treated neurons recorded in current clamp mode. The electrical activity of neurons is elicited by a 55 pA current step, lasting 800 ms duration. The treatment with 10 nM $A\beta_M$ increases the firing activity of immature neurons.

In addition, values reported in table 2 show that the passive properties of 7 DIV control cells and those exposed to 10 nM $A\beta_M$ are comparable.

Table 3 - Passive properties of untreated and 10 nM $A\beta_M$-treated neurons at 7 DIV

	Ctrl	10 nM $A\beta_M$	P value
RMP (mV)	-59.9 ± 2.1	-63.4 ± 1.93	0.241
	n= 8	n= 8	
R_{in} (MΩ)	896 ± 137	877 ± 116	0.916
	n=8	n= 8	
Cm (pF)	33.8 ± 2.32	37.3 ± 3.57	0.426
	n= 8	n= 8	

Passive properties calculated for untreated and 10 nM $A\beta_M$ - treated neurons at 7 DIV. Values are expressed as mean ± SEM. *p<0.05, unpaired t-test.

Synaptic activity modifications in 10 nM $A\beta_M$ - treated cells at 7 DIV

We observed that both electrical activity and morphology of immature neurons were affected by a chronic treatment (72 hours) with 10 nM $A\beta_M$ and this effect is reproducible in both 4 DIV and 7 DIV developing neurons (Fig. 2, 8, 10).

We were therefore able to determine whether the synaptic activity was also affected by chronic exposure to 10 nM $A\beta_M$. We firstly recorded spontaneous excitatory postsynaptic currents (sEPSC) by blocking GABA-inhibitory synaptic transmission (5 μM Gabazine) and maintaining the spike-mediated release. sEPSC were not detectable in some cells confirming that neurons at 7 DIV were still integrating into the network. Changes in sEPSC properties (such as frequency, amplitude, rise and decay times) reflect modifications in either post- or pre-synapses. In particular, any modification in the amplitude of EPSC is related to both different postsynaptic density receptors and amount of release neurotransmitter in functional synapses whereas EPSC frequency is dependent upon pre-synaptic vesicular release probability and number of functional synapses. The area of sEPSC is related to the total charge carried by the synaptic events, whereas their kinetic features are represented by the rise and decay time. Any alterations in these parameters suggest the presence of a different receptor subunit population at the post-synapses.

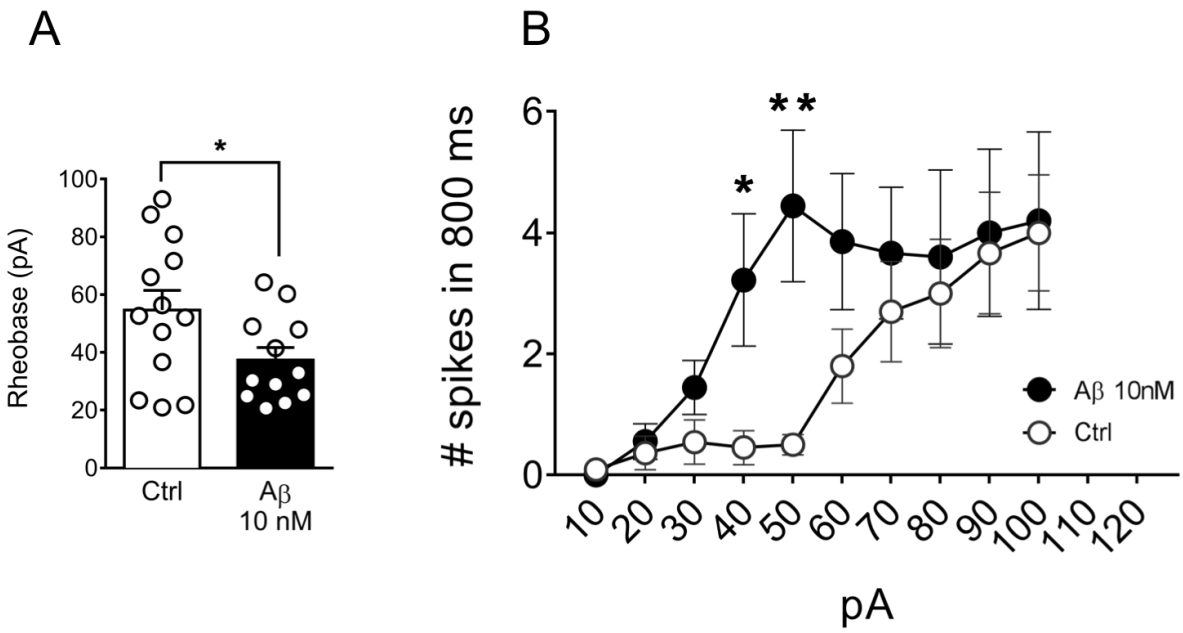

Figure 10 - 7 DIV neurons treated with 10 nM $A\beta_M$ show increased excitability

A. The reduced rheobase values of 10 nM AβM-treated neurons show that less current is needed to elicit an AP with respect of control neurons (untreated 54.66 ± 6.819 pA n=13; 10 nM $A\beta_M$ 37.40 ± 4.309 pA n=12, *p<0.05 unpaired t-test). **B.** The number of spikes generated by a step of current is plotted against the amount of current injected at each step. 10 nM $A\beta_M$ - treated (black) neurons reach their maximum firing rate when about 50 pA of current are injected, a condition that fails to induce any electrical response in untreated neurons (white) (*p<0.05, unpaired t-test)

We therefore analyzed frequency, amplitude, area as well as rise and decay time of sEPSC comparing the values obtained in control and treated-neurons. As shown in Fig.11A (inset), the average sEPSC amplitude was significantly increased after 72 hours 10 nM $A\beta_M$ treatment, as denoted by the rightward shift of the cumulative probability distribution (Fig. 11A main panel). In addition, the size of the synapses remains unchanged after treatment with 10 nM $A\beta_M$ as shown by the presence of only one population of sEPSC, with the amplitude values ranging from 10 to 20 pA, in the cumulative probability distribution.

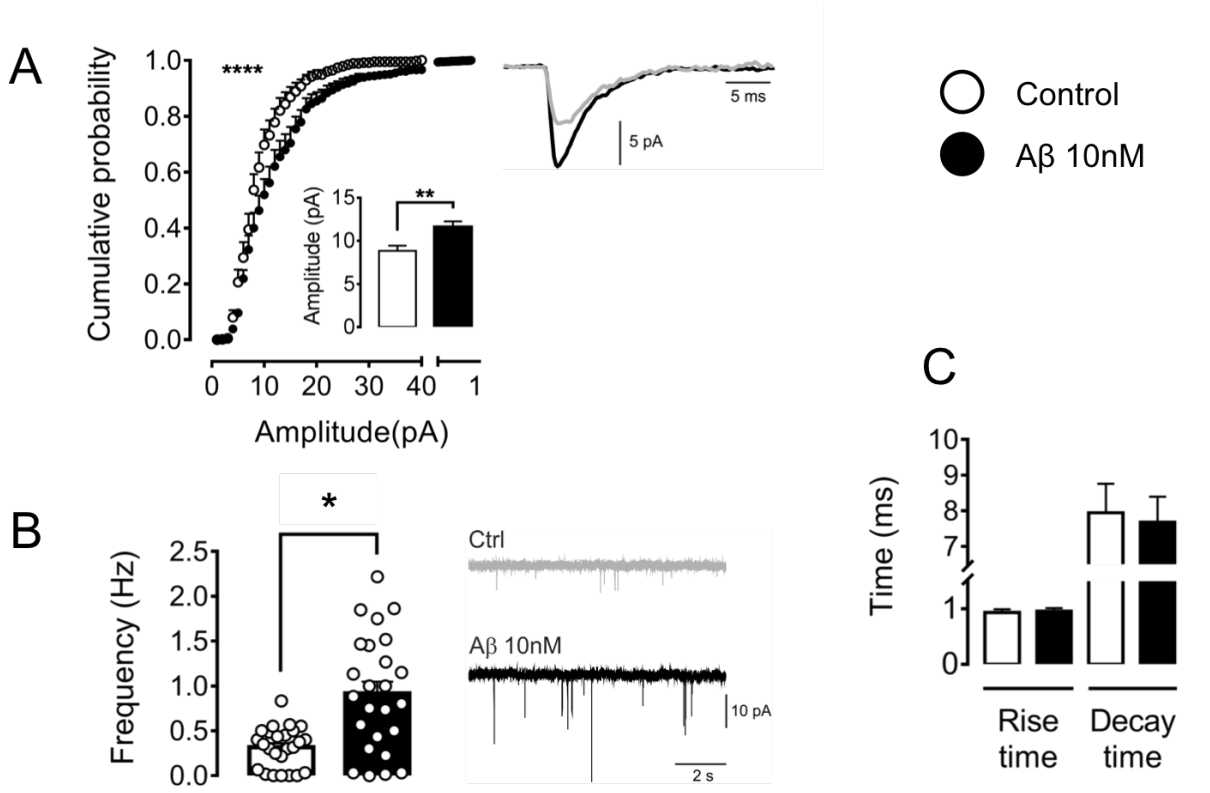

Figure 11 - sEPSC parameters of control cells are altered after 10 nM $A\beta_M$ - treatment

A. sEPSC were recorded at -70 mV in voltage-clamp mode. Gabazine (5 μM) was added to the external solution to block the GABA mediated transmission. On the left, the main plot represents the amplitude cumulative probability while the small plot represents the average values of sEPSC amplitudes of untreated (white) and treated neurons (black) (two-tailed Kolmogorov-Smirnov *p<0.0001). On the right, the representative traces of the average events recorded in one cell (untreated cells in grey, treated neurons in black). (Control cells 8.86 ± 0.58 pA n=18; 10 nM $A\beta_M$ cells 11.6 ± 0.65 pA n=18; unpaired t-test *p<0.05) **B.** On the left, the average values of the sEPSC frequency in untreated (white) and treated neurons (black). On the right, representative traces of sEPSC in untreated (grey) and treated neurons (black). Control 0.32 ± 0.04 Hz n=25; 10 nM $A\beta_M$ 0.92 ± 0.13 Hz n=25; * p<0.05 unpaired t-test **C.** Rise and decay times were measured in untreated (white) and treated neurons (black). Rise time: Control 0.93 ± 0.06 ms n=25; 10 nM $A\beta_M$ 0.96 ± 0.06 ms n=25; ; decay time: Control 7.94 ± 0.81 ms n=18; 10 nM $A\beta_M$ 7.67 ± 0.72 ms n=20; unpaired t-test *p<0.05.

Also the frequency of the events was increased by 3-fold in treated neurons compared to control cells, as illustrated in Fig. 11B. Conversely, none of the conditions considered exhibited significant changes in rise time and decay time (Fig. 11C). Furthermore, the sEPSC area was not affected in 7 DIV 10 nM $A\beta_M$-treated cells (Table 4).

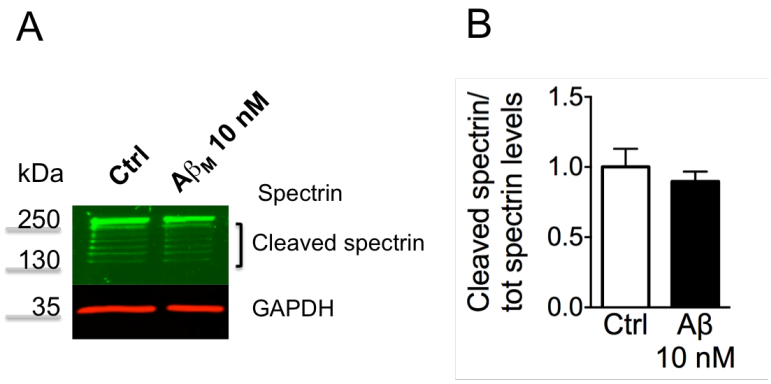

Figure 12 - Increased neuronal activity in 10 nM $A\beta_M$-treated neurons is not associated with excitotoxicity.

A. Western blotting for cleaved spectrin and total spectrin in lysates of neurons at 7 DIV, untreated and treated with 10 nM $A\beta_M$. **B.** The plotted values represent the ratio between the levels of cleaved spectrin over total spectrin normalized for the control (untreated 1.0 ± 0.13; 10 nM $A\beta_M$ treated 0.89 ± 0.07; one culture preparation)

The sAMPA-response induced by chronic treatment with 10 nM $A\beta_M$ could be associated to excitotoxicity, which is a pathological process caused by an over-activation of glutammatergic receptors, such as AMPA and NMDA receptors, leading to neuronal death [191]. To assess a possible glutamate-induced toxicity in cultures exposed to 10 nM $A\beta_M$, we performed a preliminary WB analysis of spectrin protein (Fig. 12). Spectrin is a cytoskeleton-linked protein, which is cleaved during excitotoxicy processes [192], thus we analyzed the levels cleaved spectrin in untreated and $A\beta_M$-treated cells. As shown in Fig.13, the ratio between cleaved and total spectrin did not change in the two conditions analyzed, suggesting that the overall effects on sEPSC induced by 10nM $A\beta_M$ treatment are not associated with increased vulnerability to excitotoxicity.

$A\beta_M$-induced electrical activity regulates synaptic strengthening and dendritic arborization

Data reported in Fig.11 show that treatment with 10 nM $A\beta_M$ caused an increase in both sEPSC amplitude and frequency of developing neurons, thus an improvement in excitatory synaptic transmission. However any modifications in spontaneous EPSC,

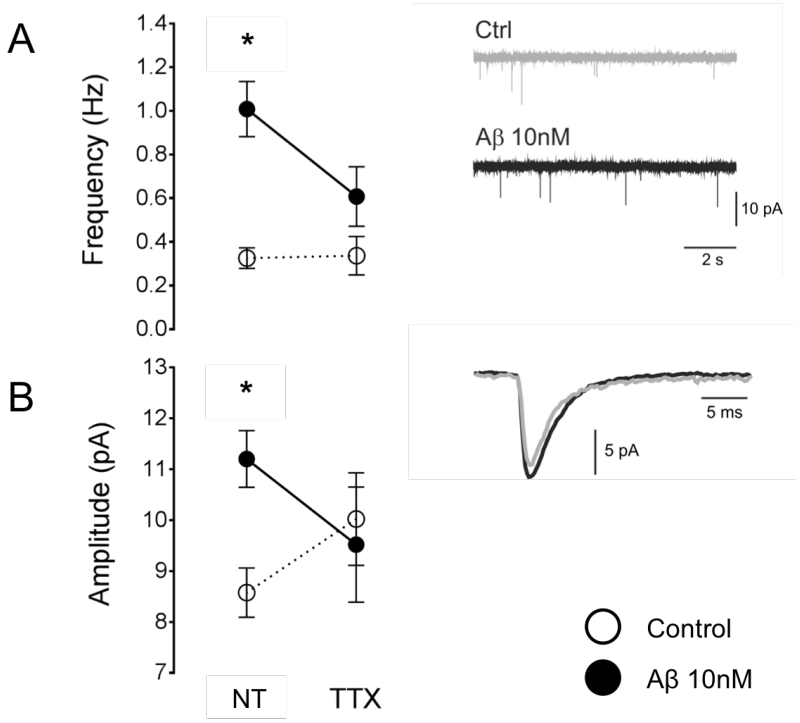

Figure 13 - The effects of 10 nM $A\beta_M$ on sEPSC is dependent on neuronal excitability

Neurons were cultured in two conditions: TTX alone or TTX and 10 nM $A\beta_M$ at 4 DIV for 72 hours, sEPSC were recorded at 7 DIV. **A.** On the left average values of sEPSC frequency in control neurons (white circles, not treated with $A\beta_M$) and 10 nM $A\beta_M$ treated neurons (black circles). On the right, representative traces of sEPSC in control (grey, TTX) and 10 nM $A\beta_M$ condition (black, TTX + 10 nM $A\beta_M$) (Control 0.326 ± 0.04 pA; w/ TTX Control 0.34 ± 0.08 pA; 10 nM $A\beta_M$ 1.01 ± 0.12 pA; w/ TTX 10 nM $A\beta_M$ 0.61 ± 0,14 pA; unpaired t-test *p<0.05) **B.** On the left average values of sEPSC amplitude in control neurons (white circles, not treated with $A\beta_M$) and 10 nM $A\beta_M$ treated neurons (black circles). On the right, representative average sEPSC events recorded from one single cell in control (grey, TTX) and 10 nM $A\beta_M$ condition (black, TTX + 10 nM $A\beta_M$) (Control 8.58 ± 0.48 pA; w/ TTX Control 10 ± 0.9 pA; 10 nM $A\beta_M$ 11.2 ± 0.55 pA; w/ TTX 10 nM $A\beta_M$ 9.52 ± 1.13 pA; unpaired t-test *p<0.05). NT=Not Treated

, which are APs-driven events, are caused by alterations in the properties of pre- or post-synaptic cells and/or by modifications in the network activity. The presynaptic strengthening, seen as an increased sEPSC frequency in $A\beta_M$-treated cells, is likely due to a rise in the number of spiking neurons and also to an enhanced firing activity of those cells. Further experiments on miniature EPSC (mEPSC) are therefore needed to elucidate the properties of synaptic currents generate by APs-independent release in both conditions.

To assess whether the increase in the firing frequency occurs before the strengthening of synapses or vice versa, we chronically cultured cells with 10 nM $A\beta_M$ and 1 μM TTX (a sodium channel blocker) for 72 hours to inhibit the spontaneous electrical activity. We therefore recorded sEPSC by using the regular external solution, thus removing the TTX blocker.

As shown before, both sEPSC amplitude and frequency were increased after treatment with 10 nM $A\beta_M$ w/o TTX applying (Fig. 13 A, B) However, control neurons showed a peculiar enhancement of sEPSC amplitude after the complete block of APs firing with TTX. This phenomenon is commonly known as "synaptic scaling"; it is a form of synaptic plasticity that allows neurons to sense the level of our own electrical activity in order to adjust and stabilize the firing by scaling up or down the strength of excitatory synapses and so maintain an homeostatic stability [193]. Basically, a neuron deprived of electrical activity - such as under TTX treatment – enhances the strength of excitatory synapses by improving the amplitude of EPSC and vice versa. Thus, the increased sEPSC amplitude displayed by control cells cultured with TTX is

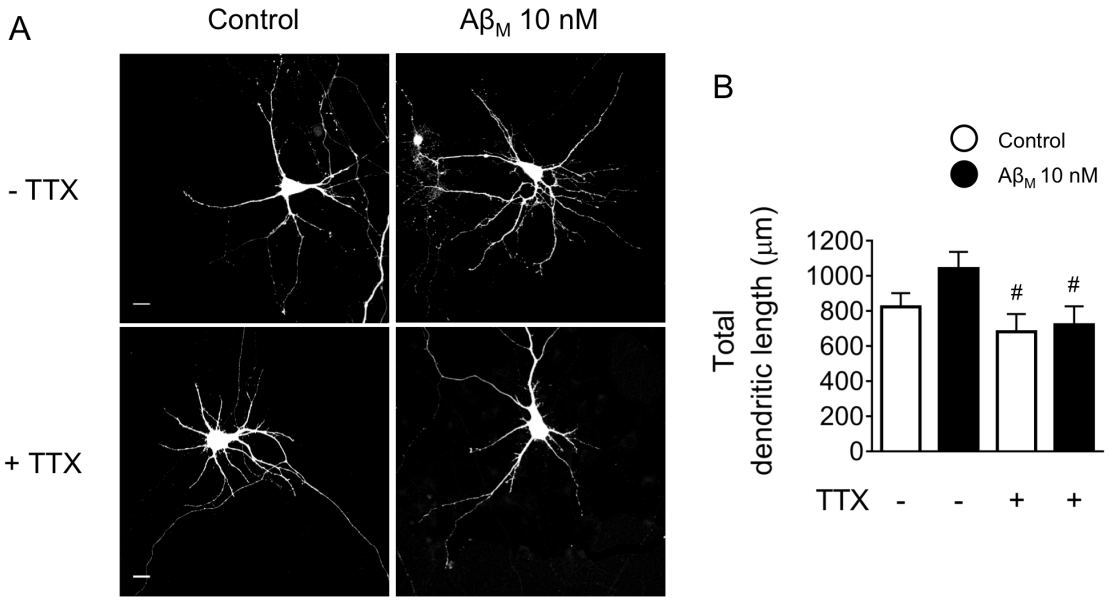

Figure 14 - The growth of dendritic processes is regulated by $A\beta_M$-induced excitability

A. Example images of 7 DIV untreated and 10 nM $A\beta_M$ treated neurons in control (- TTX) or activity-deprived condition (+ TTX, 1 μM). Neurons were treated at 4 DIV, transfected with GFP at 6 DIV and fixed at 7 DIV. Images were acquired at the confocal microscope from 2 different culture preparations, minimum 5 cells were analyzed for each conditions **B.** Analysis of total dendritic length of control cells and treated neurons culture with or without TTX (Control 823 ± 78.8 μm; w/ TTX Control 681 ± 101 μm; 10 nM $A\beta_M$ 1040 ± 96.1 μm; w/ TTX 10 nM $A\beta_M$ 720 ± 106 μm). #$p<0.05$ vs10 nM w/o TTX, two-way ANOVA followed by Fisher test

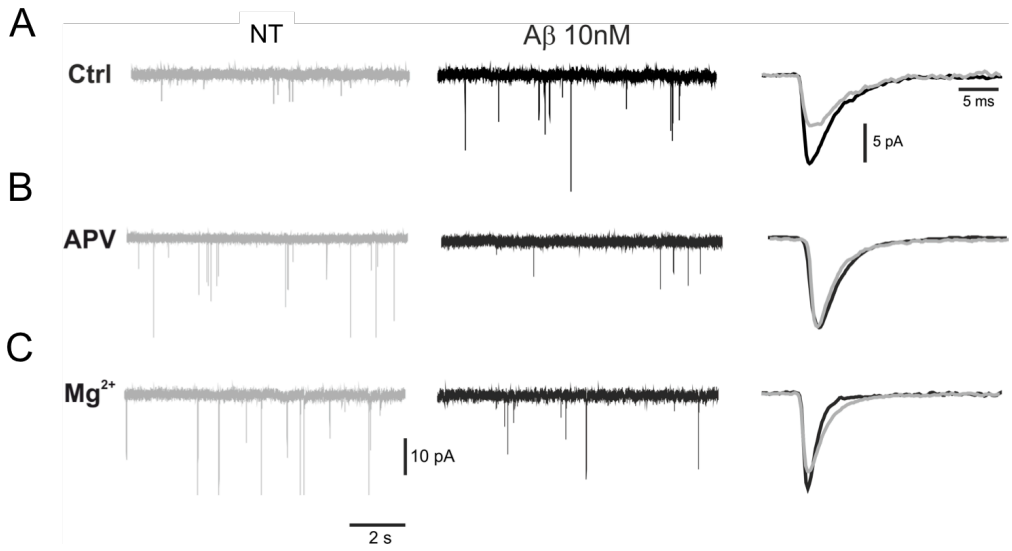

Figure 15 - On the left, representative traces of sEPSC recordings of control (grey) and 10 nM $A\beta_M$-treated neurons (black) cultured with APV or Mg^{2+} at 4 DIV for 72 hours. sEPSC were recorded at 7 DIV. APV was used at 50 μM whereas Mg^{2+} was used at 1 mM. On the right, representative spontaneous events recorded from control (grey) and 10 nM $A\beta_M$ treated neurons (grey) **A.** sEPSC frequency and amplitude increase after 10 nM $A\beta_M$ treatment **B-C.** The sEPSC frequency is altered after treatment with APV **(B)** or Mg^{2+} **(C)** but only in control neurons, whereas the amplitude remains unchanged in both untreated and treated cells.

a common homeostatic regulation of excitatory neurons.

Both sEPSC frequency and amplitude of 10 nM $A\beta_M$ –treated neurons has decreased close to control values (Fig. 13A,B) after 72 hours of in activity-deprived condition (Fig. 13B). Thus, the strengthening of excitatory synapses caused by 10 nM $A\beta_M$ seems to take place after the increase of firing activity which actually prompts the synaptic improvement probably due to a "synaptic scaling"-independent mechanism. We next measured the total dendritic length of activity-deprived neurons in control and 10 nM $A\beta_M$-condition. Blocking the firing activity for 72 hours has significantly inhibited the length of the dendritic processes displayed by $A\beta_M$-treated neurons (Fig. 14B) (#P<0.05 Two-way ANOVA). Conversely, the dendritic trees growth of control neurons was weakly affected by TTX treatment (Fig. 14B). This data is consistent with previous results that have shown a strong influence of neuronal activity on dendritic arborization [190], [194], [195].

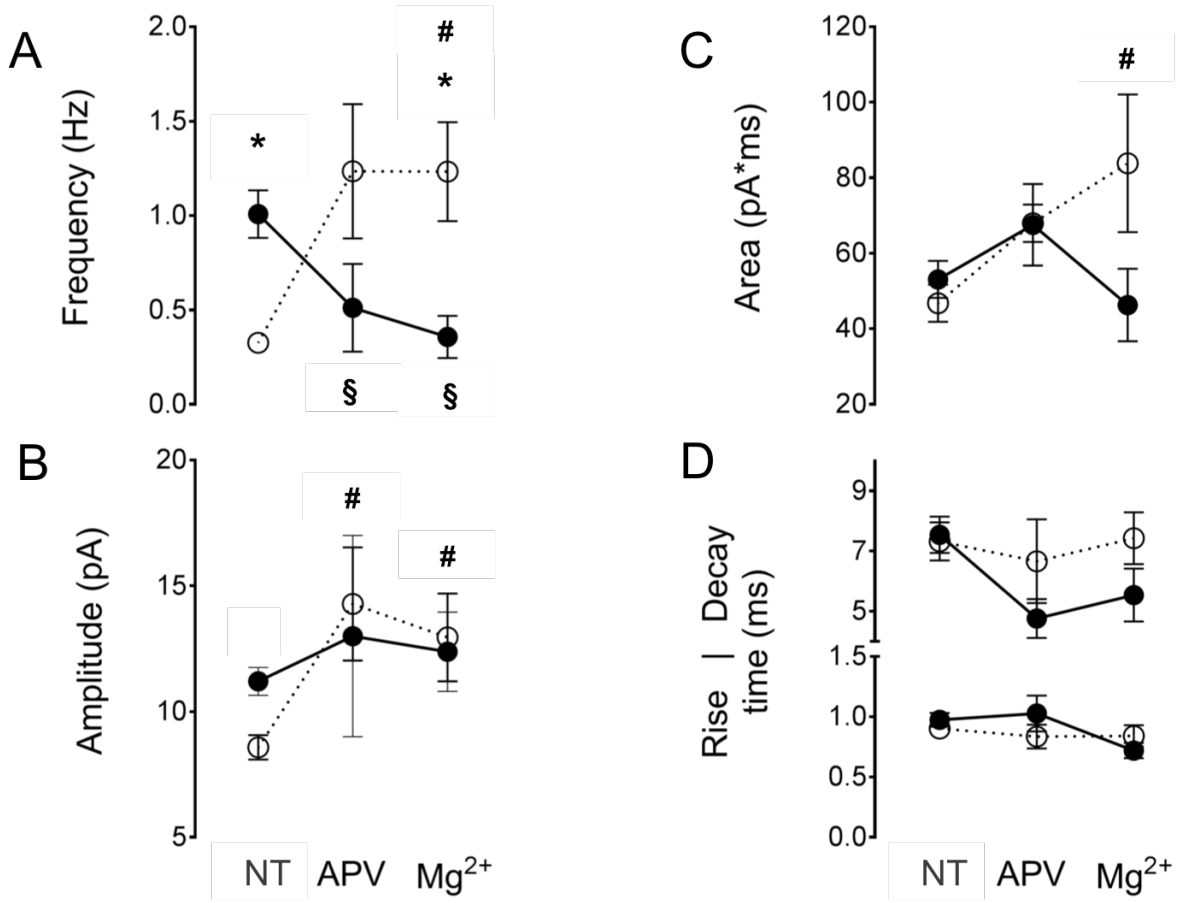

Figure 16 - Analysis of sEPSC parameters in NMDA-deprived conditions

Average values of sEPSC frequency (**A)**, amplitude **(B)**, area **(C)**, rise and decay time **(D)** in control neurons (white circles, not treated with $A\beta_M$) and 10 nM $A\beta_M$ treated neurons (black circles). * $p<0.05$ Ctrl vs 10 nM $A\beta_M$; #$P<0.05$ NT vs APV or NT vs Mg^{2+} for both control and $A\beta_M$ - treated neurons, two-way ANOVA followed by Tukey's post hoc test.

Effects of NMDA receptors in $A\beta_M$-induced outcomes on sEPSC

The levels of glutamate ionotropic receptors, both NMDA and AMPA receptors, are finely regulated during neuronal development. At early stages of maturation, neurons displays "silent synapses" that lack of functionally AMPA receptors (AMPAR). Their sequential development and insertion into post-synaptic membranes – the so-called "AMPAfication" [196]– is a process mainly mediated by NMDA receptors (NMDAR). Thus, the synaptic strength improvement induced by low concentrations of $A\beta_M$ on immature neurons (Fig. 11) could be an NMDA-dependent process. For this reason, we blocked the NMDAR for 72 hours using 50 μM D-2-amino-5-phosphonovalerate

(APV) in culture medium and we subsequently recorded sEPSC in control cells and neurons treated with 10 nM $A\beta_M$ using the regular external solution thus washing away the NMDA-blocker. When NMDAR are chronically blocked both sEPSC frequency and amplitude were strongly affected in control cells (Fig 15B, 16A-B) (#P<0.05 two-way ANOVA). Indeed, it was recorded a 3-fold increment of sEPSC frequency (Fig. 16A) and a 2-fold increase in the sEPSC amplitude of control neurons cultured with APV (Fig. 16B) (#P<0.05 two-way ANOVA). Conversely, 10 nM $A\beta_M$-treatment, in NMDAR-activity deprived condition, completely abolished the increase in sEPSC frequency and amplitude showed by APV-treated control cells (Fig. 15B). sEPSC frequency of $A\beta_M$-treated neurons went back to control values (Fig. 16A) whereas the amplitude was unaffected compared to that of control cells exposed to APV (Fig.16B) (*P<0.05, two-way ANOVA).

Chronic inhibition of NMDAR activity caused an increase in both sEPSC amplitude and frequency in control cells; it is probably due to a compensatory mechanism of synapses to counteract the chronic block of the excitatory receptors. This is also supported by sEPSC recordings performed in control neurons chronically cultured with high concentrations of Mg^{2+} (1 mM added to the culture medium) that saturate NMDAR even at depolarized potential. Both pre- and post-synapses were found to be

Table 4

	NT		APV		Mg^{++}	
	Ctrl	$A\beta_M$ 10 nM	Ctrl	$A\beta_M$ 10 nM	Ctrl	$A\beta_M$ 10 nM
Frequency (Hz)	0.32 ± 0.04	1.01 ± 0.12	1.23 ± 0.26	0.51 ± 0.23	1.23 ± 0.26	0.356 ± 0.11
Amplitude (pA)	8.58 ± 0.48	11.2 ± 0.55	14.28 ± 2.25	13.0 ± 4.0	12.95 ± 1.74	12.38 ± 1.58
Area (pA*ms)	46.76 ± 4.94	53.08 ± 4.9	67.94 ± 4.95	67.53 ± 10.79	83.84 ± 18.24	46.29 ± 9.61
Rise time (ms)	0.9 ± 0.04	0.97 ± 0.06	0.84 ± 0.1	1.03 ± 0.15	0.84 ± 0.09	0.72 ± 0.06
Decay time (ms)	7.33 ± 0.63	7.54 ± 0.6	6.67 ±1.39	4.76 ± 0.65	7.43 ± 0.86	5.54 ± 0.88

Average values of sEPSC parameters in control neurons and 10 nM $A\beta_M$ treated neurons when cultured in normal condition (NT), with APV or Mg^{2+} for 72 hours.

potentiated with increased frequency and amplitude compared to control condition (Fig. 15C, 16A-B) (*P<0.05 two-way ANOVA). Cells treated with both 10 nM $A\beta_M$ and high Mg^{2+} for 3 days has maintained the same trend seen after the chronic block of NMDAR with APV: sEPSC frequency decreased at control values (*P<0.05 two-way ANOVA) while the amplitude was not affected compared to $A\beta_M$-untreated neurons (Fig. 15C, 16A-B). Moreover, the area and the sEPSC kinetics parameters (rise and decay times) of the excitatory events were comparable in all groups (Fig. 16C) (Fig. 16D).

Discussion

So far, the Aβ peptide has been addressed as a pathological peptide, linked to AD development and progression. Thus, in the last 30 years, the scientific community has been focused on studying the multiple ways in which the peptide can exert its toxicity upon neurons and to find a way to eradicate Aβ from the brain of patients. Considered mainly an aberrant peptide or wasting product of cell metabolism, little research has ever been dedicated to the study of Aβ peptide possible role in physiological conditions.

However, growing evidences are highlighting the biological function(s) of APP and its derivatives - including Aβ - as crucial factors in maintaining neuronal homeostasis [47]. Aβ is found at low concentrations (pM and nM) in both human and murine ISF collected from healthy and AD brains [111], [112], [113], [177]; furthermore the accumulation of the peptide in extracellular plaques, a well-known hallmark of the disease, has been shown to be asymptomatic in certain cases and not related to AD onset [93]. The failure of Aβ-centric treatments, that aim to remove or reduce the concentration of the Aβ peptide from brain compartments, is a further evidence of its relevance for the cerebral homeostasis (see chapter 4). An emerging physiological role of Aβ is sustained by recent results indicating that the peptide may work as a modulator of synaptic plasticity at low concentrations (pM). By acting directly at pre-synapses [170] or indirectly on post-synaptic α7-nicotinic receptors (nAChRs) [197], [198], [199] it has been shown that Aβ positively regulates the synaptic transmission by enhancing both the presynaptic strength and LTP.

Our work starts from these assumptions and gives more information about Aβ effects on neuronal activity. In particular, our data support the hypothesis that Aβ has a modulatory effect on neuronal synaptic transmission and also demonstrate that low concentrations (10 nM) of $A\beta_{1\text{-}42}$ monomers ($A\beta_M$) can enhance the electrical activity of immature cortical neurons.

The *in vitro* maturation of neuronal cultures reaches its peak at 14 DIV at which neurons display enhanced connectivity and firing rate compared to younger neurons [200], [201]. For our experiments we used primary cultures of embryonic neurons at

4 DIV and 7 DIV in order to study the alterations induced by $A\beta_M$ on the neuronal activity of electrically silent or low-frequency firing cells.

Our investigations are based on a chronic treatment (72 hours) with exogenous $A\beta_{1-42}$ monomers. The $A\beta_{1-42}$ preparation used was synthetized through the solid phase protein synthesis (SPPS) which allows to obtain a pure solution of soluble monomers of $A\beta_{1-42}$ in its native structure [179]. We used this solution at different concentrations (10 nM, 100 nM, 500 nM) to treat neurons and we found that $A\beta_M$ modifies the electrical behavior of the cells in a concentration-dependent manner. $A\beta_M$ 500 nM zeroed the effects caused by lower concentrations (10 nM) of $A\beta_M$ on neuronal excitability **(Fig.2)**. High levels of monomeric Aβ have been reported to be deleterious (0.2 μM [202]), (1 μM [203]) prompting its oligomerization [204], a process known to be involved in AD progression. Indeed, in physiological conditions, the processes of production and clearance of Aβ are finely regulated to avoid undesired accumulations of the peptide and subsequent aggregation, since oligomerization is likely to occur whenever the peptide is present in a solution at 37°C and pH 7.4, as the physiological brain environment [205]. Thus the overall concentration of Aβ in the extracellular space of healthy brain is maintained in the range of picomolarity and nanomolarity [111].

Our data show that 10 nM $A\beta_M$ acts on neuronal excitability of immature neurons by increasing the frequency and decreasing the width of APs. On the contrary, 500 nM $A\beta_M$ reduces the spiking rate and the APs width at control levels probably due to an ongoing oligomerization of the peptide caused by its high concentration in the culture medium. Besides confirming that $A\beta_M$ has a concentration-dependent effect on neurons, these results are of particular interest because they suggest that there is a concentration threshold under which not only $A\beta_M$ has a lower tendency to aggregate, but it also has a totally different effect than that exerted at higher concentrations. We think that these observations can be explained by the fact that after 72 hours in the culture medium, in the 10 nM preparation the predominant species of $A\beta_M$ are monomers while in the 500 nM preparation the predominant species are aggregated forms. Thus, depending on the proportions of the different conformations of Aβ in the culture medium, different effects on neuronal activity can be observed. Indeed, the most ambivalent $A\beta_M$ effects are induced by 100 nM treatment; it is perhaps due

to a mixed Aβ population of monomers and oligomers that leads to a balance of enhancing and inhibitory effects exerted by the peptide on neuronal activity **(Fig.2)**.
These evidences must be discussed in the light of the current results obtained from Aβ-overproducing transgenic mice that overexpress familial AD (FAD)-associated mutant APP. Most of the studies using mouse models of amiloidopathy are focused on the analysis of the synaptic function and plasticity. However, attention has also been paid on the intrinsic excitability modifications that occur in neuronal cells. The epileptiform electrical activity recorded in APP-overexpressing mice [123], also confirmed in AD sufferers [206], was the first indication of the hyperexcitability later identified in several mouse models of AD [127], [126], [131], [129]**.** The most reported alteration is a reduced width of APs that therefore facilitate an increase in the firing rate [131], [127], [129], [132]. Our results are in accordance with the literature. Indeed, the alterations in neuronal excitability that we report are very similar to that commonly observed in AD mouse models. However, with some important differences in the experimental conditions that allow us to interpret the results in an alternative fashion, attributing to Aβ-induced excitability a trophic rather than a toxic effect. In fact, all our experiments were performed using primary cultures of neurons at early stages of development (4 DIV and 7 DIV), with a highly controllable $A\beta_M$ preparation that we applied chronically on neurons. In our opinion, the modifications induced by the peptide are surely dependent on its conformational form, but what we want to highlight as a critical issue in the study of Aβ is that every effect of the peptide can be toxic or trophic depending on the stage of development on the neuron.
An Aβ-induced hyperexcitability appears to be toxic in adult brains while in juvenile neurons it may favor the insertion of newborn cells into neuronal network as well as the communication between excitable cells through synaptic activity regulation.
Indeed, the peptide is not only produced during pathological conditions; the endogenous Aβ is released by APP-processing as early as the beginning of embryonic development and during the whole life of individuals [207]. Moreover, Brody and colleagues have shown that microdialysate Aβ levels in human ISF decrease almost immediately after an acute brain injury then increase over time until reaching a steady state concentration that correlates with improved neurological status [112]. Thus, it seems that Aβ levels increase when there is an injury in the brain, suggesting a fascinating hypothesis that sees Aβ as a peptide involved in brain repairing

processes. With this in mind, the increased excitability found in our immature neuronal cultures chronically exposed to $A\beta_M$, would not be a toxic event but it may drive/help the maturation of excitable cells. Indeed the 10 nM $A\beta_M$-induced APs narrowing resembles that displayed by neurons at more mature stages of development **(Fig. 4)**.

APs waveform is mainly controlled by the gating properties and membrane density of two voltage gated channels, Na^+ and K^+ both increasing over time during development [185]**.** In particular, the AP duration could be modified by an increase in the potassium currents, which contribute to the repolarization phase of AP, or an increase in the Na^+ peak current. In our recordings, the inward sodium current was not affected by 10 nM $A\beta_M$ treatment **(Fig.5)**, while we found a decrease in both the potassium currents analyzed, IK_A and IK_V **(Fig.6)**. There are many studies about the effects induced by Aβ on potassium channels, such as IK_A enhancement [208], [209], [210], [211] or reduction [212], [213], [132] as well as an increase in Kv3.1b delayed-rectifier channels in a mouse model of AD [129]**.** However, the alterations caused by Aβ on potassium currents are still unclear due to the different Aβ isoforms and model systems used in these studies. According to our results, a decrease in IK_A fits well with the resulting decrease in APs width found in Aβ-treated neurons; it is instead not easy to identify a reason for the reduction of IK_V since its increase is known to be necessary to reduce the AP duration. This discrepancy may be probably due to the early stage of development at which neurons were treated and analyzed.

The total dendritic length is enhanced by about 20% following $A\beta_M$ treatment at 10 nM **(Fig.8)**, reinforcing the idea that this concentration of $A\beta_M$ enhances neuronal maturation and affects the neuronal functioning in a positive way. Dendritic elongations and branching as well as synapses formation are very sensitive to neuronal activity [195], [214], due to its involvement in the modulation of vesicular release. Under developing conditions, the long-range communication between cells lead to a concentration gradient of glutamate neurotransmitter in the neuronal environment that may be detected from filopodia. The dendritic processes thus spread towards the pre-synapses in order to achieve an active innervation. Subsequently, NMDA dependent-calcium flux on the post-synapses can activate several intracellular pathways that subsequently lead to plasticity and synaptic strength [215], [216].

So, electrical activity and glutamate release play an important role in dendritic arborization and synaptic maturation. For this reason, we decided to monitor spontaneous synaptic activity in immature neurons treated with 10 nM $A\beta_M$ to see if the increased dendritic length and increased electrical activity also influence synaptic transmission.

Synapse strengthening was successfully measured in 7 DIV immature neurons treated with 10 nM $A\beta_M$ for 72 hours. At this stage of *in vitro* development, the levels of glutammatergic receptors (AMPA and NMDA receptors) are still increasing, as it happens at 4 DIV; however the synaptic markers are now detectable and many nascent synaptic junctions are present, while at 4 DIV it is still too early to record any synaptic event [217]. We then recorded the spontaneous release of excitatory neurotransmitters at 7 DIV after chronic treatment with 10 nM $A\beta_M$ and untreated neurons. Analysis of sEPSC showed that 10 nM $A\beta_M$ act at the synaptic level by strengthening both pre- and post-synapses. Since recordings were done using a TTX-free external solution, sEPSC frequency and amplitude are likely augmented due to the strong increase in the excitability caused by the treatment **(Fig. 11)**. The rise in sEPSC frequency seems to alter the post-synaptic receptor density, as demonstrated by the amplitude enhancement of sEPSC that can be due to an increase in the AMPA receptors levels at the plasma membrane. Although both frequency and amplitude are increased, rise and decay time of the synaptic events are unchanged meaning that 10 nM $A\beta_M$ treatment does not alter the subunit composition of AMPA receptors. The general strengthening of synapses caused by $A\beta_M$ may involve the activation of newly formed "silent synapses" [218]: thanks to the 10 nM $A\beta_M$ – induced vesicle release, a strong postsynaptic depolarization may activate the NMDA dependent CaMKII pathway resulting in the appearance of a solid AMPA response in immature neurons. It is worthy to notice that these changes in the synaptic activity do not lead to excitotoxicity **(Fig.12)**.

By chronically blocking (72 hours) the electrical activity of the cells with TTX we show that the effect of $A\beta_M$ on synaptic activity is almost zeroed, demonstrating that the augmented spiking activity of 10 nM $A\beta_M$-treated neurons is fundamental for the strengthening of synapses **(Fig.13)**. Moreover, by blocking the electrical activity with TTX for 72 hours, we show that the dendritic arbor spreading no longer occurs in neurons treated with $A\beta_M$, thus demonstrating that also the dendritic length is

dependent from the enhanced neuronal activity that occurs in $A\beta_M$ -treated neurons **(Fig.14)**.

The constant rise of AMPA receptors during early stages of neuronal development is strictly dependent on NMDA receptors activity [196], which quantal size is stable during synaptogenesis [219]. Thus, when an increase in the AMPA signal is needed, an NMDA activity-deprivation may cause a compensatory reaction of cells that over-produce AMPA receptors. Indeed the chronic block (72 hours) of NMDA receptors (with APV or high Mg^{2+}) correlates with an increased AMPA response, as shown by the increase of both sEPSC frequency and amplitude recorded from Aβ-untreated neurons. However, sEPSC frequency of neurons cultured with both 10 nM $A\beta_M$ and APV (or high Mg^{2+}) drastically decreases at control values whereas the amplitude remains unchanged from APV-control neurons **(Fig.16A, B)**. This is an intriguing result in light of the reported Aβ function as a Ca^{2+} like ion channel. It has been reported that Aβ peptides induce ionic conductances in both artificial membranes and plasma membranes [220], [221]–[223], [224]. Unpublished data obtained from our laboratory also confirmed this idea revealing pore formation in artificial membrane when exposed to $A\beta_M$ at 100 nM. Current recordings in artificial lipid bilayer showed that Aβ, in its monomeric form, not only is able to form ion pores with low conductance (15-20 pS) but also that this ion flux is mainly calcium and potassium selective. We speculate that the tiny calcium flux mediated by monomeric Aβ channels is able to recover the effects obtained during NMDA activity-deprived conditions. As described by Nicoll's group [225], the strength of developing synapses is modulated by the magnitude of NMDA receptors activation. That is, the basal NMDA activity seems to have an inhibitory role on AMPA receptors membrane insertion in developing conditions. This inhibitory pathway may ensure that synapses become functional only after strong activity, which instead triggers AMPA receptors insertion because of the sustained intracellular calcium flux mediated by NMDA receptors in this condition. Eliminating NMDA receptors during development, the inhibitory modulation of the synaptic strength is also abolished, leading to an increase in the active AMPA receptors on post-synaptic membranes [225]. Thus, when NMDA receptors are blocked with APV or high Mg^{2+}, Aβ-mediated calcium flux seems to override the NMDA current. When neurons are exposed to both APV and $A\beta_M$ the sEPSC amplitude remains unchanged, meaning that the calcium currents

mediated by $A\beta_M$ may mimic the current mediated by NMDA receptors when synapses are hyper-stimulated.

In light of this, post-synaptic strengthening induced by the monomeric peptide may trigger a retrograde pathway that reduces the probability of vesicular release, thus the sEPSC frequency, as observed in our sEPSC recordings **(Fig. 16A)**. In summary, Aβ might act on synapses by mediating a calcium flux that mimics or enhances NMDA receptors role in synaptogenesis and by increasing the electrical activity of neurons.

It has been demonstrated that the release of the native peptide in the brain ISF is regulated by neuronal activity [161], [160]. Although the physiological concentrations of the peptide is reported to be lower than 10 nM, monomeric Aβ levels probably fluctuate into the neuronal network within a range of nano-to-picomolar concentrations in which the peptide may exert different effects on neuronal cells. Indeed, it has been already suggested a mechanism by which Aβ and the synaptic activity are mutually controlled: picomolar concentrations of Aβ, like physiological, enhance LTP and memory [164]. The resulting increase in the synaptic activity increases in turn the peptide concentrations leading to the formation of oligomers responsible for the synaptic activity depression. Our evidences suggest a modulatory role of monomeric Aβ on both electrical and synaptic activity of immature cortical neurons, probably through partially overlapping mechanisms. Although the cell viability is not affected by the exposure to increasing amounts of monomers (10 nM, 100 nM, 500 nM), only 10 nM $A\beta_M$ positively alter the activity of juvenile neurons. As shown, the $A\beta_M$-induced firing activity increase is fundamental to drive the growth of the dendritic arbor and also the strengthening of synapses in developing neurons. Moreover, monomeric Aβ, as calcium like channel, could be involved in the stimulation of several processes involved in the maturation of a neuron. It has been already described a trophic function of Aβ on both proliferation and differentiation of neuronal stem cells (NSC) but the precise effect is still unknown due to the contradictory results so far obtained [173]. The overall evidences described in my thesis work suggest that the $A\beta_M$-dependent modulation of immature neuronal activity might be crucial for the insertion of newborn neurons into a pre-existing network.

In conclusion, this work wants to give an input to reassess the physiological role of Aβ that must be considered to further develop most efficient therapeutic interventions for AD.

References

[1] A. Association, “2017 Alzheimer’s disease facts and figures,” *Alzheimer’s Dement*, vol. 13, pp. 325–373, 2017.

[2] J. Cummings, G. Lee, T. Mortsdorf, A. Ritter, and K. Zhong, “Alzheimer’s disease drug development pipeline: 2017,” *Alzheimers Dement (N Y)*, vol. 3, no. 3, pp. 367–384, 2017.

[3] M. B. Colovic, D. Z. Krstic, T. D. Lazarevic-Pasti, A. M. Bondzic, and V. M. Vasic, “Acetylcholinesterase inhibitors: pharmacology and toxicology,” *Curr Neuropharmacol*, vol. 11, no. 3, pp. 315–335, 2013.

[4] N. M. and P. K. Andrea Witt, “Memantine hydrochloride,” *Nat. Rev. DRUG Discov.*, 2004.

[5] A. Alzheimer, “Uber eine eigenartige Erkrankung der Hirnrinde.,” *Allg Zeitschr f Psychiatr. u Psych-Gerichtl Med*, vol. 64, no. 64, pp. 146–8, 1907.

[6] M. Strassnig and M. Ganguli, “About a peculiar disease of the cerebral cortex. By Alois Alzheimer, 1907,” *Psychiatry*, no. 412, pp. 30–33, 2005.

[7] M. Prince, A. Wimo, M. Guerchat, G.-C. Ali, Y.-T. Wu, and M. Prina, “World Alzheimer Report 2015,” *Alzheimer’s Disease International- World Alzheimer Report 2015*. pp. 1–84, 2015.

[8] N. C. Fox, R. I. Scahill, W. R. Crum, and M. N. Rossor, “Correlation between rates of brain atrophy and cognitive decline in AD.,” *Neurology*, vol. 52, no. 8, pp. 1687–1689, 1999.

[9] A. M. Fjell *et al.*, “One-Year Brain Atrophy Evident in Healthy Aging,” *J. Neurosci.*, vol. 29, no. 48, pp. 15223–15231, 2009.

[10] C. R. McDonald *et al.*, “Regional rates of neocortical atrophy from normal aging to early Alzheimer disease,” *Neurology*, vol. 73, no. 6, pp. 457–465, 2009.

[11] N. C. Fox and J. M. Schott, “Imaging cerebral atrophy: normal ageing to Alzheimer’s disease,” *Lancet*, vol. 363, no. 9406, pp. 392–394, 2004.

[12] F. M. Gunning-Dixon, A. M. Brickman, J. C. Cheng, and G. S. Alexopoulos, “Aging of cerebral white matter: A review of MRI findings,” *International Journal of Geriatric Psychiatry*, vol. 24, no. 2. pp. 109–117, 2009.

[13] H. Braak and E. Braak, “Neuropathological stageing of Alzheimer-related changes,” *Acta Neuropathol.*, vol. 82, no. 4, pp. 239–259, 1991.

[14] N. Schuff *et al.*, “MRI of hippocampal volume loss in early Alzheimers disease in relation to ApoE genotype and biomarkers,” *Brain*, vol. 132, no. 4, pp. 1067–1077, 2009.

[15] D. P. Devanand *et al.*, “Hippocampal and entorhinal atrophy in mild cognitive impairment: Prediction of Alzheimer disease,” *Neurology*, vol. 68, no. 11, pp. 828–836, 2007.

[16] H. Rusinek *et al.*, “Regional Brain Atrophy Rate Predicts Future Cognitive Decline: 6-year Longitudinal MR Imaging Study of Normal Aging,” *Radiology*, vol. 229, no. 3, pp. 691–696, 2003.

[17] C. R. Jack, “Alliance for Aging Research AD Biomarkers Work Group: Structural MRI,” *Neurobiology of Aging*, vol. 32, no. SUPPL. 1. 2011.

[18] L. Pini *et al.*, “Brain atrophy in Alzheimer’s Disease and aging,” *Ageing Res Rev*, vol. 30, pp. 25–48, 2016.

[19] A. Serrano-Pozo, M. P. Frosch, E. Masliah, and B. T. Hyman, “Neuropathological alterations in Alzheimer disease,” *Cold Spring Harb Perspect Med*, vol. 1, no. 1, p. a006189, 2011.

[20] J. G. Wood, S. S. Mirra, N. J. Pollock, and L. I. Binder, “Neurofibrillary tangles of Alzheimer disease share antigenic determinants with the axonal microtubule-associated protein tau (tau),” *Proc Natl Acad Sci U S A*, vol. 83, no. 11, pp. 4040–4043, 1986.

[21] A. Delacourte and A. Defossez, “Alzheimer’s disease: Tau proteins, the promoting factors of microtubule assembly, are major components of paired helical filaments,” *J. Neurol. Sci.*, vol. 76, no. 2–3, pp. 173–186, 1986.

[22] K. S. Kosik, C. L. Joachim, and D. J. Selkoe, “Microtubule-associated protein tau (tau) is a major antigenic component of paired helical filaments in Alzheimer disease.,” *Proc. Natl. Acad. Sci. U. S. A.*, vol. 83, no. 11, pp. 4044–8, 1986.

[23] F. Braak, H. Braak, and E. M. Mandelkow, “A sequence of cytoskeleton changes related to the formation of neurofibrillary tangles and neuropil threads,” *Acta Neuropathol.*, vol. 87, no. 6, pp. 554–567, 1994.

[24] J. P. Brion, D. P. Hanger, M. T. Bruce, A. M. Couck, J. Flament-Durand, and B. H. Anderton, “Tau in Alzheimer neurofibrillary tangles. N- and C-terminal regions are differentially associated with paired helical filaments and the location of a putative abnormal phosphorylation site,” *Biochem J*, vol. 273(Pt 1), pp. 127–133, 1991.

[25] M. Morris, S. Maeda, K. Vossel, and L. Mucke, “The Many Faces of Tau,” *Neuron*, vol. 70, no. 3. pp. 410–426, 2011.

[26] S. Millecamps and J. P. Julien, “Axonal transport deficits and neurodegenerative diseases,” *Nature Reviews Neuroscience*, vol. 14, no. 3. pp. 161–176, 2013.

[27] H. Braak and E. Braak, “Staging of alzheimer’s disease-related neurofibrillary changes,” *Neurobiol. Aging*, vol. 16, no. 3, pp. 271–278, 1995.

[28] G. G. Glenner and C. W. Wong, “Alzheimer’s disease: initial report of the purification and characterization of a novel cerebrovascular amyloid protein,” *Biochem Biophys Res Commun*, vol. 120, no. 3, pp. 885–890, 1984.

[29] M. R. Brier *et al.*, “Tau and Abeta imaging, CSF measures, and cognition in Alzheimer’s disease,” *Sci Transl Med*, vol. 8, no. 338, p. 338ra66, 2016.

[30] P. Giannakopoulos *et al.*, “Tangle and neuron numbers, but not amyloid load,

predict cognitive status in Alzheimer's disease," *Neurology*, vol. 60, no. 9, pp. 1495–1500, 2003.

[31] J. Hardy and D. Allsop, "Amyloid deposition as the central event in the aetiology of Alzheimer's disease," *Trends Pharmacol Sci*, vol. 12, no. 10, pp. 383–388, 1991.

[32] D. J. Selkoe, "Amyloid protein and Alzheimer's disease," *Sci Am*, vol. 265, no. 5, p. 68–71,74–76,78, 1991.

[33] J. A. Hardy and G. A. Higgins, "Alzheimer's disease: the amyloid cascade hypothesis," *Science (80-.).*, vol. 256, no. 5054, pp. 184–185, 1992.

[34] J. Dorszewska, M. Prendecki, A. Oczkowska, M. Dezor, and W. Kozubski, "Molecular Basis of Familial and Sporadic Alzheimer's Disease," *Curr. Alzheimer Res.*, vol. 13, no. 9, pp. 952–963, 2016.

[35] R. E. Tanzi, "The genetics of Alzheimer disease," *Cold Spring Harb Perspect Med*, vol. 2, no. 10, 2012.

[36] D. J. Selkoe, "Alzheimer's Disease," *Cold Spring Harb. Perspect. Biol.*, vol. 3, no. 7, pp. a004457–a004457, 2011.

[37] L. M. Bekris, C. E. Yu, T. D. Bird, and D. W. Tsuang, "Review article: Genetics of Alzheimer disease," *Journal of Geriatric Psychiatry and Neurology*, vol. 23, no. 4. pp. 213–227, 2010.

[38] D. Campion *et al.*, "Early-onset autosomal dominant Alzheimer disease: prevalence, genetic heterogeneity, and mutation spectrum.," *Am. J. Hum. Genet.*, vol. 65, no. 3, pp. 664–70, 1999.

[39] T. D. Bird, "Genetic aspects of Alzheimer disease," *Genetics in Medicine*, vol. 10, no. 4. pp. 231–239, 2008.

[40] A. Goate *et al.*, "Segregation of a missense mutation in the amyloid precursor protein gene with familial Alzheimer's disease.," *Nature*, vol. 349, no. 6311, pp. 704–6, 1991.

[41] M. Mullan *et al.*, "A pathogenic mutation for probable Alzheimer's disease in the APP gene at the N–terminus of β–amyloid," *Nat. Genet.*, vol. 1, no. 5, pp. 345–347, 1992.

[42] R. Sherrington *et al.*, "Cloning of a gene bearing missense mutations in early-onset familial Alzheimer's disease," *Nature*, vol. 375, no. 6534, pp. 754–760, 1995.

[43] E. I. Rogaev *et al.*, "Familial Alzheimer's disease in kindreds with missense mutations in a gene on chromosome 1 related to the Alzheimer's disease type 3 gene," *Nature*, vol. 376, no. 6543, pp. 775–778, 1995.

[44] E. Levy *et al.*, "Mutation of the Alzheimer's disease amyloid gene in hereditary cerebral hemorrhage, Dutch type.," *Science*, vol. 248, no. 4959, pp. 1124–6, 1990.

[45] S. S. Sisodia and P. H. St George-Hyslop, "gamma-Secretase, Notch, Abeta and Alzheimer's disease: where do the presenilins fit in?," *Nat. Rev. Neurosci.*, vol.

3, no. 4, pp. 281–90, 2002.

[46] E. Levy-Lahad *et al.*, “Candidate gene for the chromosome 1 familial Alzheimer’s disease locus,” *Science*, vol. 269, no. 5226. pp. 973–977, 1995.

[47] U. C. Muller, T. Deller, and M. Korte, “Not just amyloid: physiological functions of the amyloid precursor protein family,” *Nat Rev Neurosci*, vol. 18, no. 5, pp. 281–298, 2017.

[48] A. Saunders *et al.*, “Association of apolipoprotein E allele epsilon 4 with late-onset familial and sporadic Alzheimer’s disease.,” *Neurology*, vol. 43, no. 8, pp. 1467–1472, 1993.

[49] W. J. Strittmatter *et al.*, “Apolipoprotein E: high-avidity binding to beta-amyloid and increased frequency of type 4 allele in late-onset familial Alzheimer disease.,” *Proc. Natl. Acad. Sci.*, vol. 90, no. 5, pp. 1977–1981, 1993.

[50] G. Bu, “Apolipoprotein e and its receptors in Alzheimer’s disease: Pathways, pathogenesis and therapy,” *Nature Reviews Neuroscience*, vol. 10, no. 5. pp. 333–344, 2009.

[51] Y. Andrews-Zwilling *et al.*, “Apolipoprotein E4 Causes Age- and Tau-Dependent Impairment of GABAergic Interneurons, Leading to Learning and Memory Deficits in Mice,” *J. Neurosci.*, vol. 30, no. 41, pp. 13707–13717, 2010.

[52] C. C. Liu, T. Kanekiyo, H. Xu, and G. Bu, “Apolipoprotein e and Alzheimer disease: Risk, mechanisms and therapy,” *Nature Reviews Neurology*, vol. 9, no. 2. pp. 106–118, 2013.

[53] Y. Ji, Y. Gong, W. Gan, T. Beach, D. M. Holtzman, and T. Wisniewski, “Apolipoprotein E isoform-specific regulation of dendritic spine morphology in apolipoprotein E transgenic mice and Alzheimer’s disease patients,” *Neuroscience*, vol. 122, no. 2, pp. 305–315, 2003.

[54] J. Kim, J. M. Basak, and D. M. Holtzman, “The Role of Apolipoprotein E in Alzheimer’s Disease,” *Neuron*, vol. 63, no. 3. pp. 287–303, 2009.

[55] G. McKhann, D. Drachman, M. Folstein, R. Katzman, D. Price, and E. M. Stadlan, “Clinical diagnosis of Alzheimer’s disease: Report of the NINCDS-ADRDA Work Group* under the auspices of Department of Health and Human Services Task Force on Alzheimer’s Disease,” *Neurology*, vol. 34, no. 7, pp. 939–939, 1984.

[56] C. R. Jack *et al.*, “Introduction to the recommendations from the National Institute on Aging-Alzheimer’s Association workgroups on diagnostic guidelines for Alzheimer’s disease,” *Alzheimer’s and Dementia*, vol. 7, no. 3. pp. 257–262, 2011.

[57] G. M. McKhann *et al.*, “The diagnosis of dementia due to Alzheimer’s disease: recommendations from the National Institute on Aging-Alzheimer’s Association workgroups on diagnostic guidelines for Alzheimer’s disease,” *Alzheimers Dement*, vol. 7, no. 3, pp. 263–269, 2011.

[58] T. G. Beach, S. E. Monsell, L. E. Phillips, and W. Kukull, “Accuracy of the clinical diagnosis of Alzheimer disease at National Institute on Aging Alzheimer

Disease Centers, 2005-2010," *J. Neuropathol. Exp. Neurol.*, vol. 71, no. 4, pp. 266–273, 2012.

[59] M. F. Folstein, S. E. Folstein, and P. R. McHugh, "'Mini-mental state'. A practical method for grading the cognitive state of patients for the clinician," *J. Psychiatr. Res.*, vol. 12, no. 3, pp. 189–198, 1975.

[60] S. Borson, J. Scanlan, M. Brush, P. Vitaliano, and A. Dokmak, "The mini-cog: A cognitive 'vital signs' measure for dementia screening in multi-lingual elderly," *Int. J. Geriatr. Psychiatry*, vol. 15, no. 11, pp. 1021–1027, 2000.

[61] B. Sheehan, "Assessment scales in dementia," *Ther. Adv. Neurol. Disord.*, vol. 5, no. 6, pp. 349–358, 2012.

[62] D. Perani *et al.*, "Validation of an optimized SPM procedure for FDG-PET in dementia diagnosis in a clinical setting," *NeuroImage Clin.*, vol. 6, pp. 445–454, 2014.

[63] B. Dubois *et al.*, "Research criteria for the diagnosis of Alzheimer's disease: revising the NINCDS-ADRDA criteria," *Lancet Neurology*, vol. 6, no. 8. pp. 734–746, 2007.

[64] C. R. Jack *et al.*, "Update on hypothetical model of Alzheimer's disease biomarkers," *Lancet Neurol.*, vol. 12, no. 2, pp. 207–216, 2013.

[65] A. M. Fagan, C. M. Roe, C. Xiong, M. a Mintun, J. C. Morris, and D. M. Holtzman, "Cerebrospinal fluid tau/beta-amyloid(42) ratio as a prediction of cognitive decline in nondemented older adults.," *Arch. Neurol.*, vol. 64, no. 3, pp. 343–349, 2007.

[66] T. Tapiola *et al.*, "Cerebrospinal fluid {beta}-amyloid 42 and tau proteins as biomarkers of Alzheimer-type pathologic changes in the brain.," *Arch. Neurol.*, vol. 66, no. 3, pp. 382–389, 2009.

[67] C. R. Jack *et al.*, "Hypothetical model of dynamic biomarkers of the Alzheimer's pathological cascade," *Lancet Neurol.*, vol. 9, no. 1, pp. 119–128, 2010.

[68] P. Scheltens *et al.*, "Alzheimer's disease," *Lancet*, vol. 388, no. 10043, pp. 505–517, 2016.

[69] A. Keshavan, A. Heslegrave, H. Zetterberg, and J. M. Schott, "Blood Biomarkers for Alzheimer's Disease: Much Promise, Cautious Progress," *Mol. Diagnosis Ther.*, vol. 21, no. 1, pp. 13–22, 2017.

[70] R. E. Tanzi, R. D. Moir, and S. L. Wagner, "Clearance of Alzheimer's A?? peptide: The many roads to perdition," *Neuron*, vol. 43, no. 5. pp. 605–608, 2004.

[71] Jucker Mathias, Konrad Beyreuther, C. Haass, R. M. Nitsch, and Y. Christen, *Alzheimer: 100 Years and Beyond*. Springer, Berlin, Heidelberg, 2006.

[72] E. D. Eanes and G. G. Glenner, "X-ray diffraction studies on amyloid filaments," *J Histochem Cytochem*, vol. 16, no. 11, pp. 673–677, 1968.

[73] C. W. Wong, V. Quaranta, and G. G. Glenner, "Neuritic plaques and

cerebrovascular amyloid in Alzheimer disease are antigenically related," *Proc Natl Acad Sci U S A*, vol. 82, no. 24, pp. 8729–8732, 1985.

[74] C. L. Masters, G. Simms, N. A. Weinman, G. Multhaup, B. L. McDonald, and K. Beyreuther, "Amyloid plaque core protein in Alzheimer disease and Down syndrome," *Proc Natl Acad Sci U S A*, vol. 82, no. 12, pp. 4245–4249, 1985.

[75] D. J. Selkoe and M. S. Wolfe, "Presenilin: running with scissors in the membrane," *Cell*, vol. 131, no. 2, pp. 215–221, 2007.

[76] D. Goldgaber, M. I. Lerman, O. W. McBride, U. Saffiotti, and D. C. Gajdusek, "Characterization and chromosomal localization of a cDNA encoding brain amyloid of Alzheimer's disease," *Science (80-.).*, vol. 235, no. 4791, pp. 877–880, 1987.

[77] J. Kang *et al.*, "The precursor of Alzheimer's disease amyloid A4 protein resembles a cell-surface receptor," *Nature*, vol. 325, no. 6106, pp. 733–736, 1987.

[78] N. K. Robakis *et al.*, "Chromosome 21q21 sublocalisation of gene encoding beta-amyloid peptide in cerebral vessels and neuritic (senile) plaques of people with Alzheimer disease and Down syndrome," *Lancet*, vol. 1, no. 8529, pp. 384–385, 1987.

[79] R. E. Tanzi *et al.*, "Amyloid beta protein gene: cDNA, mRNA distribution, and genetic linkage near the Alzheimer locus," *Science (80-.).*, vol. 235, no. 4791, pp. 880–884, 1987.

[80] R. Ehehalt, P. Keller, C. Haass, C. Thiele, and K. Simons, "Amyloidogenic processing of the Alzheimer beta-amyloid precursor protein depends on lipid rafts," *J Cell Biol*, vol. 160, no. 1, pp. 113–123, 2003.

[81] T. A. Bayer and O. Wirths, "Intracellular accumulation of amyloid-Beta - a predictor for synaptic dysfunction and neuron loss in Alzheimer's disease," *Front Aging Neurosci*, vol. 2, p. 8, 2010.

[82] U. Das *et al.*, "Visualizing APP and BACE-1 approximation in neurons yields insight into the amyloidogenic pathway," *Nat Neurosci*, vol. 19, no. 1, pp. 55–64, 2016.

[83] U. Das, D. A. Scott, A. Ganguly, E. H. Koo, Y. Tang, and S. Roy, "Activity-induced convergence of APP and BACE-1 in acidic microdomains via an endocytosis-dependent pathway," *Neuron*, vol. 79, no. 3, pp. 447–460, 2013.

[84] R. G. Nagele, M. R. D'Andrea, W. J. Anderson, and H. Y. Wang, "Intracellular accumulation of beta-amyloid(1-42) in neurons is facilitated by the alpha 7 nicotinic acetylcholine receptor in Alzheimer's disease," *Neuroscience*, vol. 110, no. 2, pp. 199–211, 2002.

[85] V. N. Uversky, "Amyloidogenesis of natively unfolded proteins," *Curr Alzheimer Res*, vol. 5, no. 3, pp. 260–287, 2008.

[86] S. A. Gravina *et al.*, "Amyloid beta protein (A beta) in Alzheimer's disease brain. Biochemical and immunocytochemical analysis with antibodies specific for forms ending at A beta 40 or A beta 42(43)," *J.Biol.Chem.*, vol. 270, no.

0021–9258, pp. 7013–7016, 1995.

[87] C. J. Barrow and M. G. Zagorski, “Solution structures of beta peptide and its constituent fragments: relation to amyloid deposition.,” *Science*, vol. 253, no. 5016, pp. 179–82, 1991.

[88] T. Iwatsubo, A. Odaka, N. Suzuki, H. Mizusawa, N. Nukina, and Y. Ihara, “Visualization of A beta 42(43) and A beta 40 in senile plaques with end-specific A beta monoclonals: evidence that an initially deposited species is A beta 42(43).,” *Neuron*, vol. 13, no. 1, pp. 45–53, 1994.

[89] E. Gowing *et al.*, “Chemical characterization of Aβ 17-42 peptide, a component of diffuse amyloid deposits of Alzheimer disease,” *J. Biol. Chem.*, vol. 269, no. 15, pp. 10987–10990, 1994.

[90] S. W. Snyder *et al.*, “Amyloid-beta aggregation: selective inhibition of aggregation in mixtures of amyloid with different chain lengths,” *Biophys. J.*, vol. 67, no. 3, pp. 1216–1228, 1994.

[91] V. N. Uversky, “Amyloidogenesis of natively unfolded proteins.,” *Curr. Alzheimer Res.*, vol. 5, no. 3, pp. 260–287, 2008.

[92] M. D. Kirkitadze, M. M. Condron, and D. B. Teplow, “Identification and characterization of key kinetic intermediates in amyloid beta-protein fibrillogenesis,” *J Mol Biol*, vol. 312, no. 5, pp. 1103–1119, 2001.

[93] L. Mucke and D. J. Selkoe, “Neurotoxicity of amyloid beta-protein: synaptic and network dysfunction,” *Cold Spring Harb Perspect Med*, vol. 2, no. 7, p. a006338, 2012.

[94] G. Merlini and V. Bellotti, “Molecular mechanisms of amyloidosis,” *N Engl J Med*, vol. 349, no. 6, pp. 583–596, 2003.

[95] R. Roychaudhuri, M. Yang, M. M. Hoshi, and D. B. Teplow, “Amyloid beta-protein assembly and Alzheimer disease.,” *J. Biol. Chem.*, vol. 284, no. 8, pp. 4749–4753, 2009.

[96] K. Ono, M. M. Condron, and D. B. Teplow, “Structure-neurotoxicity relationships of amyloid -protein oligomers,” *Proc. Natl. Acad. Sci.*, vol. 106, no. 35, pp. 14745–14750, 2009.

[97] M. P. Lambert *et al.*, “Diffusible, nonfibrillar ligands derived from Abeta1-42 are potent central nervous system neurotoxins,” *Proc Natl Acad Sci U S A*, vol. 95, no. 11, pp. 6448–6453, 1998.

[98] J. P. Cleary *et al.*, “Natural oligomers of the amyloid-beta protein specifically disrupt cognitive function,” *Nat Neurosci*, vol. 8, no. 1, pp. 79–84, 2005.

[99] D. M. Walsh *et al.*, “Naturally secreted oligomers of amyloid beta protein potently inhibit hippocampal long-term potentiation in vivo,” *Nature*, vol. 416, no. 6880, pp. 535–539, 2002.

[100] B. H. Toyama and J. S. Weissman, “Amyloid structure: conformational diversity and consequences,” *Annu Rev Biochem*, vol. 80, pp. 557–585, 2011.

[101] T. Dyrks, E. Dyrks, C. L. Masters, and K. Beyreuther, “Amyloidogenicity of

rodent and human beta A4 sequences," *FEBS Lett*, vol. 324, no. 2, pp. 231–236, 1993.

[102] S. J. Webster, A. D. Bachstetter, P. T. Nelson, F. A. Schmitt, and L. J. Van Eldik, "Using mice to model Alzheimer's dementia: An overview of the clinical disease and the preclinical behavioral changes in 10 mouse models," *Front. Genet.*, vol. 5, no. APR, 2014.

[103] M. Kitazawa, R. Medeiros, and F. M. Laferla, "Transgenic mouse models of Alzheimer disease: developing a better model as a tool for therapeutic interventions," *Curr Pharm Des*, vol. 18, no. 8, pp. 1131–1147, 2012.

[104] J. Hardy and D. J. Selkoe, "The amyloid hypothesis of Alzheimer's disease: progress and problems on the road to therapeutics," *Science (80-.).*, vol. 297, no. 5580, pp. 353–356, 2002.

[105] C. Van Cauwenberghe, C. Van Broeckhoven, and K. Sleegers, "The genetic landscape of Alzheimer disease: clinical implications and perspectives," *Genet Med*, vol. 18, no. 5, pp. 421–430, 2016.

[106] M. Gatz *et al.*, "Role of genes and environments for explaining Alzheimer disease," *Arch Gen Psychiatry*, vol. 63, no. 2, pp. 168–174, 2006.

[107] K. G. Mawuenyega *et al.*, "Decreased clearance of CNS beta-amyloid in Alzheimer's disease," *Science (80-.).*, vol. 330, no. 6012, p. 1774, 2010.

[108] J. E. Kang *et al.*, "Amyloid-beta dynamics are regulated by orexin and the sleep-wake cycle," *Science (80-.).*, vol. 326, no. 5955, pp. 1005–1007, 2009.

[109] P. D. Mehta, T. Pirttilä, S. P. Mehta, E. a Sersen, P. S. Aisen, and H. M. Wisniewski, "Plasma and cerebrospinal fluid levels of amyloid beta proteins 1-40 and 1-42 in Alzheimer disease.," *Arch. Neurol.*, vol. 57, no. 1, pp. 100–105, 2000.

[110] J. M. Castellano *et al.*, "Human apoE isoforms differentially regulate brain amyloid-beta peptide clearance," *Sci Transl Med*, vol. 3, no. 89, p. 89ra57, 2011.

[111] J. R. Cirrito *et al.*, "In vivo assessment of brain interstitial fluid with microdialysis reveals plaque-associated changes in amyloid-beta metabolism and half-life," *J Neurosci*, vol. 23, no. 26, pp. 8844–8853, 2003.

[112] D. L. Brody *et al.*, "Amyloid-beta dynamics correlate with neurological status in the injured human brain," *Science (80-.).*, vol. 321, no. 5893, pp. 1221–1224, 2008.

[113] C. A. McLean *et al.*, "Soluble pool of Abeta amyloid as a determinant of severity of neurodegeneration in Alzheimer's disease," *Ann Neurol*, vol. 46, no. 6, pp. 860–866, 1999.

[114] G. M. Shankar *et al.*, "Amyloid-beta protein dimers isolated directly from Alzheimer's brains impair synaptic plasticity and memory," *Nat Med*, vol. 14, no. 8, pp. 837–842, 2008.

[115] D. M. Kullmann and K. P. Lamsa, "Long-term synaptic plasticity in hippocampal interneurons," *Nat Rev Neurosci*, vol. 8, no. 9, pp. 687–699,

2007.

[116] E. M. Snyder *et al.*, “Regulation of NMDA receptor trafficking by amyloid-beta,” *Nat Neurosci*, vol. 8, no. 8, pp. 1051–1058, 2005.

[117] M. D. Greicius, G. Srivastava, A. L. Reiss, and V. Menon, “Default-mode network activity distinguishes Alzheimer’s disease from healthy aging: evidence from functional MRI,” *Proc Natl Acad Sci U S A*, vol. 101, no. 13, pp. 4637–4642, 2004.

[118] W. W. Seeley, R. K. Crawford, J. Zhou, B. L. Miller, and M. D. Greicius, “Neurodegenerative diseases target large-scale human brain networks,” *Neuron*, vol. 62, no. 1, pp. 42–52, 2009.

[119] R. L. Buckner, J. R. Andrews-Hanna, and D. L. Schacter, “The brain’s default network: anatomy, function, and relevance to disease,” *Ann N Y Acad Sci*, vol. 1124, pp. 1–38, 2008.

[120] M. A. Busche *et al.*, “Clusters of hyperactive neurons near amyloid plaques in a mouse model of Alzheimer’s disease,” *Science (80-.).*, vol. 321, no. 5896, pp. 1686–1689, 2008.

[121] L. Verret *et al.*, “Inhibitory interneuron deficit links altered network activity and cognitive dysfunction in Alzheimer model,” *Cell*, vol. 149, no. 3, pp. 708–721, 2012.

[122] D. Pandis and N. Scarmeas, “Seizures in Alzheimer disease: clinical and epidemiological data,” *Epilepsy Curr*, vol. 12, no. 5, pp. 184–187, 2012.

[123] J. J. Palop *et al.*, “Aberrant excitatory neuronal activity and compensatory remodeling of inhibitory hippocampal circuits in mouse models of Alzheimer’s disease,” *Neuron*, vol. 55, no. 5, pp. 697–711, 2007.

[124] S. Ziyatdinova *et al.*, “Spontaneous epileptiform discharges in a mouse model of Alzheimer’s disease are suppressed by antiepileptic drugs that block sodium channels,” *Epilepsy Res*, vol. 94, no. 1–2, pp. 75–85, 2011.

[125] X. X. Yan *et al.*, “Chronic temporal lobe epilepsy is associated with enhanced Alzheimer-like neuropathology in 3xTg-AD mice,” *PLoS One*, vol. 7, no. 11, p. e48782, 2012.

[126] R. Minkeviciene *et al.*, “Amyloid beta-induced neuronal hyperexcitability triggers progressive epilepsy,” *J Neurosci*, vol. 29, no. 11, pp. 3453–3462, 2009.

[127] J. T. Brown, J. Chin, S. C. Leiser, M. N. Pangalos, and A. D. Randall, “Altered intrinsic neuronal excitability and reduced Na+ currents in a mouse model of Alzheimer’s disease,” *Neurobiol Aging*, vol. 32, no. 11, p. 2109 e1-14, 2011.

[128] M. A. Busche *et al.*, “Critical role of soluble amyloid-beta for early hippocampal hyperactivity in a mouse model of Alzheimer’s disease,” *Proc Natl Acad Sci U S A*, vol. 109, no. 22, pp. 8740–8745, 2012.

[129] R. Wykes, A. Kalmbach, M. Eliava, and J. Waters, “Changes in the physiology of CA1 hippocampal pyramidal neurons in preplaque CRND8 mice,” *Neurobiol Aging*, vol. 33, no. 8, pp. 1609–1623, 2012.

[130] V. Kellner, N. Menkes-Caspi, S. Beker, and E. A. Stern, “Amyloid-beta alters ongoing neuronal activity and excitability in the frontal cortex,” *Neurobiol Aging*, vol. 35, no. 9, pp. 1982–1991, 2014.

[131] T. L. Kerrigan, J. T. Brown, and A. D. Randall, “Characterization of altered intrinsic excitability in hippocampal CA1 pyramidal cells of the Abeta-overproducing PDAPP mouse,” *Neuropharmacology*, vol. 79, pp. 515–524, 2014.

[132] F. Scala *et al.*, “Intraneuronal Abeta accumulation induces hippocampal neuron hyperexcitability through A-type K(+) current inhibition mediated by activation of caspases and GSK-3,” *Neurobiol Aging*, vol. 36, no. 2, pp. 886–900, 2015.

[133] F. Tamagnini, S. Scullion, J. T. Brown, and A. D. Randall, “Intrinsic excitability changes induced by acute treatment of hippocampal CA1 pyramidal neurons with exogenous amyloid beta peptide,” *Hippocampus*, vol. 25, no. 7, pp. 786–797, 2015.

[134] F. Tamagnini, J. Novelia, T. L. Kerrigan, J. T. Brown, K. Tsaneva-Atanasova, and A. D. Randall, “Altered intrinsic excitability of hippocampal CA1 pyramidal neurons in aged PDAPP mice,” *Front Cell Neurosci*, vol. 9, p. 372, 2015.

[135] A. Marcantoni, E. F. Raymond, E. Carbone, and H. Marie, “Firing properties of entorhinal cortex neurons and early alterations in an Alzheimer’s disease transgenic model,” *Pflugers Arch*, vol. 466, no. 7, pp. 1437–1450, 2014.

[136] M. J. D. E. LEON, *An atlas of Alzheimer’s disease. The encyclopedia of visual medicine series*. 1999.

[137] B. Reisberg, “Functional assessment staging (FAST),” *Psychopharmacol Bull*, vol. 24, no. 4, pp. 653–659, 1988.

[138] G. Livingston *et al.*, “Dementia prevention, intervention, and care,” *Lancet*, 2017.

[139] “IPA Complete Guides to Behavioral and Psychological Symptoms of Dementia (BPSD).”

[140] S. Barao, D. Moechars, S. F. Lichtenthaler, and B. De Strooper, “BACE1 Physiological Functions May Limit Its Use as Therapeutic Target for Alzheimer’s Disease,” *Trends Neurosci*, vol. 39, no. 3, pp. 158–169, 2016.

[141] F. Amirrad, E. Bousoik, K. Shamloo, H. Al-Shiyab, V. V Nguyen, and H. Montazeri Aliabadi, “Alzheimer’s Disease: Dawn of a New Era?,” *J Pharm Pharm Sci*, vol. 20, no. 0, pp. 184–225, 2017.

[142] J. L. Ables, J. J. Breunig, A. J. Eisch, and P. Rakic, “Not(ch) just development: Notch signalling in the adult brain,” *Nat Rev Neurosci*, vol. 12, no. 5, pp. 269–283, 2011.

[143] L. Lannfelt, N. R. Relkin, and E. R. Siemers, “Amyloid-ss-directed immunotherapy for Alzheimer’s disease,” *J Intern Med*, vol. 275, no. 3, pp. 284–295, 2014.

[144] J. Gotz, F. Chen, J. van Dorpe, and R. M. Nitsch, “Formation of neurofibrillary tangles in P301l tau transgenic mice induced by Abeta 42 fibrils,” *Science (80-.*

)., vol. 293, no. 5534, pp. 1491–1495, 2001.

[145] L. Bakota and R. Brandt, "Tau Biology and Tau-Directed Therapies for Alzheimer's Disease," *Drugs*, vol. 76, no. 3, pp. 301–313, 2016.

[146] D. Gezen-Ak *et al.*, "BDNF, TNFalpha, HSP90, CFH, and IL-10 serum levels in patients with early or late onset Alzheimer's disease or mild cognitive impairment," *J Alzheimers Dis*, vol. 37, no. 1, pp. 185–195, 2013.

[147] L. Larkfors, T. Ebendal, S. R. Whittemore, H. Persson, B. Hoffer, and L. Olson, "Decreased level of nerve growth factor (NGF) and its messenger RNA in the aged rat brain," *Brain Res*, vol. 427, no. 1, pp. 55–60, 1987.

[148] M. Perovic *et al.*, "BDNF transcripts, proBDNF and proNGF, in the cortex and hippocampus throughout the life span of the rat," *Age*, vol. 35, no. 6, pp. 2057–2070, 2013.

[149] F. M. Longo and S. M. Massa, "Neuroprotective strategies in Alzheimer's disease," *NeuroRx*, vol. 1, no. 1, pp. 117–127, 2004.

[150] M. C. Morris, J. A. Schneider, and C. C. Tangney, "Thoughts on B-vitamins and dementia.," *J. Alzheimers. Dis.*, vol. 9, no. 4, pp. 429–33, 2006.

[151] E. R. Siemers *et al.*, "Safety and changes in plasma and cerebrospinal fluid amyloid beta after a single administration of an amyloid beta monoclonal antibody in subjects with Alzheimer disease," *Clin Neuropharmacol*, vol. 33, no. 2, pp. 67–73, 2010.

[152] J. Sevigny *et al.*, "The antibody aducanumab reduces Abeta plaques in Alzheimer's disease," *Nature*, vol. 537, no. 7618, pp. 50–56, 2016.

[153] G. P. Morris, I. A. Clark, and B. Vissel, "Inconsistencies and controversies surrounding the amyloid hypothesis of Alzheimer's disease," *Acta Neuropathol Commun*, vol. 2, p. 135, 2014.

[154] E. S. Musiek and D. M. Holtzman, "Three dimensions of the amyloid hypothesis: time, space and 'wingmen,'" *Nat Neurosci*, vol. 18, no. 6, pp. 800–806, 2015.

[155] J. Lewis *et al.*, "Enhanced neurofibrillary degeneration in transgenic mice expressing mutant tau and APP," *Science (80-.).*, vol. 293, no. 5534, pp. 1487–1491, 2001.

[156] K. Bettens, K. Sleegers, and C. Van Broeckhoven, "Genetic insights in Alzheimer's disease," *Lancet Neurol*, vol. 12, no. 1, pp. 92–104, 2013.

[157] V. P. Prasher *et al.*, "Molecular mapping of Alzheimer-type dementia in Down's syndrome," *Ann Neurol*, vol. 43, no. 3, pp. 380–383, 1998.

[158] M. Nicolas and B. A. Hassan, "Amyloid precursor protein and neural development," *Development*, vol. 141, no. 13, pp. 2543–2548, 2014.

[159] W. G. D. PUZZO O. ARANCIO, and A. PALMERI, "THE KEYSTONE OF ALZHEIMER PATHOGENESIS MIGHT BE SOUGHTIN Ab PHYSIOLOGY," *Neuroscience*, 2005.

[160] J. R. Cirrito *et al.*, “Synaptic activity regulates interstitial fluid amyloid-beta levels in vivo,” *Neuron*, vol. 48, no. 6, pp. 913–922, 2005.

[161] F. Kamenetz *et al.*, “APP processing and synaptic function,” *Neuron*, vol. 37, no. 6, pp. 925–937, 2003.

[162] J. R. Cirrito *et al.*, “Endocytosis is required for synaptic activity-dependent release of amyloid-beta in vivo,” *Neuron*, vol. 58, no. 1, pp. 42–51, 2008.

[163] J. Wegiel *et al.*, “Intraneuronal Abeta immunoreactivity is not a predictor of brain amyloidosis-beta or neurofibrillary degeneration,” *Acta Neuropathol*, vol. 113, no. 4, pp. 389–402, 2007.

[164] D. Puzzo *et al.*, “Picomolar amyloid-beta positively modulates synaptic plasticity and memory in hippocampus,” *J Neurosci*, vol. 28, no. 53, pp. 14537–14545, 2008.

[165] D. Puzzo *et al.*, “Endogenous amyloid-beta is necessary for hippocampal synaptic plasticity and memory,” *Ann Neurol*, vol. 69, no. 5, pp. 819–830, 2011.

[166] J. E. Morley, S. A. Farr, W. A. Banks, S. N. Johnson, K. A. Yamada, and L. Xu, “A physiological role for amyloid-beta protein:enhancement of learning and memory,” *J Alzheimers Dis*, vol. 19, no. 2, pp. 441–449, 2010.

[167] D. H. Small *et al.*, “The beta-amyloid protein of Alzheimer’s disease binds to membrane lipids but does not bind to the alpha7 nicotinic acetylcholine receptor,” *J Neurochem*, vol. 101, no. 6, pp. 1527–1538, 2007.

[168] M. M. Lim, J. R. Gerstner, and D. M. Holtzman, “The sleep-wake cycle and Alzheimer’s disease: what do we know?,” *Neurodegener Dis Manag*, vol. 4, no. 5, pp. 351–362, 2014.

[169] G. F. Gilestro, G. Tononi, and C. Cirelli, “Widespread changes in synaptic markers as a function of sleep and wakefulness in Drosophila,” *Science (80-.).*, vol. 324, no. 5923, pp. 109–112, 2009.

[170] E. Abramov, I. Dolev, H. Fogel, G. D. Ciccotosto, E. Ruff, and I. Slutsky, “Amyloid-beta as a positive endogenous regulator of release probability at hippocampal synapses,” *Nat Neurosci*, vol. 12, no. 12, pp. 1567–1576, 2009.

[171] L. D. Plant, J. P. Boyle, I. F. Smith, C. Peers, and H. A. Pearson, “The production of amyloid beta peptide is a critical requirement for the viability of central neurons,” *J Neurosci*, vol. 23, no. 13, pp. 5531–5535, 2003.

[172] M. L. Giuffrida *et al.*, “Beta-amyloid monomers are neuroprotective,” *J Neurosci*, vol. 29, no. 34, pp. 10582–10587, 2009.

[173] M. A. Lopez-Toledano and M. L. Shelanski, “Neurogenic effect of beta-amyloid peptide in the development of neural stem cells,” *J Neurosci*, vol. 24, no. 23, pp. 5439–5444, 2004.

[174] C. Heo *et al.*, “Effects of the monomeric, oligomeric, and fibrillar Abeta42 peptides on the proliferation and differentiation of adult neural stem cells from subventricular zone,” *J Neurochem*, vol. 102, no. 2, pp. 493–500, 2007.

[175] G. J. Brewer, J. R. Torricelli, E. K. Evege, and P. J. Price, “Optimized survival of

hippocampal neurons in B27-supplemented Neurobasal, a new serum-free medium combination," *J Neurosci Res*, vol. 35, no. 5, pp. 567–576, 1993.

[176] M. S. Parihar and G. J. Brewer, *Amyloid Beta as a Modulator of Synaptic Plasticity*, vol. 22, no. 3. 2011.

[177] L.-F. Lue *et al.*, "Soluble Amyloid β Peptide Concentration as a Predictor of Synaptic Change in Alzheimer's Disease," *Am. J. Pathol.*, vol. 155, no. 3, pp. 853–862, 1999.

[178] W. B. Stine Jr., K. N. Dahlgren, G. A. Krafft, and M. J. LaDu, "In vitro characterization of conditions for amyloid-beta peptide oligomerization and fibrillogenesis," *J Biol Chem*, vol. 278, no. 13, pp. 11612–11622, 2003.

[179] M. Beeg, M. Stravalaci, A. Bastone, M. Salmona, and M. Gobbi, "A modified protocol to prepare seed-free starting solutions of amyloid-beta (Abeta)(1)(-)(4)(0) and Abeta(1)(-)(4)(2) from the corresponding depsipeptides," *Anal Biochem*, vol. 411, no. 2, pp. 297–299, 2011.

[180] D. K. Cullen, M. E. Gilroy, H. R. Irons, and M. C. Laplaca, "Synapse-to-neuron ratio is inversely related to neuronal density in mature neuronal cultures," *Brain Res*, vol. 1359, pp. 44–55, 2010.

[181] S. Li, M. Jin, T. Koeglsperger, N. E. Shepardson, G. M. Shankar, and D. J. Selkoe, "Soluble Abeta oligomers inhibit long-term potentiation through a mechanism involving excessive activation of extrasynaptic NR2B-containing NMDA receptors," *J Neurosci*, vol. 31, no. 18, pp. 6627–6638, 2011.

[182] D. Ferrera, N. Mazzaro, C. Canale, and L. Gasparini, "Resting microglia react to A??42 fibrils but do not detect oligomers or oligomer-induced neuronal damage," *Neurobiol. Aging*, vol. 35, no. 11, pp. 2444–2457, 2014.

[183] B. D. Semple, K. Blomgren, K. Gimlin, D. M. Ferriero, and L. J. Noble-Haeusslein, "Brain development in rodents and humans: Identifying benchmarks of maturation and vulnerability to injury across species," *Progress in Neurobiology*, vol. 106–107. pp. 1–16, 2013.

[184] J. C. Amatniek *et al.*, "Incidence and predictors of seizures in patients with Alzheimer's disease," *Epilepsia*, vol. 47, no. 5, pp. 867–872, 2006.

[185] H. L. Picken Bahrey and W. J. Moody, "Early development of voltage-gated ion currents and firing properties in neurons of the mouse cerebral cortex," *J Neurophysiol*, vol. 89, no. 4, pp. 1761–1773, 2003.

[186] P. Charlesworth, E. Cotterill, A. Morton, S. G. Grant, and S. J. Eglen, "Quantitative differences in developmental profiles of spontaneous activity in cortical and hippocampal cultures," *Neural Dev*, vol. 10, p. 1, 2015.

[187] J. M. Bekkers and A. J. Delaney, "Modulation of excitability by alpha-dendrotoxin-sensitive potassium channels in neocortical pyramidal neurons," *J Neurosci*, vol. 21, no. 17, pp. 6553–6560, 2001.

[188] J. M. Bekkers, "Properties of voltage-gated potassium currents in nucleated patches from large layer 5 cortical pyramidal neurons of the rat," *J Physiol*, vol. 525 Pt 3, pp. 593–609, 2000.

[189] B. Hille, *Ion channels of excitable membranes*, 3rd ed. Sunderland, Mass.: Sinauer, 2001.

[190] R. O. Wong and A. Ghosh, "Activity-dependent regulation of dendritic growth and patterning," *Nat Rev Neurosci*, vol. 3, no. 10, pp. 803–812, 2002.

[191] X. Zhou, D. Hollern, J. Liao, E. Andrechek, and H. Wang, "NMDA receptor-mediated excitotoxicity depends on the coactivation of synaptic and extrasynaptic receptors," *Cell Death Dis*, vol. 4, p. e560, 2013.

[192] S. B. Glantz, C. D. Cianci, R. Iyer, D. Pradhan, K. K. Wang, and J. S. Morrow, "Sequential degradation of alphaII and betaII spectrin by calpain in glutamate or maitotoxin-stimulated cells," *Biochemistry*, vol. 46, no. 2, pp. 502–513, 2007.

[193] G. Turrigiano, "Homeostatic synaptic plasticity: local and global mechanisms for stabilizing neuronal function," *Cold Spring Harb Perspect Biol*, vol. 4, no. 1, p. a005736, 2012.

[194] X. Yu and R. C. Malenka, "Beta-catenin is critical for dendritic morphogenesis," *Nat Neurosci*, vol. 6, no. 11, pp. 1169–1177, 2003.

[195] G. A. Wayman *et al.*, "Activity-dependent dendritic arborization mediated by CaM-kinase I activation and enhanced CREB-dependent transcription of Wnt-2," *Neuron*, vol. 50, no. 6, pp. 897–909, 2006.

[196] J. J. Zhu and R. Malinow, "Acute versus chronic NMDA receptor blockade and synaptic AMPA receptor delivery," *Nat Neurosci*, vol. 5, no. 6, pp. 513–514, 2002.

[197] D. Puzzo and O. Arancio, "Amyloid-beta peptide: Dr. Jekyll or Mr. Hyde?," *J Alzheimers Dis*, vol. 33 Suppl 1, pp. S111-20, 2013.

[198] T. M. Pirttimaki *et al.*, "alpha7 Nicotinic receptor-mediated astrocytic gliotransmitter release: Abeta effects in a preclinical Alzheimer's mouse model," *PLoS One*, vol. 8, no. 11, p. e81828, 2013.

[199] J. L. Lawrence *et al.*, "Regulation of presynaptic Ca2+, synaptic plasticity and contextual fear conditioning by a N-terminal beta-amyloid fragment," *J Neurosci*, vol. 34, no. 43, pp. 14210–14218, 2014.

[200] M. Chiappalone, M. Bove, A. Vato, M. Tedesco, and S. Martinoia, "Dissociated cortical networks show spontaneously correlated activity patterns during in vitro development," *Brain Res*, vol. 1093, no. 1, pp. 41–53, 2006.

[201] M. Ichikawa, K. Muramoto, K. Kobayashi, M. Kawahara, and Y. Kuroda, "Formation and maturation of synapses in primary cultures of rat cerebral cortical cells: an electron microscopic study," *Neurosci Res*, vol. 16, no. 2, pp. 95–103, 1993.

[202] G. Manassero *et al.*, "Beta-amyloid 1-42 monomers, but not oligomers, produce PHF-like conformation of Tau protein," *Aging Cell*, vol. 15, no. 5, pp. 914–923, 2016.

[203] M. Guglielmotto *et al.*, "Aβ1-42 monomers or oligomers have different effects on autophagy and apoptosis," *Autophagy*, vol. 10, no. 10, pp. 1827–1843, 2014.

[204] P. Hortschansky, T. Christopeit, V. Schroeckh, and M. Fandrich, "Thermodynamic analysis of the aggregation propensity of oxidized Alzheimer's beta-amyloid variants," *Protein Sci*, vol. 14, no. 11, pp. 2915–2918, 2005.

[205] O. M. El-Agnaf, D. S. Mahil, B. P. Patel, and B. M. Austen, "Oligomerization and toxicity of beta-amyloid-42 implicated in Alzheimer's disease.," *Biochem. Biophys. Res. Commun.*, vol. 273, no. 3, pp. 1003–7, 2000.

[206] J. J. Palop and L. Mucke, "Epilepsy and cognitive impairments in Alzheimer disease," *Arch Neurol*, vol. 66, no. 4, pp. 435–440, 2009.

[207] J. Franberg, H. Karlstrom, B. Winblad, L. O. Tjernberg, and S. Frykman, "gamma-Secretase dependent production of intracellular domains is reduced in adult compared to embryonic rat brain membranes," *PLoS One*, vol. 5, no. 3, p. e9772, 2010.

[208] L. D. Plant *et al.*, "Amyloid beta peptide as a physiological modulator of neuronal 'A'-type K+ current," *Neurobiol Aging*, vol. 27, no. 11, pp. 1673–1683, 2006.

[209] T. L. Kerrigan, L. Atkinson, C. Peers, and H. A. Pearson, "Modulation of 'A'-type K+ current by rodent and human forms of amyloid beta protein," *Neuroreport*, vol. 19, no. 8, pp. 839–843, 2008.

[210] E. Angulo *et al.*, "Up-regulation of the Kv3.4 potassium channel subunit in early stages of Alzheimer's disease," *J Neurochem*, vol. 91, no. 3, pp. 547–557, 2004.

[211] A. Pannaccione *et al.*, "Up-regulation and increased activity of KV3.4 channels and their accessory subunit MinK-related peptide 2 induced by amyloid peptide are involved in apoptotic neuronal death," *Mol Pharmacol*, vol. 72, no. 3, pp. 665–673, 2007.

[212] T. A. Good, D. O. Smith, and R. M. Murphy, "Beta-amyloid peptide blocks the fast-inactivating K+ current in rat hippocampal neurons," *Biophys J*, vol. 70, no. 1, pp. 296–304, 1996.

[213] C. Chen, "beta-Amyloid increases dendritic Ca2+ influx by inhibiting the A-type K+ current in hippocampal CA1 pyramidal neurons," *Biochem Biophys Res Commun*, vol. 338, no. 4, pp. 1913–1919, 2005.

[214] J. Burrone, M. O'Byrne, and V. N. Murthy, "Multiple forms of synaptic plasticity triggered by selective suppression of activity in individual neurons," *Nature*, vol. 420, no. 6914, pp. 414–418, 2002.

[215] L. C. Andreae and J. Burrone, "The role of neuronal activity and transmitter release on synapse formation," *Curr Opin Neurobiol*, vol. 27, pp. 47–52, 2014.

[216] Y. Chen, J. Bourne, V. A. Pieribone, and R. M. Fitzsimonds, "The role of actin in the regulation of dendritic spine morphology and bidirectional synaptic plasticity," *Neuroreport*, vol. 15, no. 5, pp. 829–832, 2004.

[217] C. Lesuisse and L. J. Martin, "Long-term culture of mouse cortical neurons as a model for neuronal development, aging, and death," *J Neurobiol*, vol. 51, no. 1,

pp. 9–23, 2002.

[218] G. Wu, R. Malinow, and H. T. Cline, “Maturation of a central glutamatergic synapse,” *Science (80-.).*, vol. 274, no. 5289, pp. 972–976, 1996.

[219] S. N. Gomperts, R. Carroll, R. C. Malenka, and R. A. Nicoll, “Distinct roles for ionotropic and metabotropic glutamate receptors in the maturation of excitatory synapses,” *J Neurosci*, vol. 20, no. 6, pp. 2229–2237, 2000.

[220] N. Arispe, E. Rojas, and H. B. Pollard, “Alzheimer disease amyloid beta protein forms calcium channels in bilayer membranes: blockade by tromethamine and aluminum,” *Proc Natl Acad Sci U S A*, vol. 90, no. 2, pp. 567–571, 1993.

[221] H. Lin, R. Bhatia, and R. Lal, “Amyloid beta protein forms ion channels: implications for Alzheimer’s disease pathophysiology,” *FASEB J.*, vol. 15, no. 1530–6860 SB–IM, pp. 2433–2444, 2001.

[222] H. Lin, Y. J. Zhu, and R. Lal, “Amyloid β protein (1-40) forms calcium-permeable, Zn2+-sensitive channel in reconstituted lipid vesicles,” *Biochemistry*, vol. 38, no. 34, pp. 11189–11196, 1999.

[223] Y. Hirakura, I. Carreras, J. D. Sipe, and B. L. Kagan, “Channel formation by serum amyloid A: a potential mechanism for amyloid pathogenesis and host defense,” *Amyloid*, vol. 9, no. 1, pp. 13–23, 2002.

[224] M. Kawahara, N. Arispe, Y. Kuroda, and E. Rojas, “Alzheimer’s disease amyloid beta-protein forms Zn(2+)-sensitive, cation-selective channels across excised membrane patches from hypothalamic neurons,” *Biophys. J.*, vol. 73, no. 1, pp. 67–75, 1997.

[225] H. Adesnik, G. Li, M. J. During, S. J. Pleasure, and R. A. Nicoll, “NMDA receptors inhibit synapse unsilencing during brain development,” *Proc Natl Acad Sci U S A*, vol. 105, no. 14, pp. 5597–5602, 2008.